UiT
THE ARCTIC UNIVERSITY OF NORWAY

Faculty of Science and Technology

Department of Chemistry

Mutational, structural and inhibitory investigations of metallo-β-lactamases involved in antibiotic resistance

—

Susann Skagseth

A dissertation for the degree of Philosophiae Doctor – February 2017

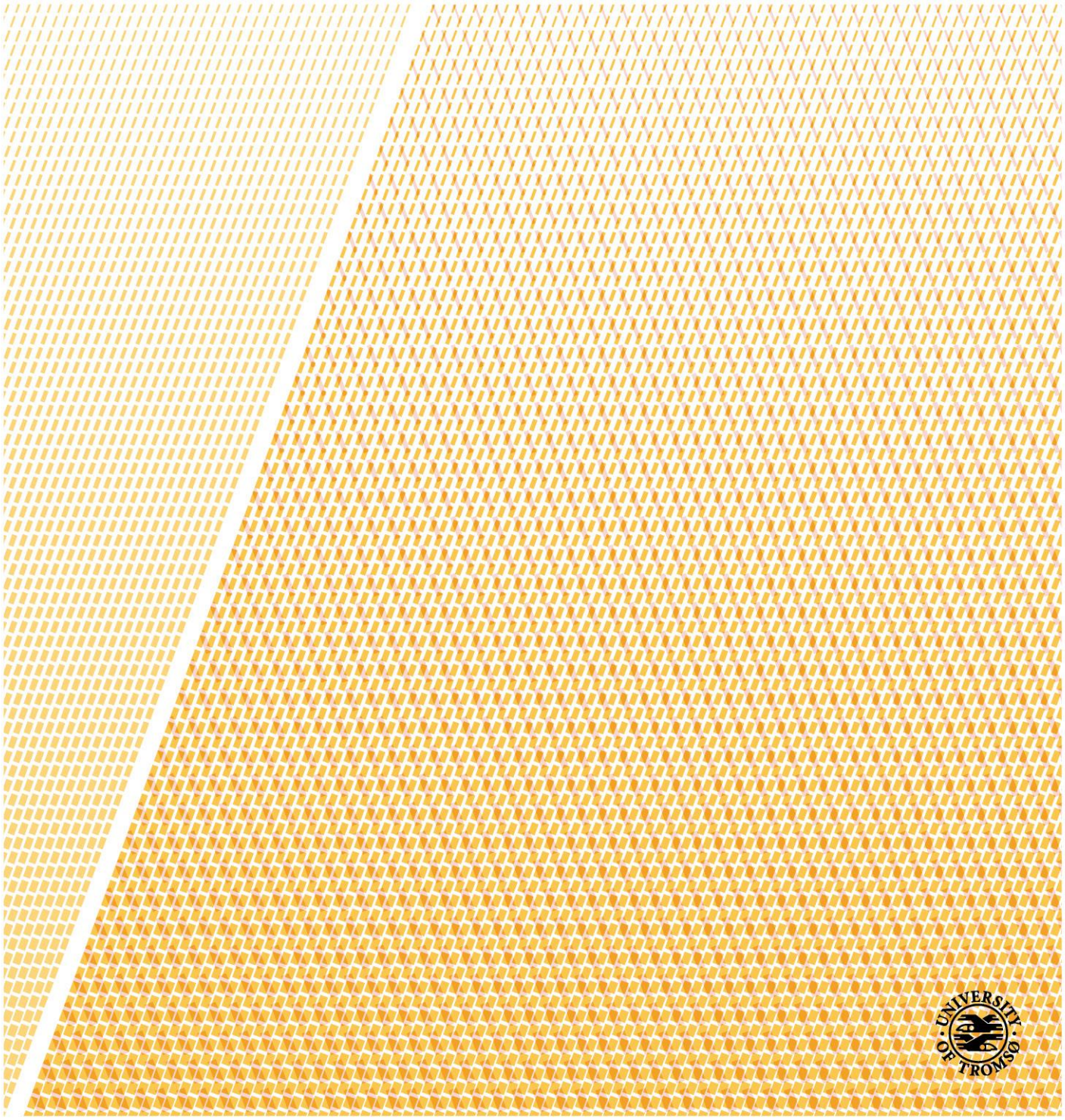

Mutational, structural and inhibitory investigations of metallo-β-lactamases involved in antibiotic resistance

Susann Skagseth

A dissertation for the degree of Philosophiae Doctor

Department of Chemistry

Faculty of Science and Technology, UiT

December 2015

To my mom, dad,

my sister Renate and brother Espen

Acknowledgement

This work was performed at the Norwegian Structural Biology Centre (NorStruct), Department of Chemistry, Faculty of Science and Technology, UiT – The Arctic University of Norway. The Research Council of Norway (RCN) through the FRIMEDBIO grant and UiT – The Arctic University of Norway, provided the financial support for this work. I would like to thank for the financial support and courses provided by BioStruct, the Norwegian Graduate School in Structural Biology.

First and foremost, I would like to thank my main supervisor Dr. Hanna-Kirsti S. Leiros for giving me the opportunity to work in this interesting field of antibiotic resistance. I am highly grateful for your excellent guidance, advice, enthusiasm, knowledge and support through the years. Thank you for your patience, understanding, and all the motivation in our discussions. Thank you for showing me the way in crystallography, and always having an open door for my many questions. Thank you for being such an amazing supervisor, always encouraging me throughout the four years of this work. Without you, this work would not have been completed. I want to thank my co-supervisor Dr. Ørjan Samuelsen for all the support, patience, knowledge and valuable feedback. I have enjoyed our discussions and I am grateful for everything I learned from you. Thanks to my co-supervisor Gro EK Bjerga for supervising me in the lab in the beginning of my PhD, and for the valuable feedback on my writing.

Thanks to Dr. James Spencer for welcoming me in Bristol and helping me in understanding the enzyme kinetics. Thanks to Annette Bayer and Sundus Akhter for the nice collaboration and discussions. Thanks to Trine for all help and talks in the lab about work- and non-work related stuff. Thanks to Tony for being patient with me while teaching me how to use the biacore, and for our discussion on the results. Thanks to Osman for showing me the way in computational modelling of GIM-1. Thanks to all co-authors on the submitted and prepared manuscripts.

A special thanks to Man Kumari for always being there for me during both good times and bad. I have appreciated our many discussions about everything between heaven and earth and our friendship. Thanks to Miriam G, Kristel, Tor Olav, Cecilie, and Titti, for listening to me over the years and all of your scientific and non-scientific discussions. Thanks to my office

mates Miriam K and Kazi for being patient with me and not complaining when I make smoothies in the office. Thanks to all fellow NorStructers for always being helpful, smiling, fun activities, the parties, and the wonderful work environment. It truly is like a big NorStruct family.

Thanks to my friends Marielle, Marthe and Marie for being there for me, cheering me on, and making me laugh so much. I would go mad without you guys! Thanks to Hahn for taking the time in your busy schedule to read through my thesis and checking the grammar for me.

Last, but not least, I want to thank my family. Thank you for all your support and for believing in me. Thanks to my parents for all the love and making my life a lot easier. Thanks to my brother Espen for making me laugh. Thanks to my sister Renate for being there for me whenever I need you, and especially driving me and picking me up from work at all times. You are the best!

Finally, a thanks to Bjørn Kristian for being so understanding and supporting in this stressful time of writing my thesis. Thank you for giving me the right amount of distraction and motivation in these last months of writing.

Susann Skagseth

December 2016, Tromsø, Norway

Summary

Metallo-β-lactamases (MBLs) are able to hydrolyze most β-lactam substrates, including carbapenems, which for a long time was considered a 'last resort' treatment for infections caused by antibiotic resistance bacteria. MBLs found on mobile genetic elements allow for rapid spread between bacteria, and are causing a major public health problem. One approach to overcome the threat of MBLs is to design or discover new inhibitors for these enzymes to use in a combination therapy of β-lactam/β-lactamase-inhibitor in order to restore the effect of β-lactams. However, to date there are no effective clinical MBL inhibitors available, and the need is urgent.

In **paper I** of this thesis, the importance of first and second sphere residues for VIM-7 were investigated for activity, stability and structure analysis. The mutation in first sphere residue D120A had a deleterious effect on the activity, stability, and the crystal structure revealed the loss of a zinc ion. The second sphere substitutions, F218Y and H224Y, showed an increase in activity and stability, and the crystal structures showed the establishment of new hydrogen bonds.

In **paper II**, the substitutions of the second sphere residues to W228R/A/Y/S and Y233N/A/I/S in GIM-1, in general showed a reduced catalytic efficiency, with no effect on the enzyme stability. The crystal structures of the W228R/A/Y/S and Y233A mutants revealed that the conformation of the L1 loop was altered instead of the L3 loop, where the substitutions were made.

In **paper III**, the search for MBL inhibitors among thiol-based compounds against VIM-2, GIM-1 and NDM-1, revealed the most potent inhibitors to contain a thioacetate and a phosphonic acid. High-resolution crystal structures of three inhibitor-VIM-2 complexes found the mercapto group bridging the two zinc ions, the thioacetate binding one zinc and the phenyl ring in stacking interactions with VIM-2.

In **paper IV**, enzyme kinetic measurements of TMB-1, TMB-2 and TMB-1 E_{119}Q/S/A mutants revealed that TMB-2 and TMB-1 mutants had a reduced efficiency compared to TMB-1. The TMB-1 crystal structure was solved to 1.75 Å. Thiol-based inhibitors tested against TMB-1 showed two potent inhibitors, **2a** and **2b**, with IC_{50} values in the nanomolar range.

In summary, through establishing the contribution from specific residues to substrate binding may give information on interactions that can be exploited in designing inhibitors able to combat the β-lactam resistance. Additionally, the study shows potent inhibitors for VIM-2, and variable results for GIM-1, TMB-1 and NDM-1 MBLs, which can be good starting points for more potent broad-spectrum MBL inhibitors.

Abbreviations

DNA	Deoxyribonucleic acid
RNA	Ribonucleic acid
MRSA	Methicillin-resistant *Staphylococcus aureus*
PBP	Penicillin binding protein
IgE	Immunoglobulin E
NAG	*N*-acetylglucosamine
NAMA	*N*-acetylmuramic acid
mDAP	Mesodiaminopimelic acid
OMP	Outer membrane proteins
SBL	Serine-β-lactamase
MBL	Metallo-β-lactamase
NDM	New Delhi metallo-β-lactamase
EDTA	Ethylemediaminetetraacetic acid
ESBL	Extended Spectrum β-lactamase
CphA	Carbapenem-hydrolyzing metallo-β-lactamase
VIM	Verona integron-encoded metallo-β-lactamase
BcII	*Bacillus cereus* β-lactamase II
GIM	German imipenemase metallo-β-lactamase
IMP	Imipenemase
BBL	Class B β-lactamase
BLAST	Basic Local Alignment Search Tool
PDB	Protein Data Bank
SPM	São Paolo metallo-β-lactamase
BlaB	β-lactamase B
MEGA7	Molecular Evolutionary Genetics Analysis, version 7
ImiS	Imipenemase from *A. veronii bv. Sobria*
AIM	Adelaide imipenemase
NMR	Nuclear magnetic resonance
MIC	Minimum inhibitory concentration

TMB	Tripoli metallo-β-lactamase
SPR	Surface Plasmon Resonance
IC_{50}	Half maximal inhibitory concentration
DMSO	Dimethyl sulfoxide
SAR	Structure activity relationship

Table of Contents

List of papers

Paper I:

His224 Alters the R2 Drug Binding Site and Phe218 Influences the Catalytic Efficiency of the Metallo-β-Lactamase VIM-7. Published in *Antimicrobial Agents and Chemotherapy*; Aug, 2014, 58 (8), p. 4826-4836.

Leiros Hanna-Kirsti S., Skagseth Susann, Edvardsen Kine Susann Waade, Lorentzen Marit Sjo, Bjerga Gro Elin Kjæreng, Leiros Ingar, Samuelsen Ørjan.

Paper II:

Role of Residues W228 and Y233 in the Structure and Activity of Metallo-β-Lactamase GIM-1. Published in *Antimicrobial Agents and Chemotherapy*; Feb, 2016, 60 (2), p 990-1002.

Skagseth Susann, Carlsen Trine Josefine, Bjerga Gro Elin Kjæreng, Spencer James, Samuelsen Ørjan, Leiros Hanna-Kirsti S.

Paper III:

Metallo-β-lactamase Inhibitors by Bioisosteric Replacement: Preparation, Activity and Binding. Submitted to *European Journal of Medicinal Chemistry*.

Skagseth Susann, Akhter Sundus, Paulsen Marianne H., Samuelsen Ørjan, Muhammad Zeeshan, Leiros Hanna-Kirsti S., Bayer Annette

Paper IV:

Structural insight into TMB-1 and the role of residue 119 and 228 in substrate and inhibitor activity. Submitted to *Antimicrobial Agents and Chemotherapy*.

Skagseth Susann, Christopeit Tony, Akhter Sundus, Bayer Annette, Samuelsen Ørjan, Leiros Hanna-Kirsti S.

1. Introduction

1.1. Antibiotics

This thesis includes studies of metallo-β-lactamase (MBL) enzymes involved in antibiotic resistance, and the search for MBL inhibitors. Before introducing the β-lactamase enzymes, I will start with introducing antibiotics, antibiotic resistance and bacterial defense mechanisms.

1.1.1. History of antibiotics

The first antibiotic substance discovered was the β-lactam penicillin G (also known as benzylpenicillin) in 1928 by the Scottish biologist Alexander Fleming. For the achievement he was awarded the Nobel Prize in Physiology or Medicine, together with the Australian pharmacologist and pathologist Howard Florey and the British biochemist Ernst Boris Chain in 1945 [1]. The discovery was accidental, and changed the course of medicine. Petri dishes with *Staphylococci* were left uncovered on Flemings laboratory bench, and were contaminated with mold spores containing *Penicillium notatum* [2]. Bacteria were not able to grow in the area around the *Penicillium* colonies. Fleming then isolated the active substance, naming it 'penicillin' [2]. Florey and Chain were able to mass-produce penicillin for use during World War II [2]. After the war, penicillin was known as the "wonder drug" due to its effect on a wide variety of diseases, including infections caused by bacteria resistant to sulfonamides, which was the only other antibiotic therapy available at that time [3].

The discovery of antibiotics, also known as antimicrobial drugs, is considered as one of the most significant events for global health in modern times, and has had a massive impact on treatment of infectious diseases. Antibiotics target bacterial cells with limited toxicity to human cells [4]. Since the introduction of antibiotics on the market in the 1940s, antimicrobial agents have reduced illness and death from infectious diseases [5]. The antibiotics have, in addition allowed countless of medical procedures to be performed without the risk of getting infections. Many modern surgical procedures such as organ transplantations and cancer treatment would not be possible without antibiotics [6].

The American biochemist and microbiologist Selman Waksman, was the discoverer of the antibiotic streptomycin. Waksman is known for his work on screening soils for investigating biologicals, and he was the first to propose the word «antibiotic» as a noun in 1941 [7]. The

term “antibiotic” was then used as a description for a compounds use, not type of class or its natural function. Herein, an antibiotic is defined as organic molecule that kills or inhibits bacteria by specific interactions with the bacterial targets, without any consideration of the source of the particular class or compound [8]. Today, however, the term has been expanded to include antifungal and bacteriostatic antibacterial agents that may also be derived from synthetic chemical approaches, not only from natural sources [9].

There are several classes of antibiotics available with different targets in the bacteria. These include: i) inhibition of cell wall synthesis (peptidoglycan biosynthesis), ii) inhibition of protein synthesis (translation), iii) DNA replication, iv) inhibition of RNA synthesis (transcription), v) folic acid synthesis (C1 metabolism), and vi) disruption of cell membrane [5, 6]. Antibiotics can arrest cell growth (bacteriostatic) or kill the cells (bactericidal) depending on their mode of action and biochemical characteristics [6].

1.1.2. β-lactam antibiotics

The β-lactams are the most used antibiotics and account for more than 60% of all prescribed antibiotics [10]. The β-lactam antibiotics have a common feature of the molecular structure, a four-atom ring known as the β-lactam ring. The β-lactams have a broad antibacterial activity spectrum, including important Gram-positive and Gram-negative pathogenic bacteria [11]. Hundreds of different β-lactams are made based on natural product scaffolds, and they are classified according to their chemical structure [9]. Clinically relevant β-lactams are divided into penicillins, cephalosporins, carbapenems and monobactams as discussed below [11].

a) Penicillins

Penicillins have the β-lactam fused together with a five-membered ring containing a carboxyl group at the C-3 position [11]. Penicillin G and other natural penicillins are mainly active against Gram-positive bacteria, while extended-spectrum penicillins, such as ampicillin and piperacillin also offer modest Gram-negative coverage as well. In comparison with other antibiotics such as aminoglycosides and second- and third-generation cephalosporins, the toxicity associated with penicillin is low [12]. The two penicillins, mecillinam and temocillin, are some of the latest penicillins introduced on the market being approved in the late 70s and mid 80s [4]. Piperacillin (introduced in the early 80s), ampicillin, amoxicillin and ticarcillin are still useful against Gram-negative bacteria, however, must be used in combination with an

appropriate β-lactamase inhibitor [4]. The chemical structure of the penicillin backbone is given in **Figure 1a**.

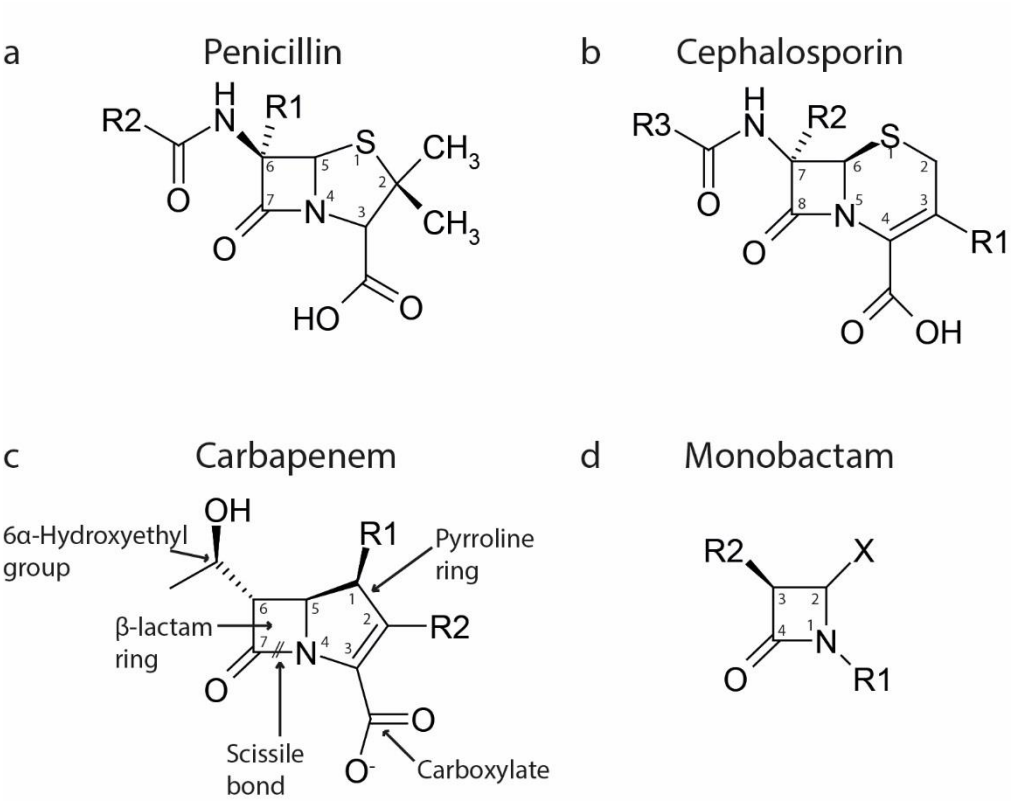

Figure 1: The chemical backbone structures of β-lactam antibiotics; a) penicillin, b) cephalosporin, c) carbapenem and d) monobactam, all with common β-lactam rings. The R groups differs in various antibiotics. The X in the monobactam chemical structure represents α-methyl. Figure adapted from [4].

b) Cephalosporins

The first cephalosporin (**Figure 1b**) compound discovered was derived from the cultures of *Cephalosporium acremonium* in 1948 by the Italian scientist Giuseppe Brotzu who identified the cultures in sewer samples in Sardinia [13]. The cephalosporins are structurally related to the penicillins with a β-lactam ring fused to a dihydrothiazoline ring [12]. Chemical group substitutions give varying antimicrobial activities and pharmacological properties.

After the first discovery of cephalosporin, there have been several groups of cephalosporins divided into five major groups or "generations" according to their antibacterial activity. First generation cephalosporins have good activity against gram-positive aerobic bacteria, such as methicillin-susceptible *Staphylococci* and *Streptococci*, and some Gram-negative bacteria, e.g.: *Proteus mirabilis, Escherichia coli,* and *Klebsiella* species. Second generation

cephalosporins, such as cefuroxime and cefoxitin, have a more extended spectrum of activity against Gram-negative bacteria, e.g.: *Haemophilus influenzae,* and some *Neisseria*, and some are active against Gram-negative anaerobes [14, 15]. Third-generation cephalosporins, like ceftazidime, show activity against many Gram-negative bacteria, and ceftazidime is unique among third-generation cephalosporins because of its activity against *P. aeruginosa, Acinetobacter, Citrobacter, Enterobacter*, and other *Pseudomonas* strains [12, 16]. Third-generation cephalosporins are useful against meningitis caused by *pneumococci, meningococci, H. influenzae, E. coli, Klebsiella*, and penicillin-resistant *Neisseria gonorrhoeae*. The only currently available fourth-generation cephalosporin, cefepime, shows activity similar to ceftazidime against *P. aeruginosa*, and has better activity against *Enterobacter* and *Citrobacter* [17]. There are fifth-generation cephalosporin, ceftaroline and ceftobiprole, with activity against methicillin-resistant *Staphylococcus aureus* (MRSA) and many Gram-negative bacteria [4, 12]. The latest cephalosporin available on the market is the fifth generation ceftolozane, used in combination with tazobactam inhibitor against enteric bacteria and shows antipseudomonal activity [4].

In general, each newer cephalosporin generation show a better activity against Gram-negative bacteria compared to the previous generation, but with a lower activity against Gram-positive bacteria, in most cases.

c) Carbapenems

The first carbapenem β-lactam antibiotic, thienamycin, was developed as a naturally derived product of *Streptomyces cattleya* in the mid-1970s [18]. As thienamycin is chemically unstable, it was later altered to the more stable imipenem. Meropenem, ertapenem and doripenem are all chemically more stable than imipenem. All four carbapenems are widely used [4]. The group of carbapenems have a broad-spectrum activity against most Gram-negative (including *P. aeruginosa*), Gram-positive bacteria and anaerobes, and are currently used as a 'last resort' treatment of infections caused by antibiotic-resistant bacteria [19]. Carbapenems have a β-lactam ring fused to a penicillin-like five-membered ring containing a carbon at C-1 replacing the sulfur in penicillin with a double bond between C-2 and C-3 (**Figure 1c**) [11]. An important feature for carbapenems is their resistance to inactivation by most serine β-lactamases enzymes. Carbapenems can act as inhibitors by forming a long-lived acyl-enzyme intermediate through interaction with the active site serine in many serine β-lactamases [20, 21].

Carbapenems have an affinity for penicillin binding proteins (PBPs), where the targets carboxypeptidases and transpeptidases are used by bacteria to build the cell walls in both Gram-positive and Gram-negative organisms [20]. Tebipenem is of the latest approved carbapenem, however, along with biapenem, are only available in Japan [4].

d) Monobactams

In contrast to other β-lactams, the monobactams do not contain a fused ring system, but named due to its monocyclic β-lactam ring (**Figure 1d**). The β-lactam ring has a linked sulfonic acid group at the position analogous to the carboxylate group in penicillins and cephalosporins [11]. Monobactams are effective against aerobic Gram-negative bacteria (e.g., *Neisseria* and *Pseudomonas*) [4]. The only marketed monobactam is aztreonam [22]. The clinical use of aztreonam is limited due to the third-generation cephalosporins available which have a broader activity spectrum [22]. Aztreonam is structurally similar to penicillins, however, a cross-reactivity with immunoglobulin E (IgE, an antibody produced by the immune system) is absent; consequently aztreonam can be used in patients with IgE-mediated penicillin allergy [22]. Another monobactam is BAL30072, a monosulfactam with similar spectrum of activity as aztreonam, and is currently in phase I trials [4].

1.1.3. Mechanism of action of β-lactam antibiotics

The β-lactam antibiotics have a bactericidal effect since the β-lactam ring is a substrate for the transpeptidase enzymes involved in cell wall biosynthesis [11]. Transpeptidases, also known as penicillin-binding proteins (PBPs), are found in large numbers and usually several in each organism. The peptidoglycan layer is a major component of the bacterial cell wall, and the support for the cell wall is important for maintaining the bacterial morphology [23]. In a rigid cell wall, the osmotic stability is maintained due to the presence of *N*-acetylglucosamine (NAG) and *N*-acetylmuramic acid (NAMA) units. Transglycosidases are linking these glycosidic units. Each NAMA unit has a pentapeptide attached to it, and two D-Ala–D-Ala NAMA pentapeptides are cross-linked by PBPs [24, 25]. The PBPs contain a specific sequence SXXK motif with active-site serine central to the catalytic mechanism. The active-site serine in PBPs forms a covalent acyl-enzyme complex with the stem peptide, and the last D-Ala amino acid is released from the 'donor' peptide (**Figure 2**). In transpeptidases, the D-Ala amino acid carbonyl, is in an ester linkage with the active site serine, and undergoes a nucleophilic "attack" by a second 'acceptor' stem peptide (**Figure 2**). A peptide bridge is created and links the glycan strands.

The ‘donor’ stem peptides are eliminated from the peptidoglycan through hydrolyzing the acyl-enzyme intermediate [26].

The rigidity of the bacterial cell wall is due to this cross-linking of the adjoining glycan strands [27]. The D-Ala–D-Ala of the NAMA pentapeptide is sterically similar to the β-lactam ring, and the β-lactam can mimic the D-Ala-D-Ala in an elongated conformation and act as inhibitor. The PBP active site serine attacks the β-lactam ring carbonyl, instead of the D-Ala amino acid (**Figure 2 (1.)**), opens the β-lactam ring and makes a covalent acyl-enzyme complex. As a result, the PBPs have an acetylated active site serine causing the acyl-enzyme complex to hydrolyze slowly, and preventing further crosslinking reactions (**Figure 2 (2.)**) [26]. The biosynthesis of the cell wall slowly comes to a stop, causing autolysis. The specific details on bactericidal effects of penicillins are still being investigated [28].

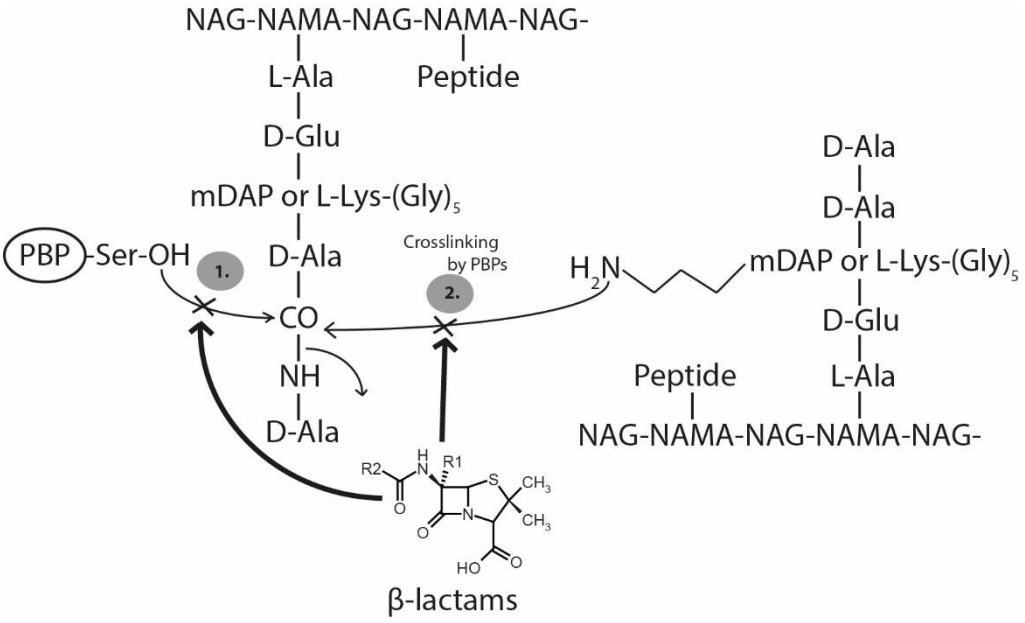

Figure 2: The mechanism of β-lactam antibiotics on the peptidoglycan layer in the bacteria. 1. The β-lactam antibiotic is attacked by the PBP preventing the PBP to bind to the D-Ala amino acid in the NAMA pentapeptides. **2.** As a result, the crosslinking of the two glycan strands by PBP are prevented. The PBPs become acetylated and lose their ability to catalyze transpeptidation, ultimately causing the cells to autolyze. NAG: *N*-acetylglucosamine, NAMA: *N*-acetylmuramic acid, Ala: alanine, Glu: glutamic acid, Lys: lysine, Gly: glycine, mDAP: mesodiaminopimelic acid. Figure modified from [29].

1.2. Antibiotic resistance

Antibiotic resistance happens when the bacteria have the ability to resist the effect of an antibiotic [29]. Bacterial genes can change through random mutations resulting in resistance genes, and bacteria can acquire antibiotic resistance genes from other bacteria. The existence of antibacterial genes might be just as old as the bacteria, 3.5 billion years [30]. A study of microorganisms collected from a 4 million year old cave showed bacterial strains investigated possessing antibiotic resistance genes, with β-lactam-destroying activity [31]. Although antibiotic resistance dates back before modern antibiotics were introduced, the ongoing mass-production and use of antibiotics from the 1940s have given an exceptional selection pressure on bacteria. Fleming warned about the risk of antibiotic resistance in his Nobel Prize lecture already in 1945 [31]. The increase in antibiotic resistance genes in bacteria is due to anthropogenic activities, environmental pollution originating in human activities. Antibiotics are widely used in: (i) animals for growth promotion and disease-prevention; (ii) humans for therapeutic and disease-prevention; (iii) in aquaculture as therapeutics and disease-prevention; (iv) in household pets as therapeutics and disease-prevention; (v) pest control and cloning for plants and agriculture; (vi) in cosmetics and household cleaning products as biocides; and (vii) molecular cloning, as selection markers in research and industry [8]. Each year millions of kilograms of antibiotics are used in treatment of people, animals and agriculture globally [32, 33]. The heavy use of β-lactam antibiotics have resulted in resistant organisms with multiple β-lactamases and other resistance mechanisms, commonly termed “superbugs” [8].

Antibiotic resistance can be natural or acquired. Bacteria evolve, and will naturally acquire resistance, either through random mutagenesis or from outer pressure. Intrinsic antibiotic resistance means that the bacterial species is resistant without any additional alteration of genes [34]. Due to the lack of peptidoglycans, *Mycoplasma* is always resistant to β-lactam antibiotics. Further, many enteric bacterial species like *P. aeruginosa* are intrinsically resistant to hydrophobic antibiotics like macrolides due to the difficulties of penetrating the outer membrane [35]. Acquired antibiotic resistance arise either from mutations (deletions, insertions, inversions or point mutations in relevant genes) or from horizontal gene transfer [34]. The spread of resistance amongst bacteria is possible through mobile genetic elements such as plasmids, naked DNA, bacteriophages or transposons (also known as transposable

elements) [5, 33]. Transposons can contain integrons, which are more complex transposons containing sites for integrating a variation of antibiotic resistance genes and other gene cassettes alongside each other for expression regulated by a single promoter [36]. Integrons have been located in both Gram-negative and Gram-positive bacteria. Plasmids and transposons containing resistance genes generally cause high level of resistance, but when these mobile genetic elements are not present, a step-wise process from low- to high-level resistance can occurs through mutations in the bacterial chromosomes [33, 37, 38]. The initial emergence of penicillin- and tetracycline-resistant *N. gonorrhoeae* were due to this process [5]. Resistance on the chromosome is spread through horizontal gene transfer, such as conjugation, transformation, and transduction. In addition to having a wide variety of ways to spread resistance, bacteria have evolved mechanisms against antibiotic drugs.

1.3. Bacterial defense mechanisms

The widespread use of antibiotics has caused the bacteria to evolve defense mechanisms to resist the lethal effects of antimicrobial agents. Bacteria are becoming more and more resistant, and the activity of important antibiotics is diminishing. This is a growing concern to clinicians today. Diseases and pathogenic bacteria once controlled by antibiotics are returning containing new resistance mechanisms towards available therapies [5]. One example is the re-emergence of tuberculosis, which is now often found to be multidrug resistant [39]. The therapeutic options for the multi-drug resistant pathogens are now so limited that clinicians have to take in use older, previously rejected drugs. The polypeptide antibiotic colistin is an example of such a drug previously not used due to significant toxicity and there were limited data on dosage or duration of the therapy [40]. Better living conditions in the western world result in an increase in population and a growing number of elderly patients. An increasing number of intensive care events, such as surgery and chemotherapy, is putting more immunocompromised individuals at risk of infections [40]. Bacteria have developed a number of different defense mechanisms to fight antibacterial agents. The most common modes of bacterial defense mechanisms are: a) replacement or modification of the drug target, b) reduced uptake of drugs, c) active drug efflux, and d) enzymatic drug inactivation (**Figure 3**, **Table 1**), including antibiotic classes, examples of antibiotics and bacterial targets [29].

Table 1: Available antibiotics with some examples, their target in bacteria and the bacterial mode of resistance towards these antibiotics. The modes of resistance are ranged according to most common defense mechanism for each class of antibiotics, with reference to chapter in this thesis in parentheses and part describing by which process the antibiotics are inactivated. Modified from [6].

Antibiotic class	Example(s)	Target	Mode of resistance (chapter)
β-lactams	Penicillins (ampicillin) Cephalosporins (cephamycin) Carbapenems (meropenem) Monobactams (aztreonam)	Peptidoglycan biosynthesis	Hydrolysis (1.3.4.) Efflux (1.3.3.) Altered target (1.3.1.) Reduced drug uptake (1.3.2.)
Aminoglycosides	Gentamicin Streptomycin Spectinomycin	Translation	Phosphorylation, acetylation or nucleotidylation (1.3.4.) Efflux (1.3.3.) Altered target (1.3.1.)
Glycopeptides	Vancomycin Teicoplanin	Peptidoglycan biosynthesis	Reprogramming of peptidoglycan biosynthesis (1.3.1.)
Tetracyclines	Minocycline Tigecycline	Translation	Monooxygenation (1.3.4.) Efflux (1.3.3.) Altered target (1.3.1.)
Macrolides	Erythromycin Azithromycin	Translation	Hydrolysis, glycosylation or phosphorylation (1.3.4.) Efflux (1.3.3.) Altered target (1.3.1.)
Lincosamides	Clindamycin	Translation	Nucleotidylation (1.3.4.) Efflux (1.3.2.) Altered target (1.3.1.)
Streptogramins	Quinupristin Dalfopristin	Translation	C-O lyase (type B streptogramins), Acetylation (type A streptogramins) (1.3.4.) Efflux (1.3.3.) Altered target (1.3.1.)
Oxazolidinones	Linezolid	Translation	Efflux (1.3.3.) Altered target (1.3.1.)
Phenicols	Chloramphenicol	Translation	Acetylation (1.3.4.) Efflux (1.3.3.) Altered target (1.3.1.)
Quinolones	Ciprofloxacin	DNA replication	Acetylation (1.3.4.) Efflux (1.3.3.) Altered target (1.3.1.) Reduced drug uptake (1.3.2.)
Pyrimidines	Trimethoprim	C1 metabolism	Efflux (1.3.3.) Altered target (1.3.1.)
Sulfonamides	Sulfamethoxazole	C1 metabolism	Efflux (1.3.3.) Altered target (1.3.1.)
Rifamycins	Rifampin	Transcription	ADP-ribosylation (1.3.4.) Efflux (1.3.3.) Altered target (1.3.1.)
Lipopeptides	Daptomycin	Cell membrane	Altered target (1.3.1.)
Cationic peptides	Colistin	Cell membrane	Altered target (1.3.1.) Efflux (1.3.3.)

1.3.1. Replacement or Modification of the Drug Target

A bacterial target can be replaced or structurally modified making the drug unable to bind and stop the activity of the bacterial cell (**Figure 3**). Modification of target can be associated with resistance to nearly any antibacterial agent, as shown in **Table 1**. From a clinical perspective, however, this mechanism is important for resistance to β-lactams, glycopeptides, macrolides, lincosamides, and streptogramines in Gram-positive bacteria and for resistance to quinolones in both Gram-positive and Gram-negative bacteria (**Table 1**) [29]. Changes in the active site of PBPs can reduce the affinity for β-lactam antibiotics, and MRSA is a clinical challenge due to an alteration of PBP2a. The PBP2a has a broad spectrum of resistance to methicillin and all other β-lactam antibiotics used clinically [41].

1.3.2. Reduced Drug Uptake

Hydrophobic drugs enters bacterial cells through the phospholipid layer, while hydrophilic drugs enters through porins, in Gram-negative bacteria. Some bacterial species, such as *P. aeruginosa*, has an outer membrane which is less permeable than other species (approximately 10% of that of *E. coli*) [42], causing the bacteria to be less susceptible to antimicrobial agents. Resistance to various antibacterial drugs can be acquired through mutations causing loss, reduced size, or decreased expression of outer membrane proteins (OMPs) in bacteria (**Figure 3**). In Gram-negative bacteria, such as *P. aeruginosa* and *Enterobacteriaceae*, reduced uptake is a clinical important mechanism of resistance to β-lactams and fluoroquinolones. PBPs are linked to the inner cell membrane and active in the periplasmic space, hence the β-lactams can access the proteins by either diffusion through or directly through porin channels in the outer membrane of the Gram-negative bacterial cell wall [27]. Insertion sequences and point mutations in porin-encoding genes can result in proteins with lower activity, and therefore lower permeability to β-lactam antibiotics and higher level of resistance [43]. This mechanism often gives low-level resistance, meaning that the disruption of porin proteins alone is alone not always enough to cause clinical resistance. In association with other mechanisms of resistance, like enzymatic drug inactivation through the expression of β-lactamase enzymes, porin mutations contribute to the resistant phenotype of multi-resistant clinical strains [29, 43].

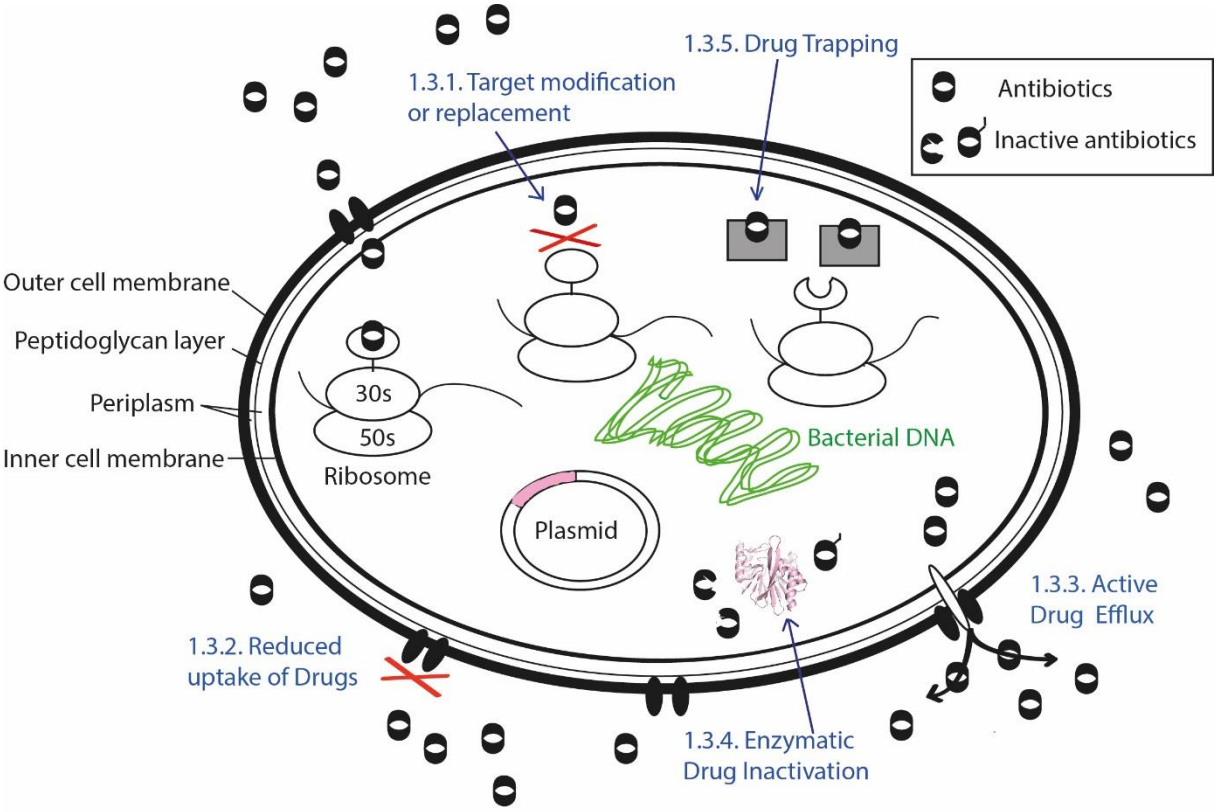

Figure 3: Bacterial defense mechanisms in Gram-negative bacteria. 1.3.1. Drug target modification or replacement is when the antibiotic drug cannot bind to the target to stop the cellular processes. 1.3.2. Reduced antibiotic drug uptake can be through mutation resulting in loss, reduced size, or decreased expression of outer membrane porins (OMPs). 1.3.3. Active antibiotic efflux limits the intracellular accumulation of toxic antibiotics. 1.3.4. Enzymatic drug inactivation is the most common defense mechanism, where production of enzymes able to modify or inactivate the antibiotics, such as β-lactamases. 1.3.5. Antibiotics can be trapped and not be able to act on the bacteria. Figure based on Figure 3 in chapter 1 of [29].

1.3.3. Active Drug Efflux Pumps

Efflux pumps are transmembrane proteins in bacteria capable of exporting metabolites and foreign toxic compounds, including drugs, from the periplasm in cells to the external environment [44, 45]. Drugs are pumped out of the cytoplasm, reducing the effective drug concentration in that compartment, thus preventing or limiting the access of the drug to its target, causing drug resistance (**Figure 3**) [29]. The efflux pumps can be part of an intrinsic or acquired resistance phenotype. An upregulation of efflux pumps can increase the carbapenem resistance given by a catalytically poor β-lactamase, like shown in OXA-23-producing strains [46]. From all bacterial genes, ~5-10% have been estimated to be involved in transport and many of these encode efflux pump proteins. Several different efflux pumps are found in all studied bacterial genomes, indicating their ancestral origin. Therefore, transmembrane

proteins that efflux multiple substrates, have most likely not evolved due to the stresses of the antibiotic era [44, 47].

1.3.4. Enzymatic Drug Inactivation

Some Gram-negative and Gram-positive bacteria are able to express enzymes that modify or hydrolyze the active core of the drug, causing the drug to be unable to bind to its target and lose its antimicrobial activity (**Figure 3**). The enzymes modify either by addition of a chemical group, such as phosphorylation, acetylation, glycosylation or nucleotidylation by aminoglycosides, or by cleavage of the molecule, such as the hydrolysis of β-lactam antibiotics by β-lactamases (**Table 1**). Generally, drug-inactivating enzymes are associated with mobile genetic elements, e.g. as plasmids. The aminoglycoside-modifying enzymes and the β-lactamases are the most widespread and clinically important enzymes [29]. The focus in this thesis is the metallo-β-lactamases, a class of enzymes inactivating through hydrolysis the β-lactam antibiotics, one of the most commonly used antibiotic drugs. These enzymes will be described later in the introduction.

1.3.5. Other Bacterial Defense Mechanisms

Other bacterial defense mechanisms include *target protection*, where the antibiotic target is protected through mutations that reduces the affinity of the antibiotics, or through synthesis of protective molecules covering the target. *Drug trapping* or *titration* is another defense mechanism, where the bacteria increases its production of the drug target or other molecules with drug affinity, resulting in a reduced concentration of free drug at the target site (titration) [29].

1.4. β-lactamases

The main mechanism of resistance towards β-lactam antibiotics in Gram-negative bacteria is the expression of hydrolytic enzymes, β-lactamases, which hydrolyze the β-lactam ring resulting in an inactive drug. The first β-lactamase were reported by Abraham and Chain in 1940 [48], the year before penicillin was put into clinical use [49]. The β-lactamases presumably evolved to degrade naturally occurring β-lactams. Some β-lactamases are believed to have evolved from enzymes (PBPs) involved in cell wall biosynthesis, due to their structural resemblance [23, 50]. Both β-lactamases and PBPs are located in the periplasmic space in Gram-negative bacteria. The PBPs are present on the outer surface of the cytoplasmic

membrane while the β-lactamases are either bound or excreted to the cytoplasmic membrane in Gram-positive bacteria (lacking the outer membrane) [51]. The growing number of β-lactams antibiotics and their massive therapeutic use have contributed to the spread and acquirement of a wide number of β-lactamase genes in pathogenic bacteria [52].

1.4.1. Classification of β-lactamases

Over 1300 unique, naturally occurring β-lactamases are known, and these enzymes have historically been classified according to a several schemes [53]. Today, β-lactamases are mainly divided according to two major classification schemes: (1) the Ambler classes A to D, based on amino acid sequence homology and conserved motifs, and (2) the Bush-Jacoby-Medeiros functional groups 1 to 3, based on substrate and inhibitor profile [53-55], shown in **Table 2**.

Most β-lactamases belong to the serine-β-lactamase (SBL) group, due to an active site serine residue essential for their activity. Ambler classes A, C and D are SBLs according to amino acid sequence alignments and conserved motifs. All three classes have an active site motif of Ser-X-X-Lys, however, the serine may be given different residue numbers [56-58]. In addition, the three classes have two other conserved sequences, the (Ser/Tyr)-X-Asn motif and the Lys-(Thr/Ser)-Gly motif [53]. Ambler class B are the metallo-β-lactamases (MBLs), containing zinc atom(s) in the active site important for their catalytic activity. Metal ion chelators inhibit the MBL enzymes. The MBLs have further been divided into three subgroups due to a wide structural diversity. Structural and functional characteristics of the enzymes were used to divide the MBLs into subgroups B1, B2 and B3. However, after this classification, the structurally dissimilar New Delhi metallo-β-lactamase (NDM-1) was discovered, possessing only 32.4% sequence identity to already established MBLs, resulted in a second B1 subgroup, B1b [59]. Structurally, the subgroups B1 and B3 contain two zinc ions in the active site involved in β-lactam hydrolysis, while subgroup B2 only need one zinc ion in the active site to effectively hydrolyze β-lactam antibiotics [53].

The Bush-Jacoby-Medeiros classification uses functional properties which takes into account substrate and inhibitor profiles [54]. The classification is based on hydrolytic activity against key β-lactam substrates and β-lactamase inhibitors. Inhibitors being the metal chelator ethylenediaminetetraacetic acid (EDTA) to identify MBLs and clavulanic acid to identify group

2 SBLs, while group 1 cephalosporinsases would not respond to clavulanic acid [53]. The Ambler class A β-lactamases are categorized into functional group 2 (except for group 2d), class B β-lactamases belong to functional group 3, class C cephalosporinases are in functional group 1, and class D β-lactamases in functional group 2d. There are several subgroups according to their substrate profile, as shown in **Table 2**.

Table 2: β-lactamase classification schemes according to Ambler classes and the Bush-Jacoby-Medeiros functional groups. The different groups given whether they have penicillinase, cephalosporinase, Extended-Spectrum β-Lactamase (ESBL), carbapenemase, and monobactamase activities with examples of enzymes. The + sign is for activity, the – sign for no activity, while ± means variable within the group. Activity data inconsistent with published substrate profiles are in red. Table modified from [53].

Ambler class	Functional group	Penicillinase activity[1]	Cephalo-sporinase activity[2]	ESBL activity[3]	Carba-penemase activity	Mono-bactam activity	Examples of enzymes
A	**2a**	+	-	-	-	-	PC1
	2b	+	+	-	-	-	TEM-1, SHV-1
	2be	+	+	+	-	+	CTX-M-14
	2br	+	+	-	-	-	TEM-30, SHV-10
	2ber	+	+	+	-	±	TEM-50
	2c	+	-	-	-	-	PSE-4
	2ce	+	-	-[4]	-	-	RTG-4
	2e	+	+	+	-	±	SFO-1, L2
	2f	+	+	+	+	+	KPC-2, SME-1
B	**3a**[5]	+	+	+	+	-	VIM, NDM, GIM, L1
	3b	+	-	-	+	-	CphA
C	**1**	-	+	-	-	-	AmpC
	1e	-	+	+	-	-	CMY-37
D	**2d**	+	-	-	-	-	OXA-1, OXA-10
	2de	+	+	±	-	-	OXA-11, OXA-15
	2df	+	-	+	-[6]	-	OXA-23, OXA-48

[1] + means reported $k_{cat} > 5\ s^{-1}$, while – means reported $k_{cat} < 5\ s^{-1}$. [2] hydrolysis of cephaloridine or cephalothin. [3] Hydrolysis of cefepime, ceftazidime, or cefotaxime. [4] The k_{cat} values are generally ≤ 1 s^{-1}, however resistance to cefepime and cefpirome has been reported. [5] Subclasses B1 and B3 are included. [6] The k_{cat} values are generally ≤ 1 s^{-1}, however resistance to carbapenem is seen.

These groups contain enzymes with hydrolytic activity against extended-spectrum ("e") cephalosporins similar to class A Extended-Spectrum β-Lactamases (ESBLs). However, according to structural features, they belonged to class C (subgroup 1e, the *e*xtended-spectrum AmpC), class A (subgroup 2ce), and class D (subgroup 2de) [53]. The subgroups containing "r" have shown resistance to clavulanic acid, sulbactam and tazobactam inhibitors. The new class D β-lactamase subgroup 2df with carbapenem-hydrolysing ability was introduced to differentiate from the class A serine carbapenemases subgroup 2f, shown in **Table 2**.

1.5. Metallo-β-lactamases

Metallo-β-lactamases (MBLs) hydrolyze an extended spectrum of substrates, including penicillins, cephalosporins and carbapenems. The substrate specificity of MBLs may extend from a narrow range, like the Carbapenem-hydrolyzing metallo-β-lactamase (CphA) enzyme from *Aeromonas hydrophila*, to an extended range, as seen for Verona integron-encoded Metallo-β-lactamase (VIM) variants, which are able to hydrolyze almost all β-lactam classes [60, 61]. In addition to their potent carbapenemase activity, MBLs are resistant to clinically available β-lactamase inhibitors such as clavulanic acid, sulbactam, tazobactam and avibactam [11, 62]. The hydrolytic profile of MBLs do not include the monobactam aztreonam [63], however, the sensitivity of the bacteria towards this group of antibiotics is usually weakened due to the co-expression of serine-β-lactamases [51]. The naming of MBLs is not conserved, some are named according to the bacterial species they was discovered in, e.g. β-lactamase II (BcII) from *Bacillus cereus*, while some are named according to the geographic location they were first found, such as German imipenemase (GIM) and New Delhi Metallo-β-lactamase (NDM).

The first MBL was discovered in the 1960s as a chromosomal enzyme of a non-pathogenic *B. cereus* bacteria, identified to be zinc dependent and inhibited by the metal chelating agent EDTA [64]. In general, the first MBLs described were encoded by chromosomally located genes in non-pathogenic bacteria, and thus were not considered a serious problem for antibiotic therapy [11]. In the 1980s, chromosomally encoded MBLs were found in several pathogenic bacteria such as *Stenotrophomonas maltophilia* [65], *Bacteroides fragilis* [66], various *Chryseobacterium* [67-69] and *Aeromonas* strains [70, 71]. However, in Japan in 1991 the first acquired MBL, an Imipenemase-1 (IMP-1) was discovered in *Serratia marcescens* [72].

Subsequently, additional MBL genes were found on mobile genetic elements in a variety of Gram-negative pathogenic bacteria including Enterobacteriaceae species, *P. aeruginosa* and *Acinetobacter* species [60, 73]. The mobile genetic elements containing carbapenemase genes often carry other genes coding for resistance enzymes towards other classes of antibiotics, such as quinolones and aminoglycosides, resulting in multi-drug resistant bacterial strains [59]. Examples are MBL enzymes such as VIM-2 and IMP-1, found to be encoded as gene cassettes together with other resistance genes in integrons [74, 75]. Integrons are frequently linked with transposons and that can move antibiotic resistance genes within plasmids or on to the bacterial chromosome, hence facilitating movement of resistance genes between plasmids and between bacterial species [61, 76]. Outbreaks of Gram-negative pathogens producing VIM-2, IMP-1 or NDM-1 are observed all over the world. Their ability to hydrolyze carbapenems and their resistance to available inhibitors, are causing clinical difficulty in treatment of infections of bacteria carrying MBLs.

MBL enzymes are synthesized with a native leader sequence in the bacterial cytoplasm, translocated through the cytoplasmic membrane where the leader sequence is cleaved off leaving the resulting protein folded in the periplasm [77]. In the periplasm, the metal availability can be critical at the time of refolding, in order to get the optimal activity *in vivo* [78]. MBL enzymes have a characteristic αβ/βα sandwich fold with the active site between the two αβ-domains. The scaffold is supporting up to six active site residues, which coordinates either one or two zinc ions important for the MBLs catalytic activity [11]. The metal binding motif consists of H/N116-X-H118-X-D120-H/R121, and the zinc biding residues H196, C/S221, and H263, according to the standard BBL numbering scheme [79]. The MBL proteins belong to an ancestral superfamily of metallohydrolases, which include more than 30 000 genes coding for enzymes hydrolyzing thiol esters, sulfuric ester bonds, phosphodiesters, and enzymes which are oxidoreductases [80]. MBLs do not have a bridging aspartate residue as most non-β-lactamase hydrolases, but a hydroxide ion is bridging the two zinc ions [11, 62]. The MBL fold is universal in all living organisms and not exclusive to bacteria [10]. The αβ/βα MBL core fold is widely distributed and supports a range of catalytic activities, including redox reactions [80], nonetheless the enzymes within the MBL fold with β-lactamase activity are restricted to bacteria [10].

1.5.1. Sub-classification of MBLs

Metallo-β-lactamases belongs to the class B of Ambler structural classification scheme of β-lactamases, and are a divergent group. The MBL sequence identity between the subclasses can be as low as 10%. MBLs have been further divided into three structural subclasses based on sequence alignment guided by distinctive structural characteristics within the active sites of each subclass B1, B2 and B3 enzymes [79]. The available X-ray structures facilitated the sub-classification of class B MBLs, by using corresponding secondary structure elements, even due to the low sequence similarity of these enzymes [79]. A selection of crystal structures is given in **Table 3**. The first solved three-dimensional structure of a MBL was the mono-zinc form of the B1 enzyme BcII [81]. Since then, several subclass B1 structures have been solved, such as CcrA [82], the di-zinc form of BcII [83], IMP-1 [84], BlaB [85], VIM-2 [86], VIM-7 [87], SPM-1 [88], NDM-1 [89], GIM-1 [90], subclass B2 enzyme CphA [91], and subclass B3 MBLs, L1 [92], FEZ-1 [93], AIM-1 [94], BJP-1 [95], in addition to other variants of MBLs, have been solved (some shown in **Table 3**).

After the discovery of the first MBL, a wide variety of MBLs have emerged, some chromosome-borne and some found on mobile genetic elements, as shown for selected MBLs in **Table 3**. According to the Lahey β-lactamase database http://www.lahey.org/studies/ there are reported 53 IMP-variants and 46 VIM-variants, for example. However, the website has not been updated since July 2015. Another database for β-lactamases is the National Center for Biotechnology Information, which reports 58 IMP and 51 VIM variants; however, this page does not seem actively maintained. A BLAST (Basic Local Alignment Search Tool) search as per 17.11.16 showed 64 IMP and 51 VIM variants. The different variants of a MBL family, such as the VIMs, are numbered according to their discovery, and have nothing to do with the sequence similarity. E.g. the difference between VIM-1 and VIM-2 is 17 residues, while the VIM-1 and VIM-4 differs with one single residue [96].

Table 3: Metallo-β-lactamase subclasses. The year of discovery or reported of the MBL enzymes are listed with organisms they are found in, whether they are chromosome-borne or on mobile genetic elements, one PDB-ID if crystal structure is available. Not all the variants of MBLs are included in the table, which is modified from [11, 62, 97].

Sub-class	Enzyme	Year	Organism(s)[a]	Location	PDB-ID
B1a	BcII	1966	*B. cereus*	Chromosome	1BMC
	IMP-1	1988	*S. marcescens, P. aeruginosa*	Plasmid or chromosome	1DD6
	CcrA	1990	*B. fragilis*	Chromosome	1ZNB
	VIM-1	1997	*P. aeruginosa, A. baumanii*	Plasmid or chromosome	-
	BlaB	1998	*Elizabethkingia meningoseptica*	Chromosome	1M2X
	IND-1	1999	*Chryseobacterium indologenes*	Plasmid	-
	VIM-2	2000	*P. aeruginosa, A. baumanii*	Plasmid or chromosome	4NQ2
	IMP-2	2000	*A. baumanii, S. marcescens*	Plasmid	4UBQ
	SPM-1	2001	*P. aeruginosa*	Chromosome	4BP0
	VIM-7	2001	*P. aeruginosa, A. baumanii*	Plasmid	4D1T
	GIM-1	2002	*P. aeruginosa*	Plasmid	2YNT
	SIM-1	2003	*A. baumanii*	Chromosome	-
	DIM-1	2007	*P. stutzeri*	Plasmid	4WD6
	TMB-1	2011	*Achromobacter xylobacter*	Plasmid or chromosome	Paper IV
B1b	NDM-1	2006	*K. pneumonia, E. coli*	Plasmid or chromosome	3S0Z
B2	CphA	1991	*Aeromonas veronii*	Chromosome	1X8G
	ImiS	1999	*A. veronii*	NR	-
	Sfh-1	2004	*Serratia fonticola*	Chromosome	3SD9
B3	L1	1991	*Stenotrophomonas maltophilia*	Plasmid	1SML
	GOB-1	2000	*E. meningoseptica*	Chromosome	-
	FEZ-1	2000	*Legionella gormannii*	Chromosome	1K07
	THIN-B	2001	*Janthinobacterium lividium*	Chromosome	-
	Mbl1b	2001	*C. crescentus*	Chromosome	-
	CAU-1	2002	*Caulobacter vibrioides*	Chromosome	-
	BJP-1	2006	*Bradyrhizobium japonicum*	Chromosome	3LVZ
	AIM-1	2012	*P. aeruginosa*	Chromosome	4AWY

[a] The organism listed are the original species where the genes were identified.

1.5.1.1. B1 (a and b) MBLs

Subclass B1 is binuclear Zn(II) monomeric enzymes with a broad substrate spectrum, including all β-lactams except monobactams [84, 98, 99]. Enzymes in subclass B1 have sequence identity higher than 23% [62]. Subclass B1 MBLs include the chromosomally encoded enzymes like *B. cereus* BcII [100], *E. meningoseptica* (formerly known as *Flavobacterium meningosepticum*,

and *Chryseobacterium meningosepticum*) BlaB (β-lactamase B) [67], and *B. fragilis* CcrA [101]. Almost all clinically relevant MBLs are found in the B1 group. These includes enzymes like NDM [59], VIM [75], IMP [102], GIM [103], TMB [104], and SPM-1 (São Paulo MBL) [105]. The NDM-1 MBL is structurally dissimilar to other B1 class MBLs, and has an amino acid sequence identity of 32.4 % with VIM-2. Hence, a second B1 subclass (B1b) was suggested [59]. The phylogenetic tree in **Figure 4** shows the similarity of some acquired B1 MBLs. [59]

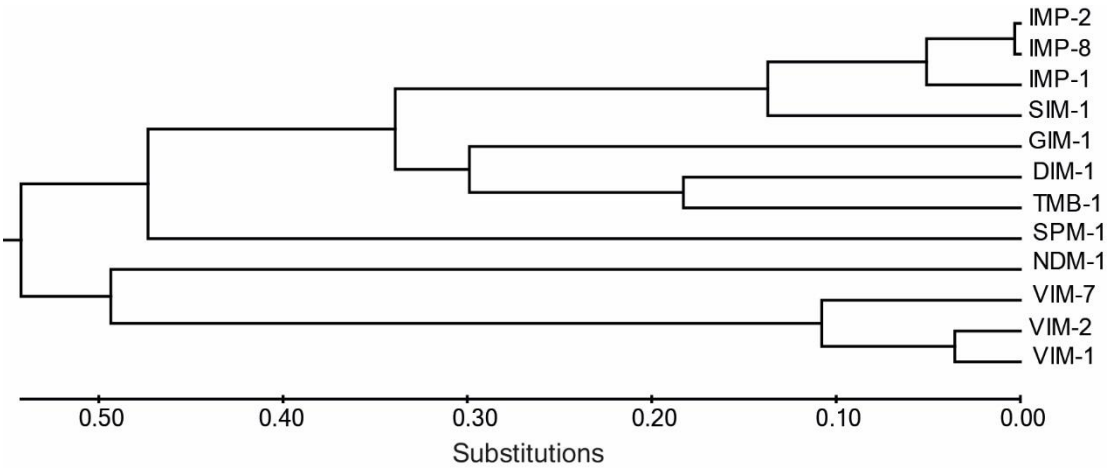

Figure 4: Phylogenetic tree based on the amino acid sequence of some acquired B1 MBLs, selected based on enzymes in our studies and frequently reported enzymes. The tree is drawn to scale, with branch lengths in the same units as those of the evolutionary distances used to deduce the phylogenetic tree. The alignment and the phylogenetic tree were made using MEGA7 software (Kumar, 2016, MEGA7: Molecular Evolutionary Genetic Analysis version 7). The GenBank accession numbers used are: IMP-1, S71932; IMP-2, AJ243491; IMP-8, AF322577; VIM-1, Y18050; VIM-2, AF191564; VIM-7, CAO91763; GIM-1, AJ620678; SPM-1, AJ492820; SIM-1, AY887066; TMB-1, FR771847; DIM, GU323019; NDM-1, FN396876.

1.5.1.2. B2 MBLs

Subclass B2 is a mononuclear Zn(II) monomeric enzyme group effectively hydrolyzing carbapenems [106], while showing weak activity, if any, towards penicillins and cephalosporins. A second zinc ion in the active site of subclass B2 MBLs has a noncompetitive inhibiting effect on the B2 enzymes [106]. Phylogenetically the B2 subclass is closer to B1 than B3 enzymes [107], and the B2 MBLs share 11% sequence identity to B1 subclass enzymes [62]. B2 enzymes are found entirely as chromosomally located in Gram-negative bacteria [107]. Enzymes of the B2 subclass MBLs include *A. hydrophilia* CphA [108], *Serratia fonticola* Sfh-I [109], and *A. veronii* ImiS (Imipenemase from *A. veronii bv. Sobria*) [71].

1.5.1.3. B3 MBLs

Like B1 enzymes, the subclass B3 are binuclear Zn(II) enzymes and have a broad substrate preference including penicillins, cephalosporins and carbapenems. However in phylogenetic analysis the B3 class is the most distant subclass, with low sequence identity and enzymes containing only nine common residues with the other MBL groups [10]. The B3 genes are mostly chromosomally located in Gram-negative bacteria [107]. Subclass B3 genes include chromosome-borne MBLs *E. meningoseptica* GOB [110] and *Legionella (Fluoribacter) gormanii* FEZ-1 [111]. The L1 MBL was reported as being on plasmids in *Stenotrophomonas maltophilia* [112] and Adelaide Imipenemase (AIM-1) was recently reported encoded in a mobile genetic element [113]. The majority of the B3 enzymes are monomeric, like the B1 and B2 enzymes, with exception of the tetrameric L1 enzyme [92].

1.5.2. Structural diversity of MBLs

Several crystal structures of MBLs are available, and despite their low sequence identity, all subclasses share the same characteristic αβ/βα fold, composed of two β-sheets with five or more surrounding α-helices exposed to the solvent, shown for some examples in **Figure 5**. The active site is located at the edge of the ββ sandwich, in all reported structures.

B1 MBL enzymes have in the N-terminal domain incorporated a loop, called L1 loop in this thesis. The L1 loop includes residues 60-66 (standard BBL numbering), which together with some preceding and continuing residues can interact with β-lactam substrates or MBL inhibitors, and it contains many hydrophobic side-chains (**Figure 5A**, **E**). In the native form of the enzyme, the L1 loop is very flexible. As the substrate or inhibitor molecule enters the active site, the loop can bind to trap the molecule in the active site. In addition, the loop is involved in crystal packing, which gives it different conformations [94]. In the IMP-1 enzyme, the loop is moved due to the interaction of e.g. the W64 residue with a hydrophobic substrate side-chain [114]. Binding of inhibitors in the active site stabilizes the L1 loop [84], and the active site can be transformed to a tunnel-shaped cavity. By deleting the L1 loop (residues 61-66) in IMP-1 the enzymatic activity was seriously reduced due to a weaker binding of substrate to the enzyme, except with imipenem as substrate [114]. The only carbapenem substrate tested in the study was Imipenem, and the kinetic parameters were barely affected by the missing L1 loop. One explanation might be that imipenem is a less bulky substrate compared to both penicillins and cephalosporins, which usually include bulky aromatic ring structures. An

exception in the B1 subclass is the SPM-1 enzyme that contains an insertion region of 24 amino acids in an extended α3-α4 region instead of the mobile L1 loop (**Figure 5C**). When considering the SPM-1 sequence identity compared to other MBLs, it shows closest relations to IMP-1 (35.5%) and the B2 enzymes ImiS (32.2%) and CphA (32.1%). As a result, structurally the subclass B1a SPM-1 enzyme is a hybrid between subclasses B1 and B2.

The L1 loop is not present in B2 and B3 subclasses. Instead, subclass B2 CphA enzyme has an extended α3 helix, including residues R140-L161, located close to the active site groove. At approximately W150 residue there is a turn in the helix that lets the α3 to follow the protein surface curvature and contributes to a hydrophobic face, aiding in binding of carbapenem [91]. Hence, the active site of CphA is very well defined and explaining the very narrow spectrum activity of the enzyme. The extended α3 helix is observed in B2 CphA enzyme crystal structure, as shown in **Figure 5G**.

Subclass B3 enzymes possess a mobile loop including residues 151-166, between α3 and β7, able to close the active site [92, 93], presented in **Figure 5I** for the L1 B3 enzyme. L1 MBL crystal structure found this loop extended over the active site, and modelling studies suggested that residues in the loop are involved in contacts with large, hydrophobic substituents on penicillin, cephalosporin and carbapenem β-lactams [92]. Modelling and mutational studies of several residues within this loop, found them to be important in enzyme activity [92, 115, 116]. The L1 monomer contains one disulfide bridge, which is similar to the one found in the FEZ-1 structure [92, 93], whereas AIM-1 carries three disulfide bonds [94]. The subclass B1 and B2 enzymes do not have intramolecular disulfide bridges.

The five different MBL enzymes presenting in **Figure 5** reveals that there are large structural differences within the different subgroups, e.g. as seen for the B1a/b enzymes VIM-2, SPM-1 and NDM-1 loops. All MBLs have mobile loops essential for substrate and inhibitor binding, represented in in the **Figure 5**.

VIM-2 (B1a)

A

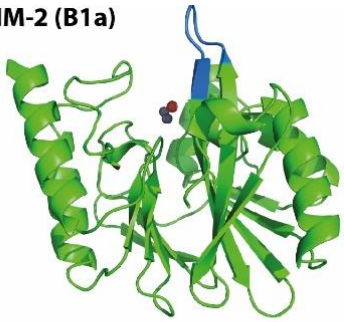

B

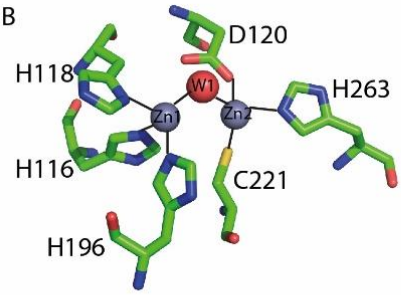

SPM-1 (B1a)

C

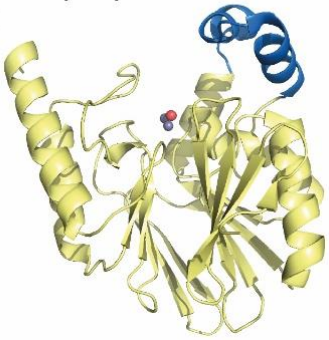

D

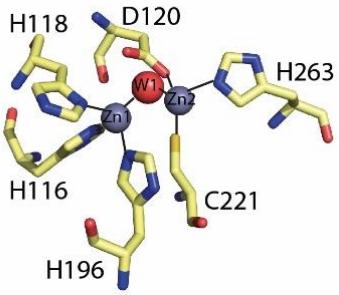

NDM-1 (B1b)

E

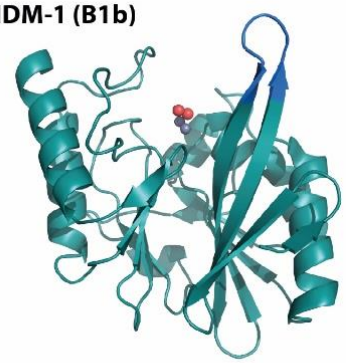

F

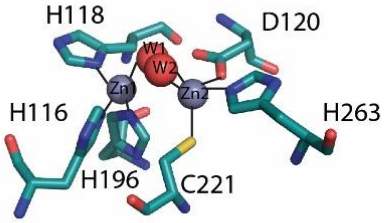

CphA (B2)

G

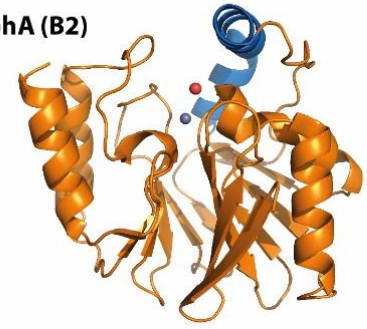

H

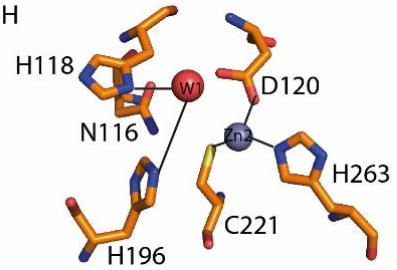

L1 (B3)

I

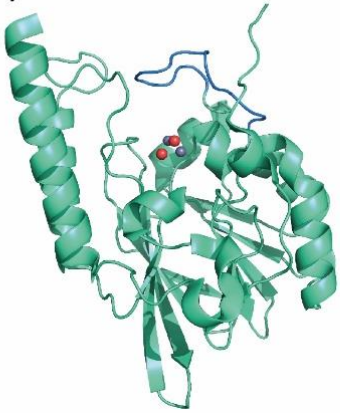

J

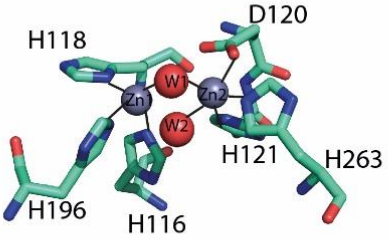

Figure 5 (previous page): Global fold and active site representation of MBLs from all subclasses. The overall fold is preserved in all subclasses. Active site loops important for the catalytic activity are represented in blue. A and B) B1a subclass VIM-2 enzyme (PDB-ID: 4NQ2; green), C and D) B1a SPM-1 enzyme (PDB-ID: 4BP0; yellow), E and F) B1b NDM-1 enzyme (PDB-ID: 3S0Z; dark green), G and H) B2 CphA enzyme (PDB-ID: 1X8G; orange), and I and J) the B3 L1 subclass enzyme (PDB-ID: 2FM6; mint). The overall fold given to the left and the active site with interactions to the right for all five MBLs. The gray spheres show zinc ions and the red spheres show hydroxyl ions/water molecules. The figure was generated using PyMOL [117].

1.5.3. Active site and zinc coordination in MBL subclasses

The MBL active site is located at the edge of a wide shallow groove between two β-sheets and has potentially two zinc ion binding sites, as presented in left panels of **Figure 5**. For the two metal sites (Zn1/Zn2), the zinc ligands are not the same and not fully conserved between the different MBL subclasses. The conserved residues in all MBL classes are H118, D120 and H196. The variation in amino acids in the MBL subclasses involved in zinc ligands are given in **Table 4** together reported with substrate preferences.

The metal binding motif H116-X-H118-X-D120 is conserved in all B1 enzymes. Herein the Zn1 binding site, also known as the 3H site, includes H116, H118 and H196 residues mostly in a tetrahedral coordination sphere including an OH^- ion. The Zn2 binding site, known as DCH site, includes D120, C221, and H263 in a trigonal-pyramidal coordination sphere including one water molecule and the same OH^- ion (**Table 4**, **Figure 5B**, **D**, **F**). One OH^- ion bridges between the two zinc ions Zn1 and Zn2, which act as ligand. Mutational studies of the zinc binding residues in B1 enzymes show that these residues are important for the full catalytic activity [118]. Most B1 enzymes needs two zinc ions in the active site for optimal activity, however, exceptions such as of the B1 enzymes BcII and BlaB have shown to be active in a mono-Zn(II) form [119], and the mono-zinc SPM-1 showed a reduced catalytic efficiency [88]. The sole metal ion in the mononuclear enzymes BcII, VIM-2 and SPM-1, are found in the 3H site [81, 86, 88].

The active site residues of B2 enzymes involved in zinc binding are D120, C221 and H263 hence the same as in the B1 enzymes (**Table 4**). The conserved H116 in B1 and B3 MBLs is in B2 enzymes replaced by an N116 (**Figure 5H**), however, is not likely the reason for the narrow substrate spectrum of B2 MBLs. A CphA N116H mutant showed to remain a low activity towards penicillins and cephalosporins [120]. Spectroscopic studies of a Co(II)-substituted ImiS enzyme indicated that the second metal binding site in B2 enzymes was not the traditional 3H

site in B1 enzymes [121]. The H118 plays a role in the catalytic mechanism (**Figure 6b**) [91, 122], which could explain inhibition when binding of a second zinc ion, as the residue H118 is prevented from performing this role (deprotonating the water molecule (W1) for nucleophilic attack on the β-lactam substrate) when immobilized as ligand of this second zinc ion in the binuclear form of the enzyme [62].

The B3 active site resembles the B1 active site, however, the B1 residue C221 is replaced by H121 in B3 enzymes (**Table 4**), and they have a square pyramidal coordination sphere of Zn2 due to a third water molecule functioning as a fifth ligand [95], as seen in the L1 crystal structure in **Figure 5J**. The active sites are not very conserved in B3 enzymes due to the replacement of H116 residue with a Q116 in GOB enzymes [62]. Most B3 enzymes require two zinc ions in the active site for activity. Despite this, the characterization of GOB-18 revealed that both the mono- and the di-Zn(II) forms were active against penicillins, cephalosporins and carbapenems [69, 123]. The zinc ion in GOB-18 was bound in the Zn2 site, shown in **Table 4**, and a solvent molecule [69]. The GOB-18 differs from GOB-1 with only three residues located far from the active site [123]. The B3 enzyme L1 has shown to be nearly fully active in a mono-Zn(II) form [119, 124], and the binding of the second zinc ion tunes the substrate specificity of the enzyme.

Table 4: Metallo-β-lactamase subclasses with zinc ligands, active site residues and substrate preference. Modified from [53].

Sub-class	Example of enzyme	No. of Zn(II) in active site	Zn1 site	Zn2 site	Substrate preference
B1a	VIMs, IMPs, GIM-1, TMB-1, CcrA, BcII, SPM-1	2	H116 H118 H196	D120 C221 H263	All β-lactams except monobactams
B1b	NDM-1	2	H116 H118 H196	D120 C221 H263	All β-lactams except monobactams
B2	Sfh-1, CphA, ImiS	1	(H118) (H196)	D120 C221 H263	Carbapenems
B3	L1, AIM-1, FEZ-1, GOB-1, BJP-1	2	H/Q116 H118 H196	D120 H121 H263	All β-lactams except monobactams

1.5.4. Catalytic mechanisms of MBL

The MBLs are dependent on zinc ions in the catalytic mechanism. Mechanistic studies of MBLs and MBL crystal structures containing β-lactam substrates in the active site, provide important information for identifying key residues for substrate binding and understanding the catalytic mechanism details. In general, β-lactam hydrolysis occurs in two steps: first, a nucleophilic attack on the carbonyl carbon (C7/C8), causing the C-N amide bond to cleave, and second, the protonation of the bridging nitrogen [125]. Crystallographic structures of MBL enzymes complexed with hydrolyzed substrate in the active site have shown that Zn2 are interacting with the carboxylate moiety present in all β-lactams, on the C3 atom in penicillins and carbapenems and on the C4 in cephalopsorins (**Figure 1**) [91, 116, 126]. In addition, the β-lactam carboxylate interacts with positively charged residues at position 224 or 228 in most B1 and B2 enzymes and residues S221 and S223 in B3 MBLs, which are highly but not strictly conserved residues [91, 116, 126]. VIM-2 and VIM-7 B1 enzymes have a tyrosine and a histidine at position 224, respectively, which indicate that surrounding residues may contribute in the binding of the β-lactams.

1.5.4.1. Reaction mechanisms of dinuclear MBLs

The dinuclear subclass B1 and B3 enzymes uses the two zinc ions, bridged by a hydroxide ion, to coordinate the β-lactam by the C3/C4 carboxylate and carbonyl group. After substrate binding, Zn1 and other enzyme residues polarize the β-lactam carbonyl, making it disposed for attack by the nucleophilic hydroxide ion [125, 127]. The deprotonated D120 residue orients the hydroxide, and the nucleophilic attack by the hydroxide is forming a tetrahedral species, which rapidly collapses into an enzyme bound intermediate (EI^1/EI^2) where the β-lactam nitrogen is anionic [128]. In the last step, protonation of the nitrogen forms the product (P^1/P). However, the identity of the proton donor is unclear, but the most accepted suggestion is a water molecule (W2) bound to Zn2 in the resting state enzyme [129], which replaces the vacant position left by the nucleophilic hydroxide ion by shifting/moving towards the Zn1 ion. This bridging water molecule between Zn1 and Zn2 in the enzyme-intermediate ($EI^{1/}EI^2$) complex assists protonation of the nitrogen and restores the nucleophilic hydroxide in the enzyme-product (P^1+E) complex (**Figure 6A**). The bridging water can be oriented by residue D120 to donate a proton to the intermediate.

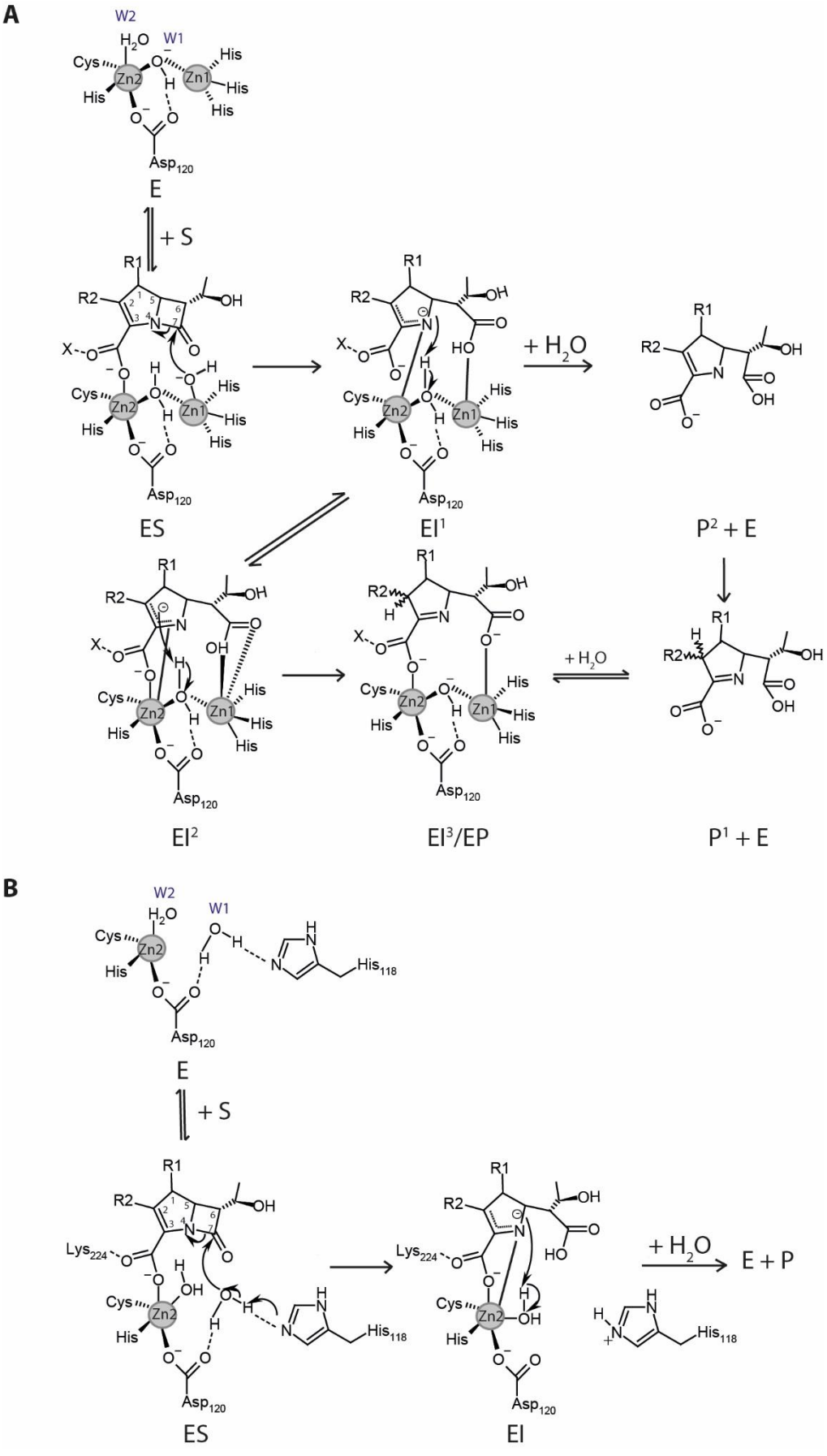
A
W2
W1
Cys
His
Zn2
Zn1
Asp120
E
+ S
R1
R2
X
OH
HO
+ H2O
ES
EI1
P2 + E
EI2
EI3/EP
P1 + E
B
His118
Lys224
E + P
ES
EI

Figure 6 (previous page): Catalytic mechanisms of MBLs on carbapenems. A) The reaction mechanism of di-Zn(II) B1 and B3 enzymes hydrolyzing a carbapenem substrate. The anionic intermediates (EI^1/EI^2) are characterized experimentally [130]. The Zn2 ion is stabilizing the intermediates. The X represents interacting residues 224/228 (mostly K/R) in B1 enzymes and residue S221 and S223 in B3 enzymes. The W1 and W2 are a hydroxide ion and a water molecule, respectively. B) The reaction mechanism of mono-Zn(II) B2 enzymes hydrolyzing carbapenem. W1 and W2 are water molecules based on Sfh-I crystal structures [131] and CphA structures in complex with biapenem and in free form [91]. The D120 residue can orient the bridging water to provide a proton to the intermediate. E, enzyme; S, substrate, I, intermediate, and P, product. Figure modified from [129].

Mechanistic and crystallographic studies of different MBLs have shown that there are differences in the catalytic mechanisms between different β-lactam antibiotics. The accumulation of anionic intermediate(s) stabilized by the Zn2 ion is dependent on the combination of enzyme and substrate [129]. Reaction intermediates have been studied by replacing the native Zn(II) ion with Co(II), giving slightly less active enzymes than the Zn(II) variants. Co(II)-substitution studies on B1 MBLs such as BcII [132], NDM-1 [133], VIM-2 [134], and L1 [135] have provided insight into reaction mechanisms.

Mechanistic studies of penicillin G hydrolysis using Co(II)-substituted BcII enzyme showed the presence of two different enzyme-substrate (ES) complexes [136, 137], giving the first evidence that the active-site metal ions change coordination geometry during the turnover. However, reaction intermediates were not shown in penicillin hydrolysis by the same BcII enzyme. The ES^1 complex with Zn2 bound to one of the oxygens, while in ES^2 the Zn2 is bound to both oxygens of the β-lactam carboxyl group (not in Figure 6)[129]. The structures and interactions of the two different ES complexes were based on the crystal structure of the enzyme-product (EP) complexes of penicillins and NDM-1 [99, 126], and the spectroscopic data of BcII enzyme [138].

Studies on hydrolysis of the cephalosporin-like reporter substrate nitrocefin show that reaction intermediates accumulates [128, 133, 139, 140]. The enzyme-bound intermediate is anionic with a negatively charged nitrogen atom after cleavage of the β-lactam amide bond and metal-bound [135]. The active mono-Zn(II) B3 GOB enzyme has the zinc ion bound in the Zn2 site (**Table 4**), and showed an accumulation of the intermediate [141]. The importance of the Zn2 ion in the catalysis was demonstrated in NDM-1 where the effect on the rate of intermediate formation was significantly reduced for a Cd(II) substitution. This implies that a Zn2 ion plays a major role in electrophilic activation of substrate and stabilization of the intermediate [133]. The mono-Zn(II) forms of B1 and B3 enzymes with the zinc bound to the

Zn1 site are not able to stabilize the anionic intermediate, shown in studies of the a mono-Zn1 form of L1 (B3 enzyme) [142] and the B1a Bla2 enzyme [143]. The dynamic loops around the active site are also affecting the accumulation of intermediates. As described above, the loop L1 (residues 60-66) in B1 enzymes is a mobile loop affecting the catalysis as it closes over the active site when substrates or inhibitors are binding [144]. Taken together, the presence of a zinc ion at the Zn2 site, the residues in mobile loops, the subtle changes between different MBL enzymes are contributing to stabilize the anionic intermediate.

Imipenem hydrolysis of di-Zn(II) BcII revealed a reaction intermediate, while the di-Co(II) BcII enzyme resulted in accumulation of two reaction intermediates, EI^1 and EI^2 (**Figure 6A**) in a branched mechanism [130]. The nucleophilic attack of the hydroxide ion results in an open-ring β-lactam structure with a negative charge involving the N4 and C3 atoms of the substrate. A direct interaction with Zn2 is stabilizing the anionic intermediate, EI^1. Next, either the EI^1 N4 can be protonated forming tautomer P^2, which rapidly will be tautomerized to P^1 in an aqueous environment, resulting in a mixture of the α and β diastereomers, or the EI^1 can remain in the enzyme pocket, with the negative charge on the C3 atom, giving EI^2. The metal-bound water can protonate the EI^2, resulting in an EI^3 or EP adduct as shown in **Figure 6A** [129]. The formation of a stable anionic intermediate was supported by studies of meropenem hydrolysis in NDM-1 [145] and SPM-1 [146] B1 enzymes.

1.5.4.2. Reaction mechanisms of mononuclear MBLs

Subclass B2 enzymes show a different reaction mechanism compared to dinuclear B1 and B3 enzymes, as proposed through mechanistic studies of the monozinc enzyme ImiS [122], and crystal structures of Sfh-I [131] and CphA [91]. Pre-steady state measurements of Sfh-I hydrolyzing imipenem revealed the presence of temporary intermediates during the catalytic cycle [129]. Regardless of the differences between B2 enzymes, carbapenem hydrolysis occurs through a reaction intermediate involved in changes in the metal site geometry, Zn2 site, in these enzymes. The Sfh-I crystal structure showed that a water molecule (W2) completed the Zn2 coordination sphere [131], similar to the position of the amide nitrogen of biapenem bound in the CphA crystal structure [91]. The distance between the Zn2 and the water (W1), being 2.24 Å, thus consistent with a water molecule rather than a hydroxide ion. A second water molecule (W2) occupies the Zn1 site, and is involved in a network of hydrogen bonds,

showing a strong interaction with residue H118 suggesting that this histidine residue activates the W2 [91].

The conserved positively charged residue in position 224, found in all B2 enzymes, assists the substrate binding to the C3 carboxylate group guided by the Zn2 ion. W1 is expected to perform the nucleophile attacking the β-lactam, causing electronic rearrangement which opens the β-lactam ring forming an anionic intermediate (EI in **Figure 6B**) [131], an analogue to the proposed mechanism for dinuclear MBLs (**Figure 6A**).

Overall, the main difference between the mechanism of dinuclear B1 and B3 MBLs and the mononuclear B2 enzymes are that B2 MBLs do not involving the Zn2 ion in the activation of the water nucleophile. On the other hand, despite the difference in metal site content and active site topologies, the role of Zn2 in binding of substrates and the stabilizing of the anionic intermediate in B2 enzymes resembles the role Zn2 in the B1 and B3 enzymes [129].

1.5.5. Studies of B1 MBL residues

MBLs of B1 subclass contain a conserved active site with six residues binding the zinc ions, known as first sphere residues, as shown in **Figure 5** and **Table 4**. The next layer of residues outside the active site is generally termed second sphere residues. B1 MBLs that are having the same scaffold and metal binding site, show diverse substrate specificities, indicating that the substrate profile are shaped by mutations in loops around the active site or in the second sphere residues [96]. Many site directed mutagenesis and crystallographic studies of MBLs have focused on the analysis of active site residues and the role of surrounding loops and the importance of their residues in binding of substrates or inhibitors [114, 147, 148]. Still, the detailed mechanism for why different B1 enzymes demonstrate very different substrate profiles is unknown [148].

1.5.5.1. Zinc-binding residue analysis

For the first sphere zinc binding residues, the histidines are highly conserved. Substitution of zinc binding residues, such as replacing each of the histidine residues individually in Zn1 site, H116, H118 and H196, with a serine amino acid in BcII resulted in lower catalytic activity, but the zinc affinity was, however, unaffected [118]. The enzyme kinetics showed as expected, a poorer binding for the serine mutant, due to a higher flexibility of the substrate in the active site due to the absence of a histidine residue. H116 substitution to asparagine or alanine

studied in CcrA showed that the alanine mutant had lower activity towards cephalosporins while the asparagine showed reduced k_{cat} for benzylpenicillin and imipenem, but could bind both zinc ions [149]. Alanine mutants of histidine residues (H116, H118, H196, H263) in IMP-1 gave the same effect on the activity, and the zinc content indicated the presence of one zinc (not two) in the active site [150]. Substitutions of H263 to a serine residue in the Zn2 site of BcII and IMP-1 were more deleterious to the activity than substitutions of histidines from the Zn1 site [118, 150]. Thus, these data point to Zn2 being more important for catalysis than Zn1.

The active site residue C221 substituted to alanine or serine amino acids in several enzymes show to drastic decrease in the hydrolytic rate in conditions with low zinc concentration [118, 149, 150]. BcII and IMP-1 mutants showed increase in rate of hydrolysis as excess zinc was added, while this was not studied for the CcrA mutant. Saturation mutagenesis of C221 in IMP-1 indicated that most substitutions destabilized the enzyme, while the mutants C221D and C221G expressed well and showed catalytic activity against β-lactams [151]. Molecular modelling indicate steric constraints on position 221, and the C221 mutants may alter the positioning of Zn2, showed in the reduced catalytic efficiency of the mutants compared to the wild-type [151]. Hence, the Cys residue is suggested to play a crucial role in maintaining the stability and the catalytic activity of the mononuclear enzyme and not for the dinuclear enzymes [118].

The residue D120 is binding the Zn2 ion in the active site. In addition, it is involved in the catalytic mechanism in all MBLs through hydrogen binding to the bridging hydroxide nucleophile between Zn1 and Zn2. The importance of the active site residue D120 was demonstrated in the IMP-1 enzyme [147]. Substitution of the D120 residue in B1 enzymes have resulted in a significant reduced catalytic activity, such as the D120N in BcII where the activity was reduced by more than a 100 fold [118]. The second zinc ion was still able to bind in BcII mutant. The D120 residue is directly involved in binding of penicillin and cephalosporin substrates in NDM-1 [99, 152] and inhibitor binding in VIM-2 [153, 154].

1.5.5.2. Second sphere residue analysis

Second sphere residues are surrounding the active site. Although not directly involved in binding of the zinc ions, these residues are involved in a network of hydrogen bonds below the active site, which can contribute to the geometry of the zinc ions [88]. The loops defining

the active site are shown in VIM-2 including loops L1 and L3 containing second sphere residues, in **Figure 7**.

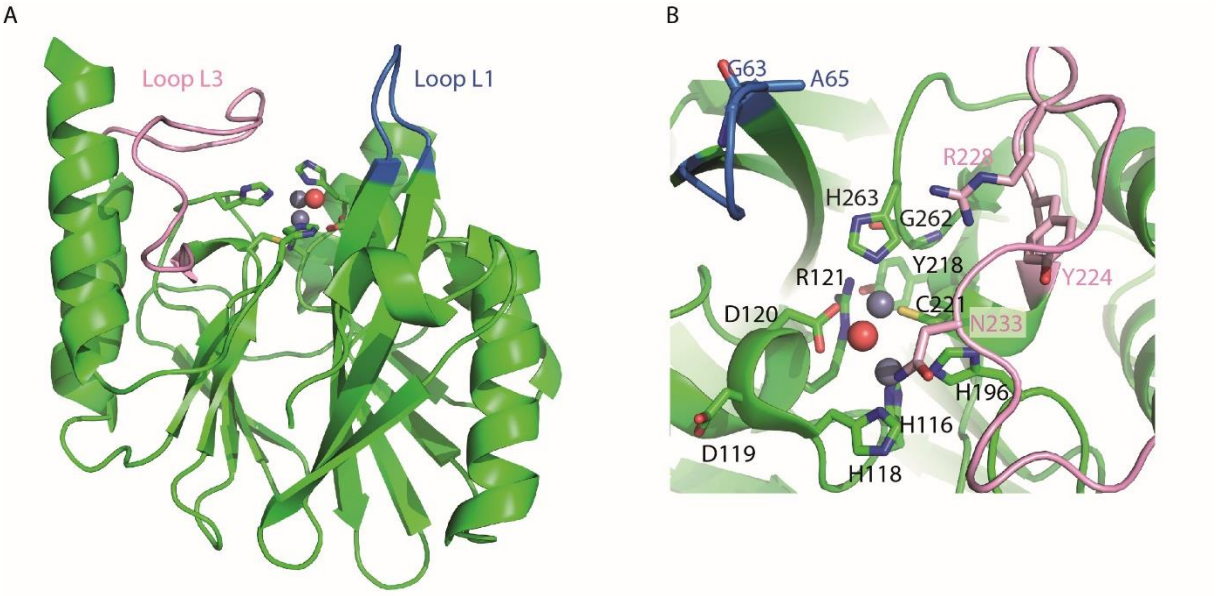

Figure 7: VIM-2 L1 and L3 loops and active site. A) The VIM-2 crystallographic structure (PDB-ID: 4NQ2) with loops L1 and L3 highlighted in blue and pink, respectively. The zinc-binding residues are shown. B) The zinc binding residues and location of the studied second sphere residues are shown. For glycine residues at position 63 and 262 main chain atoms are depicted. The active site zincs are given in grey and bridging hydroxide ion in red.

The L1 loop

Most B1 MBLs have L1 loop consisting of residues 60 to 66, shown to be involved in substrate binding especially when including some extended residues. The exception is the SPM-1 enzyme as previously described. The L1 loop show greater flexibility compared to the rest of the molecule, as shown by NMR characterization of BcII [155], and many crystal structures have an undefined L1 loop region due to the lack of well-ordered electron density depending on the crystal packing and symmetry interactions [156]. Mutational studies in IMP-1 have shown that the G65 residue is essential for catalytic activity [147]. The G65 and G63 are located in the L1 loop, contributing to the β-hairpin turn at the end of the loop. The glycine residues are suggested to be important for the structure and function of the IMP-1 enzyme, as changes may prevent antibiotic hydrolysis due to destabilization of the β-hairpin, thus, destabilization of the whole protein [147]. Crystal structures of NDM-1 with hydrolyzed benzylpenicillin, methicillin, oxacillin [99], and cephalosporins [152] in the active site shows that L1 loop residue G63 are involved in the substrate binding. These two glycine residues in the L1 loop are not conserved in all B1 MBLs, as some MBLs only have one glycine residue, e.g.

VIM-2 and VIM-7 [87]. However, not all residues in the L1 loop are significantly affecting the hydrolysis or binding of substrates [157]. The role of loop L1 studied in BcII showed that the removal of the loop had a significant effect on hydrolysis of penicillins and cephalosporins, while the imipenem hydrolysis was not altered significantly [114]. IMP-1 crystal structures with inhibitor bound to the active site show that residue W64 side-chain are interacting edge-to-face with the aromatic group of the inhibitor [84, 158]. Other loop residues can contribute with e.g. hydrophobic interactions with inhibitors bound to the active site, as shown in crystal structures of VIM-2 to a triazolylthioacetamide inhibitor or fragments with residues F61 and Y67 [154, 159]. Hence, several L1 loop residues are important for both substrate and inhibitor binding in studied MBL enzymes.

The L3 loop

The residues in the MBL loop L3 (residues 223-240) have been shown to be involved in binding of substrates or inhibitors. Crystal structures revealed that residues K224 and N233 are involved in binding of β-lactam substrates or inhibitors in NDM-1 [99, 126, 152] and inhibitors in IMP-1 enzymes [84, 158, 160-162]. Based on mutagenesis experiments K224 is thought to have a critical role for the enzyme function [163, 164]. IMP-1 K224 mutants showed significant reduced catalytic efficiency towards benzylpenicillin, cefoxitin, cefuroxime, cephalothin and imipenem [164]. Many B1 MBLs have a K224 residue, which guides substrate binding by interaction with the conserved carboxylate group on C3/C4 of the antibiotics, together with the Zn2 site interaction [84, 125]. However, VIM enzymes do not display a lysine residue at position 224. The nearby R228 residue found in most VIM enzymes, are thought to replace to role of K224 of guiding the substrates carboxylate group [86, 87, 153]. The L224 is important for substrate binding, as shown in VIM-26, a H224L mutation compared to VIM-1 [165]. Due to the L224 and S228 residues, the VIM-26 R2 drug binding site is more open than in VIM-2 and VIM-7 and naturally charged [165]. The study of VIM-13 mutations of the single mutants L224H and R228S and a double mutant L224H/R228S in comparison with VIM-1 (H224, S228), revealed lower minimum inhibitory concentration (MIC) values for VIM-13 and the single mutants with cephalosporins, concluding that the effects of the two positions are related [166].

Residue R228 is also a part of the L3 loop (**Figure 7**) and is involved in binding of inhibitor or inhibitor fragment in VIM-2, as revealed by different crystal structures of VIM-2-inhibitor

complexes [159, 161, 167]. The substitution in VIM-2 of arginine 228 to leucine (i.e. resembling VIM-24) was suggested to relieve steric clashes and enhance resistance to cephalosporins [168]. This and other studies, support that an arginine at position 228 in VIM enzymes would form a more open active site and more easily hydrolyze ceftazidime and cefepime substrates, however the hydrolysis of imipenem was unaffected by this modification as seen in MIC results of VIM-2 and VIM-23 [169].

The L3 loop residue N233 is involved in inhibitor binding in VIM-2 [154, 159, 161, 167] and BcII enzymes [161], as also found for NDM-1 and IMP. The majority of MBLs (~67%) contain an asparagine at the 233 position [170]. Substitution to each of the 19 possible amino acids in IMP-1 showed that the kinetic parameters of the enzyme were significantly altered, although the mutants could still hydrolyze a broad range of substrates [170]. An IMP-1 N233A mutant hydrolyzed ampicillin, nitrocefin, cefotaxime and cephaloridine more effectively compared to IMP-1 wild-type [163]. Alanine and aspartic acid mutants at position 233 in IMP-1 revealed that hydrolysis of benzylpenicillin and cephalothin was not affected, while the catalytic efficiency of cefuroxime, cefoxitin and imipenem were reduced [164]. The asparagine at position 233 is suggested to be crucial for imipenem resistance, and since the majority of MBLs have an asparagine at this position, the residue seems to have been selected by natural evolution in MBLs [96].

Other second sphere residues

Residue 119 is located in the conserved H116XH118XD120 motif of three zinc binding residues, the Q119 residue in NDM-1 is involved in binding of penicillin and cephalosporin β-lactams [99, 126, 152], and S119 in IMP1 is binding to a 3-aminophtalic acid inhibitor [160]. Substitutions of residue 119 studied in NDM-1 show a reduced MIC for all substrates tested. The Q119D mutant resulted in the most reduced MIC compared to the wild-type and other Q119 mutants, and the zinc content was reduced by 70% compared to the wild-type NDM-1 [171]. Hence, residue 119 may be important in maintaining the orientation of its neighboring zinc binding residues H118 and D120.

Remote mutations of residues 121, 218 and 262 were investigated in IMP-1 and IMP-6 (a G262S mutation of IMP-1), and the results could be explained by dividing the β-lactams in two types according to the molecular structures. Type I substrates contain R2 electron donor group

(nitrocefin, cefotaxime, and cephalothin), while type II substrates contain axial methyl groups (ampicillin and benzylpenicillin) or positively charged R2 side-chains (ceftazidime and imipenem). Type I substrates were hydrolyzed equally well by IMP-1, IMP-1 G262A and IMP-6 (S262), and more effectively by other mutants, whereas all mutants revealed less efficient hydrolysis of type II substrates. The G262A and F218Y mutants showed good folding properties, high MIC values, and broad substrate spectra [172]. Although residue 218 is conserved in IMP-1 through IMP-12 [173], substitutions were tolerable and did not affect the catalytic efficiency significantly.

Overall, substitutions of residues in the Zn2 site seems to have a significant impact of the catalytic activity of all MBL enzymes and binding of the zinc ion, while residues at Zn1 site shows reduced catalytic efficiency and zinc affinity not significantly altered. Mutations of second sphere residues and loop residues contributes in tuning the substrate specificity of the MBL enzymes. However, the importance of the different residues seems to be dependent on the complete enzyme sequence in whether they are essential for some substrates and not for others. The information of the MBL structures and the residues important for substrate specificity can provide knowledge of inhibitor binding in MBLs. Through this, certain MBL residues can be targeted for creating specific MBL inhibitors in the fight against these multi-resistant bacteria.

1.6. Using inhibitors as a strategy to overcome antibiotic resistance

The development of β-lactamase inhibitors for combination therapies with β-lactam antibiotics has been a successful approach to restore the β-lactam activity against pathogens producing β-lactamases [174]. Especially important are agents with activity against Gram-negative bacteria, as resistance among these organisms is an urgent clinical problem [175]. As mentioned earlier, some penicillins and cephalosporins are useful only on combination therapies with β-lactamase inhibitors. Combination therapy β-lactams/β-lactamase inhibitors have proven effective, such as the ceftolozan/tazobactam and ceftazidime/avibactam combinations [174]. However, these combination therapy are efficient towards SBLs and ineffective against MBLs. A wide variety of compounds with MBL inhibitory potential have

been reported (**Table 5**), and inhibitors have been identified from either natural product sources or from chemical synthesis.

Table 5: Selected MBL inhibitors studies. The type of inhibitor, name of representative compounds or derivatives, MBL enzyme used experimentally, and reference to studies given in the table. Table modified from [60] and extended.

Inhibitor type	Compound	Enzyme tested	Ref
Thiol	Mercaptoacetic acid	IMP-1	[176, 177]
	2-mercaptopropionic acid		
	2'-mercaptoethyl derivative	BcII	[178]
	Mercaptophosphonates	VIM-4. CphA, FEZ-1	[179]
	Mercaptocarboxylates	IMP-1, VIM-2	[84, 153]
	Thiobenzoate derivative	IMP-1, CcrA	[180]
	2-*para*-Thiomandeli acid	BcII	[181]
	Captopril and derivatives	BcII, CphA, VIM-2, IMP-1, NDM-1	[161, 182, 183]
	Bisthiazolidines	NDM-1, IMP-1, BcII, L1, Sfh-I	[162, 184]
Thioesters	Morpholinoethanesulfonic acid	CcrA	[185]
	SB214751/4752/3079/6271/6968	BcII, CfiA, L1, CphA	[186]
Triazoles	Arylsulfonyl-NH-1,2,3-triazole, Triazoleylthioacetamide	VIM-2	[154, 187]
Tricyclic natural products	SB238569	BcII, IMP-1, CcrA	[188]
Trifluoromethyl alcohols and ketones	D-alanine derivatives	BcII, L1	[189]
Sulfonic acid derivatives	N-arylsulfonyl hydrazones	IMP-1	[190]
Succinic acid derivatives	2,3-(S,S)-disubstituted succinic acid	IMP-1	[158]
Biphenyl tetrazole	Biphenylmethyl derivatives	IMP-1, CcrA	[191, 192]
Cysteinyl peptide	D-Phenylalanine derivative	BcII	[193]
1-β-Methyl carbapenem	J-110, 441	IMP-1, CcrA, L1, BcII	[194]
Penicillin derivatives	Penicillinate sulfone	L1, BcII	[195]
Thioxocephalosporin	Thioacid	BcII	[196]
Pthalic acid	Pthalic acid derivatives	IMP-1	[197]
Phenazines	SB212021, SB212305	L1, CfiA, BcII	[198]
Pyridine carboxylates	Dithioacid	CcrA, L1	[199]
Benzohydroxamic acid	2,5-substituted benzophenone hydroxamic acid	FEZ-1, IMP-1, BcII, CphA, L1	[200]
Peptides	Peptide derivatives	L1	[201]
Pyrroles	Pyrrole derivatives	IMP-1	[202]
Metal chelators	NOTA and DOTA	NDM-1, NDM-4, VIM-1, IMP-1, IMP-8, VIM-2, IMP-7	[203] [204]
	Aspergillomarasmine A		[205]
	ME1071		

Inhibitors involved in metal chelation have shown to be effective MBL inhibitors, however, a common side-effect is potent inhibition of mammalian zinc-containing enzymes such as angiotensin-converting enzymes, mammalian carboxypeptidases, or alcohol dehydrogenase [62, 206]. Compounds containing thiol groups are among the most tested inhibitors due to the promising results [207, 208]. Thiol-based mercaptocarboxylic acids are evaluated successfully

against several MBLs [27, 161, 167], and are an interesting starting point for further inhibitor optimization. Another challenge is to find broad spectrum inhibitors against several clinically relevant MBLs. This due to bacteria with already acquired β-lactamase resistance genes; more easily acquire additional resistance genes, forming genetic resistance islands [209]. In this case, an inhibitor targeting one MBL enzyme could be effectiveless due to the presence of other MBLs. However, the currently reported MBLs inhibitors are effectively inhibiting one or two enzymes and show less activity against others. Examples of experimentally promising inhibitors with good *in vitro* results are given in **Table 5**. In our research, we have searched for inhibitors through both synthetically made thiol-based compounds and from natural sources. The hits might lead to an efficient compound to block the β-lactamase activity.

1.6.1. Synthetically made thiol-based inhibitors

Large fragment-based screening using IMP-1 revealed hits containing thiol groups [210]. Thiol compounds are promising candidates as MBL inhibitors with the potential to coordinate the zinc ions in the MBL active site, due to the thiophilic nature of zinc, and thereby preventing β-lactam hydrolysis. A number of crystal structures of thiol-containing inhibitors in complex with B1 enzymes are reported [84, 161, 162, 208], and show that the sulfur atom of the thiol group replaces the catalytically important bridging hydroxide ion [10, 84, 162]. Through this coordination of active site zinc ions the thiol-containing compounds inactivate a variety of MBLs (**Table 3**) see e.g. [127, 179, 181, 211]. Structural analysis of inhibitors containing thiol groups complexed with MBLs suggested that the thiol group chelates the zinc ions of the B1 enzyme L1 and the B2 enzyme CphA [208]. Captopril is a thiol-containing small molecule targeting the zinc ion-utilizing human angiotensin-converting enzyme, used to control high blood pressure. Captopril has shown to inhibit a variety of MBLs [161], and used for comparison of potency of new inhibitors [159]. Thiol-containing inhibitors studied in MBLs such as NDM-1, VIM-2 and IMP-1 shows effective inhibition [161, 162, 212], thus optimization of thiol containing inhibitors may provide inhibitors able to inhibit a broader spectrum of MBLs.

1.6.2. Marine bioprospecting searching for new inhibitor scaffolds

Nature has been the source of many of the most effective medicines, such as the discovery of penicillin, and has been the starting point of further developed medicinal products [213]. Approximately two thirds of all commercial available pharmaceuticals originate from natural

products [214]. The oceans cover more than 70% of the Earth's surface, however, the marine organisms have not been adequately explored. Marine bioprospecting is defined as the search for bioactive molecules from marine sources containing new, unique properties [215]. The Barents Sea is part of the Arctic Ocean, and located of the northern coasts of Norway and Russia. The Barents Sea has a highly shifting environment due cold water from the Arctic and warmer temperate water from the Gulf Stream. This sea is the home to an enormous biodiversity, with marine microorganisms well adapted to extreme conditions. The organisms in the arctic environment are low-temperature extremophiles [216]. These extremophiles have evolved the ability to adapt to low temperatures in order to survive the cold environment that organisms further south do not have to face [217]. The marine microorganisms may have developed specific defense mechanisms crucial in order to survive, e.g. such as producing proteins providing protection against microbial intruders [218, 219]. These marine organisms may have evolved the expression of molecules used to combat threatening organisms, which humans may be able to utilize. Isolating of active compounds from marine extracts can provide a starting point of new active inhibitors to β-lactamases, as tested in a small-scale pilot project in this thesis. Through several purification steps of the marine extract, one single compound may inhibit MBL activity, aiming at identification of a chemical scaffold, which can be further optimized and synthesized to achieve a potent broad-spectrum MBL inhibitor.

2. Background and aim of the study

The project was funded by the Research Council of Norway, through the FriMedBio 2011 grant number 213808. The purpose was to study and gain insight into enzymes involved in antibiotic resistance and metallo-β-lactamases (MBLs) in particular. One way to restore the function of the β-lactam antibiotics is to find MBL inhibitors, and the need to find such a compound is urgent. New synthetically designed inhibitors were tested in this study.

This study had two different aims. The first objective was to investigate the importance of different residues located in or close to the active site of selected MBLs using enzyme kinetics studies, thermostability measurements, cellular assay, modelling studies, *in silico* calculations or crystallography. The focus was on following objectives:

- Investigate the effect of mutations at H224, F218 and D120 in the divergent VIM-7 MBL through enzymatic characterization, and determination of the three dimensional structures.
- Study the importance of residues W228 and Y233 in GIM-1 MBL, by creating eight mutants, through biochemical and structural characterization.
- Determine the three-dimensional structure of TMB-1 MBL, study effects in TMB-2, with a S228P mutation compared to TMB-1, and the role of residue E119 through mutations using enzyme kinetic studies.

The second objective was to search for MBL inhibitors in synthetically made compounds. The goal was to find inhibitors targeting a wide spectrum of MBLs.

- Investigate the inhibitory effect of thiol-based compounds against the MBLs, VIM-2, NDM-1, GIM-1 and TMB-1 using enzyme inhibition assay, SPR, whole cell assays and MIC.
- Solve three-dimensional structures of VIM-2 bound to inhibitors.

3. Summary of papers

3.1. Paper I

His224 Alters the R2 Drug Binding Site and Phe218 Influences the Catalytic Efficiency of the Metallo-β-lactamase VIM-7

Hanna-Kirsti S. Leiros, **Susann Skagseth**, Kine Susann Waade Edvardsen, Marit Sjo Lorentzen, Gro Elin Kjæreng Bjerga, Ingar Leiros, Ørjan Samuelsen (2014) Antimicrobial Agents and Chemotherapy. **58**(8): p. 4826-4836

Metallo-β-lactamases (MBLs) are threatening the function of our most used antibiotics, the β-lactams, including carbapenems, one of the last line drugs used for treatment of bacterial infections. One way of understanding bacterial resistance mechanisms to β-lactams is through enzyme characterization and mutational studies of MBLs involved in resistance. Verona integron-encoded MBLs-7 (VIM-7) is the most divergent variant within the important VIM group of MBLs. In this paper, three different site-directed mutations of VIM-7 were made, D120A, F218Y and H224Y, in order to investigate the residues' effect on the activity and stability of VIM-7. The D120A mutant showed no enzymatic activity, was less thermostable than VIM-7 and the crystal structure revealed only one zinc ion in the active site. The F218Y mutant showed an increase in catalytic efficiency compared to VIM-7, a slightly higher thermostability, and the crystal structure revealed establishment of a hydrogen-bonding cluster. The H224Y mutant resulted in an increased enzymatic activity, a significant higher thermostability compared to VIM-7. This was due to two additional hydrogen bonds in the active site of the VIM-7 H224Y crystal structure. The H224Y mutant in particular resulted in increased activity towards cephalosporins with a positively charged R2 group, due to substitution of the positively charged histidine to the hydrophobic tyrosine. The modelling of ceftazidime substrate in the VIM-7, VIM-7 F218Y and H224Y structures suggests that the conformation of side-chain residues 224 and R228 in the L3 loop and the Y67 in the L1 loop influence the possible conformations for the substrate binding.

3.2. Paper II

Role of Residues W228 and Y233 in the Structure and Activity of Metallo-β-lactamase GIM-1

Susann Skagseth, Trine Josefine Carlsen, Gro Elin Kjæreng Bjerga, James Spencer, Ørjan Samuelsen, Hanna-Kirsti S. Leiros (2016), Antimicrobial Agents Chemotherapy. 60(2): p. 990-1002.

Establishing the contribution from certain residues to substrate binding might give information on interactions that can be exploited in ligand design. Herein, the German Imipenemase-1 (GIM-1) MBL is unique since it includes the two aromatic side-chains W228 and Y233 in the active site making it narrower and more hydrophobic compared to other metallo-β-lactamases (MBLs). To investigate the role of these residues eight GIM-1 mutants, W228R/AY/S and Y233N/A/I/S, were made. The results presented in this paper show that the W228 and Y233 residues are important for the GIM-1 activity, and mutation at these positions influence the β-lactam substrate specificity. Mutation at position 228 could enhance activity against type 1 substrates, containing electron-donating C-3/C-4 R2 groups, while mutations at 233 position favored hydrolysis of type 2 substrates, containing axial methyl groups or positively charged R2 groups. The β-lactam enzyme kinetics of GIM-1 Y233N showed a deleterious effect. The *in silico* model of GIM-1 Y233N with hydrolyzed ampicillin in the active site showed an additional hydrogen bond between N233 and the C-7 carboxylate group of the ampicillin, however, the calculated binding affinities revealed a stronger binding of Y233 to ampicillin. The three-dimensional structures of GIM-1 W228R (1.98 Å), W228A (1.70 Å), W228Y (1.90 Å), W228S (1.81 Å), and Y233A (1.46 Å) were solved by crystallography. These GIM-1 mutant structures revealed that the conformation of L1 loop is altered instead of the L3 loop, where the mutations are located.

3.3. Paper III

Metallo-β-lactamase Inhibitors by Bioisosteric Replacement: Preparation, Activity and Binding

Susann Skagseth, Sundus Akhter, Marianne H. Paulsen, Zeeshan Muhammad, Ørjan Samuelsen, Hanna-Kirsti S. Leiros, Annette Bayer. Submitted to European Journal of Medicinal Chemistry.

Metallo-β-lactamases (MBLs) are representing an increasing clinical threat with their ability to hydrolyze an entire class of antibiotics, causing them to become inactive. One way to combat this antibiotic resistance is to find MBL inhibitors, which could restore the activity of the β-lactam antibiotics. Bacteria easily acquire MBL resistance genes, thus there is a need for inhibitors for a broad variety of MBLs. Fragment library screening and other studies have shown that compound containing thiol groups have an inhibiting effect on MBLs. In this paper, modified mercaptocarboxylic acids were prepared replacing the carboxylate group to the bioisosteric groups such as phosphonate esters, phosphonic acids and *N*H-tetrazoles. The inhibition potential was measured against the worldwide spread VIM-2 and NDM-1 MBLs, and the more geographically restricted GIM-1. The new MBL inhibitors showed half maximal inhibitory concentration (IC_{50}) values, in the low micro- and high nanomolar range for the three MBLs studies. A cell-based assay with β-lactamases-negative *E. coli* SNO3 cells inducing expression of one of the MBLs found the best inhibitors to be the **3** and **10** series. Three crystal structures of VIM-2 in complex with inhibitor **2b**, **10b** or **10c** were resolved, and showed VIM-2 residues F61, Y67, R228 and H263 contributing in stacking with the inhibitor phenyl ring, and residue N223 forming polar interaction to the P=O group of inhibitor **2b** and sulphur atom of inhibitor **10b**. Synergistic effects were not observed in bacterial strains of *P. aeruginosa* or *K. pneumoniae*, but reduced MIC for inhibitors **3b**, **10b** and **10c** was observed in a clinical isolate of *E. coli*. The results reveal that thiol-based inhibitors show promising inhibition of VIM-2 MBL. However, with GIM-1 or NDM-1 the inhibition potential is less encouraging.

3.4. Paper IV

Structural insight into TMB-1 and the role of residue 119 or 228 in substrate and inhibitor activity

Susann Skagseth, Tony Christopeit, Sundus Akhter, Annette Bayer, Ørjan Samuelsen, Hanna-Kirsti S. Leiros. Submitted to Antimicrobial Agents and Chemotherapy.

Carbapenemases effectively break down carbapenem antibiotics, our most effective β-lactam antibiotics in fighting against bacterial infections. Mutational studies of MBLs can give insight into residues important for the enzyme activities, and possibly which residues to target in the inhibitor designing. Compounds containing thiol groups have been shown to have an inhibiting effect on MBLs. In this study, synthetically made genes of TMB-1 and TMB-2 (one S228P mutation away from TMB-1), and TMB-1 mutants E119Q/S/A were studied. In general, substitutions of residue 228 and 119 reduced the catalytic efficiency compared to TMB-1. Substitutions at position 119 showed the most reduced activity, especially towards penicillins. Thermostability measurements of TMB-1 revealed that a high salt concentration buffer (1 M NaCl) had stabilizing effect. The three-dimensional structure of TMB-1 solved to 1.75 Å resolution, and showed the αββα-fold characteristic for MBLs. Thiol-based inhibitors from **Paper III** were investigated for effectiveness through enzymatic assays showing two promising inhibitors, **2a** and **2b**, with IC_{50} values of 0.6 µM, compared to the captopril with an IC_{50} of 47 µM. The inhibitor binding to TMB-1 using SPR biacore method revealed that the new synthesized inhibitor **2a** were binding 10 times better than captopril, hence more potent. The inhibitor **2b** modelled into TMB-1 showed that residue W64 and H263 may contribute in π stacking, and residue R224 in cation-π interaction with the inhibitor phenyl ring. Hydrophobic interactions from residues V61, V67, W87, E119 and Y233 may be made to the inhibitor ethyl groups on the phosphonate group in the R1 binding site.

4. Results and discussion

MBLs ability to hydrolyze all β-lactam substrates, except monobactams, limits treatment options against infections caused by bacteria harboring MBLs. Many B1 MBL resistance genes are found on mobile genetic elements, facilitating the spread between bacteria of the same and between species [60]. A strategy to restore the activity of the β-lactams, is utilizing them in combination with β-lactamase inhibitors to prevent hydrolysis of the β-lactam molecule [174]. To date, however, no MBL inhibitors are clinically available, thus there is an urgent need to find effective inhibitors [206]. To design inhibitors with activity against a variety of MBLs, a better understanding of MBL residues contributing in substrate or inhibitor binding is essential. In this thesis, the effect of substitution of residues in the first (zinc binding) and second shell interaction sphere of MBLs were investigated through various studies including enzyme kinetics, determination of MICs, thermostability measurements, modelling, *in silico* analysis, and crystal structure determination of enzymes, mutants and enzyme inhibitor complexes. In addition, we have in a collaboration searched for potential inhibitors among synthetic thiol-based compounds and in marine extracts originating from organisms in the extreme conditions in the Barents Sea. The different MBL enzymes and mutants studied in this thesis are given in **Table 6** showing our studies of enzyme kinetics, crystal structures and inhibitor binding. The overall aim of these studies were to discover new potent broad-spectrum MBL inhibitors.

Table 6: A short summary of the enzymes, mutants, enzyme kinetics, crystal structure(s) inhibitor studies performed in the thesis. Residues at position 119,218, 224 and 223 are given. x means an investigation has been done, and – indicated the same amino acid as given above.

	Enzyme	Mutant	Enzyme kinetics	Crystal structure(s)	Inhibitor assays	Residue at position:				
						119	218	224	228	233
Paper I	VIM-7		x	x		D	F	H	R	N
		F218Y	x	x		-	Y	-	-	-
		H224Y	x	x		-	F	Y	-	-
Paper II	GIM-1		x			E	F	R	W	Y
		W228R	x	x		-	-	-	R	-
		W228A	x	x		-	-	-	Y	-
		W228Y	x	x		-	-	-	Y	-
		W228S	x	x		-	-	-	S	-
		Y233N	x			-	-	-	W	N
		Y233A	x			-	-	-	-	A
		Y233I	x	x		-	-	-	-	I
		Y233S	x			-	-	-	-	S
Paper III	VIM-2			3 x	x	D	Y	Y	R	N
	GIM-1				x	E	F	R	W	Y
	NDM-1				x	Q	F	K	A	N
Paper IV	TMB-1		x	x	x	E	Y	R	S	Y
	TMB-2		x			-	-	-	P	Y
	TMB-1	E119Q	x			Q	-	-	S	-
		E119S	x			S	-	-	-	-
		E119A	x			A	-	-	-	-

4.1. Impact of residue substitutions in VIM-7, GIM-1 and TMB-1

In this thesis, the reported distribution of the MBL genes from VIM-7 (**paper I**), GIM-1 (**paper II**) or TMB-1 (**paper IV**) are all geographically restricted. In VIM-7, the first sphere zinc-binding residue D120A, and of the second sphere residues H224Y and F218Y were investigated. In GIM-1, the impact of mutations of residues in the narrow active site, W228R/A/Y/S and Y223N/A/I/S, were evaluated. Characterization of TMB-1 was performed and compared to TMB-2 (a S228P mutant of TMB-1), and three mutants of the second sphere residue E119Q/S/A. This to study the effect on the catalytic efficiency when introducing a rigid proline residue at 228 and the substitution of residue E119 in TMB-1. The residues studied through substitution have shown to be involved in substrate or inhibitor binding according to MBL crystal structures, and the catalytic efficiency of the substitutions was studied against a variety of β-lactams. The MBL mutants with single point mutations may be variants that can evolve naturally, where the mutants showing higher catalytic activity are worrisome.

4.1.1. Impact of zinc-binding residue D120A substitution in VIM-7

In **paper I**, the impact of residue D120 in VIM-7 by mutation to an alanine, showed that the substitution gave an inactive mono zinc enzyme with no activity against nitrocefin nor

ertapenem. This is in agreement with previous reports [118, 147, 220] and the reaction mechanism of MBLs, where the deprotonated D120 residue binds the Zn2 ion and orienting the bridging hydroxide ion, which makes the nucleophilic attack on the β-lactam forming an enzyme bound intermediate (**Figure 6a**). The 1.9 Å crystal structure of VIM-7 D120A (**paper I**, **Figure 2**) revealed that the Zn2 ion was lost. Thermostability measurements showed that the mutant protein was folded, but less thermostable compared to VIM-7. In the structure, a water molecule was found in the Zn2 site interacting with the other DCH site residues, C221 and H263. This water molecule is inadequate to act as nucleophile for catalysis, and together with the loss of Zn1, could explain why the enzyme was inactive.

4.1.2. Substitution of second sphere residues F218Y and H224Y in VIM-7 increases catalytic efficiency and stability

VIM-7 is the most divergent variant within the VIM class with 77% and 74% sequence identity to VIM-4 and VIM-2, respectively. VIM-7 showed a reduced catalytic activity towards cephalosporins containing a bulky, positively charged R2 side group, compared to VIM-2 [221]. VIM-2 entails Y218 and Y224 both involved in two different hydrogen binding clusters, while VIM-7 contains phenylalanine and histidine residues in these positions. In **paper I**, the single point mutations at F218 and H224 to tyrosine in VIM-7 revealed enhanced stability, ΔT_m= +1.8°C and +7.6°C, respectively, and an increased catalytic activity compared to VIM-7.

Residue 218

In particular, the VIM-7 F218Y mutant showed increased efficiency towards penicillins, the four cephalosporins tested and the carbapenem imipenem, compared to VIM-7. In the 1.7 Å VIM-7 F218Y crystal structure, three additional hydrogen bonds from F218Y to N70, D84, and R121 were observed (**paper I**, **Figure 2**). This hydrogen bond network, also present in VIM-2 [88, 221], was attributed to the enhanced stability since it makes the structure more rigid by linking together different secondary structure elements. Hydrogen bonds provide intramolecular interactions important for protein folding, and contribute to rigidity, which is favorably for protein stability [222, 223]. The increased catalytic activity is in agreement with the studies of the IMP-1 F218Y mutant, which showed an increased hydrolysis rate for substrates containing neutral or charged R2 groups [172, 224].

Residue 224

Another second sphere mutant, H224Y, is located in the L3 loop and found in the R2 substrate binding site (**paper I**). The catalytic activity of VIM-7 H224Y was increased for all β-lactams tested, except for ertapenem and meropenem. VIM-7 H224Y compared to VIM-7 hydrolyzed imipenem, cefepime and ceftazidime, with positively charged R2 groups, significantly more efficiently. The increased efficiency is likely due to removal of the positively charged histidine residue to the aromatic polar tyrosine, thus reducing repulsion from two positive charges. The VIM-7 H224Y crystal structure showed two additional hydrogen bonds, to A231 and a water-intermediated hydrogen bond to H196, which also explain the increased catalytic activity and stability (**paper I**, **Figure 2**). In addition, the VIM-7 H224Y R2 binding site is open and U-shaped while in VIM-7, R228 occupy the same binding site.

Both introductions of a VIM-2 amino acid in VIM-7 increased the catalytic efficiency and stability due to additional hydrogen bonds. A VIM-7 double mutant (F218Y/H224Y) would probably form an even more rigid and efficient enzyme due to addition of two hydrogen bond networks, as in VIM-2 which is more catalytically efficient against cephalosporins with bulky, positively charged R2 groups than VIM-7 [87]. Overall, the 218 residue in VIM-7, located below the active site, have been shown to be important for the catalytic activity, as in IMP enzymes [224], and residue 224 in L3 loop is important for the stability and activity of MBLs, generally.

Modelling of ceftazidime containing a positively charged R2 group

In order to investigate substrate binding in the VIM-7 F218Y and VIM-7 H224Y mutants, modelling studies of ceftazidime containing a bulky, positively charged R2 group were performed. Ceftazidime in the VIM-7 mutants showed that the substrate conformation did not fit into either mutant structures (**paper I**, **Figure 1**). The alternative conformation of ceftazidime in both mutants is likely due to R228, as the residue is overlapping the ceftazidime conformation in VIM-7. Another R228 conformation in the mutants would likely give modelling results with ceftazidime as shown for VIM-7 and IMP-30 [225], where the cyclic R2 group is adjacent to residue 224 and buried below residue 228. It was suggested that a stacking with Y67 residue in the VIM-7 mutant L1 loop to the positively charged R2 ring of ceftazidime is more likely to happen for the substrate in this conformation.

Residue 224 versus 228

According to several NDM-1 and IMP-1 crystal structures [84, 99, 126, 152, 161, 162], the positively charged lysine at residue 224 is involved in substrate and inhibitor binding. The VIM-2 Y224 residue is not involved in inhibitor binding, however VIM-2-inhibitor complex crystal structures shows that the positively charged R228 is involved instead [159, 161, 167]. The R228 in VIM-2 is suggested to replace the K224, in other B1 enzymes, in interaction with the carboxylate on C3 or C4 of the substrate (**Figure 6**) [86]. The residue composition of the L3 loop influences the activity, as shown in the comparative study between VIM-1 containing H224 and S228 and VIM-13 with L224 and R228 [166]. The interplay between a positively charged residue at the 224 or 228 position in the L3 loop seems to be important for the activity of MBLs, and the effects of the two positions are related.

4.1.3. Residues 228 (GIM-1 and TMB-1) and 223 (GIM-1) confers substrate specificity

Residue 228

The residues W228 and Y233 form a narrower and more hydrophobic active site in GIM-1 compared to other MBLs [90], and substitution of these residues were investigated (**paper II**). The kinetic activity of the GIM-1 W228R/A/Y/S mutants showed a slight reduction against the penicillin substrates tested (**paper II**, **Table 2**). The W228A and W228I mutants showed an increase in activity against type 1 substrates (cefoxitin and meropenem), which have electron donors at the R2 position, compared to the wild-type. The two mutants had little change in the hydrolysis rate of type II substrates (ceftazidime and imipenem), which contains a positively charged R2 group. The role of residue 228 is studied in several VIM MBLs, where most VIM MBLs contain an arginine, however, VIM-1 and VIM-23 contains a serine [169, 226], and VIM-24 and VIM-26 a leucine [165, 168]. In general, the kinetic parameters showed that the efficiencies were reduced for VIM-1, VIM-23, VIM-24 and VIM-26; however, they also showed increased efficiency towards some substrates. Our GIM-1 results are in agreement with the studies of the residue 228 in VIM-type MBLs showing that the residue is defining the substrate specificity.

Residue 233

The enzyme kinetics of GIM-1 Y233N/A/I/S mutants revealed more deleterious effects, with the exception of the Y233A mutant (**paper II**, **Table 2**). The increase in penicillin hydrolysis is reported for IMP-1, where the N233A mutant showed an increase in ampicillin hydrolysis, in addition to hydrolysis of nitrocefin, cefotaxime and cephaloridine substrates [163]. In GIM-1, substitution at position 233 showed a higher level of reduced activity towards type I substrates than type II substrates, except for the Y233N mutant, which showed reduced activity for all tested substrates. The effect on the different substrates were most prominent for the Y233I mutant showing up to 50 times reduced catalytic efficiency against type I substrates, and 5 times reduction against type II substrates, compared to the wild-type. The significant reduction in activity for GIM-1 Y233N is interesting, since ~67% of all MBLs have an asparagine in this position [170]. N233 is suggested to be crucial for imipenem resistance [96], however, this was found not to be the case for GIM-1 (**paper II**). The substitutions of N233 residue in IMP-1 showed that a wide variety of amino acids were tolerable at this position and the effect was substrate dependent [170], in agreement with our results. Taken together, the effects of the mutations were mainly due to changes in K_M, indicating that the mutations at position 228 and 233 are affecting the association steps rather than the catalytic steps in the reaction. Thermostability measurements of GIM-1 and mutants revealed no significant change; hence, the protein stability of the mutants cannot explain the difference observed in the catalytic properties. In general, the GIM-1 wild-type shows the highest catalytic efficiency compared to the mutants, showing the importance of these residues in GIM-1, distinguishing this and similar MBLs, such as DIM-1 [227], from other class B1 enzymes. Steady state kinetics of mutations of either W228 or Y233 show that both residues are important but have a nonessential role for the enzymatic activity of GIM-1 by contributing to substrate specificity.

Proline at residue 228

TMB-2, discovered shortly after TMB-1, differs with only a single point mutation: a proline at the 228 position. TMB-1 (**paper IV**) share 51 % sequence identity with GIM-1, and contains a tyrosine at the 233 position, while the 228 position holds a serine amino acid. The kinetics characterization of TMB-2, with the rigid proline residue, revealed a slightly reduced catalytic efficiency and significantly reduced for ampicillin compared to TMB-1. Substitution of R228 to all possible amino acids studied in VIM-2 showed that proline at this position was tolerable,

and the MIC values revealed a reduction for all antibiotics tested [168]. The reduced efficiency with a proline at position 228 in VIM-2 is consistent with our TMB-2 results.

Residue 119

Residue 119 is located in the conserved H116XH118XD120 motif with three zinc-binding residues, and in crystal structure complexes found involved in substrate binding in NDM-1 [99, 126, 152] or inhibitor binding in IMP-1 [160]. The effect of substitution of residue 119 is to our knowledge only studied in NDM-1 [171], therefore, mutations in TMB-1 were made. The enzyme kinetics of TMB-1 E119Q/S/A revealed a reduced catalytic efficiency compared to TMB-1, with the highest reduction against penicillin substrates (**paper IV**, **Table 3**). This is supported by studies showing that Q119 in NDM-1 is involved in binding of penicillin substrates [99, 126]. The TMB-1 mutants show through reduced efficiency, that residue 119 are involved in the hydrolysis of penicillin substrates, either through direct binding or by maintaining the orientation of its neighboring, zinc binding residues, H118 and D120. Other surrounding residues might contribute in binding of substrates in TMB-1, such as the positively charged residue R224 and the residue Y233, shown to be important for the GIM-1 activity. Overall, residue 119 contribute to tuning the substrate specificity of TMB-1.

Summary of residue substitutions

Despite the large differences between MBL enzymes, some seems to have evolved giving many similar enzyme to inhibitor/substrate interactions. When a residue involved in substrate or inhibitor binding is missing or replaced, surrounding residues may contribute to form alternative interaction. This was found in GIM-1, TMB-1, IMP-1, NDM-1, VIM-7 and VIM-2, where a positively charged residue at either the 224 or 228 position contribute in substrate binding in (**paper I**) [84, 86, 87, 90, 99, 153], and with an aromatic tryptophan at either 228 as for GIM-1 (**paper II**) or 64 position as in TMB-1 (**paper IV**). Information about the influence and importance of residues on enzymatic activity, inhibitor binding, and the interplay between residues, such as 224 and 228, are useful when trying to find inhibitors for a wide variety of MBLs. Knowledge of the contribution from residues and residue determinants in the MBLs can aid the design of specific inhibitors. In order to block the enzymes hydrolytic function, inhibitors containing specific side groups can target important enzyme residues since the structure activity relation (SAR) is explored.

4.2. Crystal structures of two different VIM-7 gene constructs show no structural difference

Obtaining high amounts of concentrated pure enzymes required for enzyme characterization and crystallization could be challenging. Consequently, in order to obtain high amounts of purified enzyme it is convenient to use affinity tags. However, one concern is whether lack of residues or additional residues from different gene construct design are influencing the recombinant enzyme structure and function. In our VIM-7 study we used two different gene constructs due to the low production yields after enzyme purification from the periplasm (**paper I**). One gene construct encoded the recombinant *native* VIM-7 with the leader sequence resulting in residues A16-E300 and this was purified from the periplasm. The other gene construct encoded a recombinant VIM-7 with a Hexa His tag, TEV cleavage site and a residue A25-E300 called tVIM-7. The catalytic efficiency of the two constructs revealed that the recombinant version of the native VIM-7 was higher compared to tVIM-7, due to both improved binding and higher turnover. The tVIM-7 crystal structure showed a RMSD for CA atoms of 0.15-0.50 Å, compared to four native VIM-7 (PDB-ID: 2Y8A, 2Y8B, and 2Y87). The differences were due to conformational changes in the L3 loop (residues 223 to 240), which also are reported for native VIM-7 structures [87]. The zinc-binding residues and second sphere residues interacting with the active site were similar in all structures from both enzyme constructs. Hence, the difference in catalytic efficiency could not be explained based on the structures.

4.2.1. D120A, F218Y and H224Y mutations do not significantly alter the VIM-7 structure

The crystal structures of the tVIM-7-D120A, VIM-7-F218Y and tVIM-7-H224Y mutants (**paper I**) were similar to the tVIM-7 structure, showing a RMSD of 0.63 Å, 0.50 Å, and 0.23 Å, respectively, for CA atoms. The major differences were observed in the flexible L1 loop, for all three mutants. The VIM-7-D120A mutant structure contained a single zinc ion in the active site, with a water molecule occupying the Zn2 site.

4.2.2. Crystal structures of GIM-1 mutants show some changed active site architectures

Crystal structures of GIM-1 W228R/A/Y/S and Y223A (**paper II, Figure 5**) compared to GIM-1 (PDB-ID: 2YNT) showed low RMSD values, and the mutant structures matched to each other with a RMSD of 0.28 to 0.76 Å, for CA atoms. The differences were mainly found in the L1 loop, known to be flexible [90]. The low RMSD indicate that the five introduced mutations in GIM-1 did not cause any profound structural changes compared to the wild-type GIM-1. All W228 mutant structures had oxidized C221 residues, in which cysteine becomes a cysteine sulfonic residue, despite the use of the reducing agent β-mercaptoethanol in the crystallization. A consequence of this oxidation might be a lower affinity for Zn2, as observed in the crystal structures showing 0 to 0.15 Zn2 per GIM-1 molecule, except Y233A, which has a fully occupied Zn2 site. However, in the structure of W228A and W228R, some electron density were observed in the Zn2 position, and modelled as a low occupancy zinc. The oxidized active-site C221 has in previous studies shown to cause reduced occupancy or even loss of one zinc ion in other MBL crystal structures [86-88]. This could be due to C221 involved in coordination of Zn2 ion. However, the oxidation of the C221 is suggested to take place in the crystallization process, as indicated in a VIM-2 study [86] or by radiation damage also shown for another VIM-2 study [154]. Hence, the oxidized C221 would not be present in the enzymatic characterization. If the C221 residue were oxidized during enzymatic measurements, it would play a role in down regulating the catalytic efficiency. In the GIM-1 W228S structure, residue D68 in the L1 loop was repositioned and made ion pair with H263 in the Zn2 site. In this structure, the Zn2 ion was lost, but whether this was only due to the W228S mutation is not clear. Other studies have showed that mutation in second sphere residues cause disruption of hydrogen bond network adjacent to the zinc ions, thus affect the enzyme activity significantly [148, 228]. The GIM-1 Y233A mutant structure showed a reduced C221 residue and two zinc ions with full occupancy (**paper II**, **Figure 5**). Compared to the W228 mutant structures, the Y233A structure differs less compared to the wild-type structure. In addition, the zinc-zinc distance in the Y233A mutant was increased due to two hydrogen bonds between the D64 and G264, which were not present in the wild-type GIM-1 structure. Both mutation at residue W228 and Y233 show some effect on the GIM-1 active site architecture and catalytic properties.

4.2.3. *In silico* modelling of hydrolyzed ampicillin binding in GIM-1 and GIM-1 Y233N

The better understand the deleterious effect of the GIM-1 Y233N mutant, *in silico* modelling of the GIM-1 wild-type and mutant with hydrolyzed ampicillin in the active sites was investigated (**paper II**, **Figure 6**). GIM-1 Y233N was modelled with a hydrogen bond from the N233 side-chain to the hydrolyzed ampicillin, not present in the ampicillin GIM-1 wild-type model. The ampicillin GIM-1 model revealed an anion π interaction from the carboxylate of the hydrolyzed ampicillin to the aromatic ring of residue Y233. Despite the hydrogen bond in the Y233N mutant, the calculation of the estimated relative binding affinities of hydrolyzed ampicillin showed stronger binding to GIM-1 wild-type. The results of the calculation is in correlation with the enzyme kinetics of ampicillin hydrolysis, giving a higher binding affinity for ampicillin to the wild-type GIM-1 enzyme. The N233 residue was described as critical for the IMP enzyme [96], although this is not the case for other MBLs [163, 164, 229]. The *in silico* modelling and calculation of GIM-1 and GIM-1 Y233N mutant with hydrolyzed ampicillin gave new insight into the positive contribution of the Y233 contribution for substrate binding in GIM-1.

4.2.4. TMB-1 reveals high salt stability and W64 closes the R2 site in the structure

TMB-1/-2 and mutants were all stabilized in buffers with high salt concentration (**paper IV**). TMB-1 was discovered in environmental isolates of *Achromobacter xylosoxidans* and clinical isolates of *Acinetobacter* spp. However, the organisms where the TMB genes were discovered are not halophilic (organisms that thrive in high salt concentration) and do not explain the high salt preference. The 1.75 Å TMB-1 crystal structure (**paper IV**), contains two catalytic zinc ions coordinated by the conserved residues in the B1 subclass: H116, H118, and H196 in the Zn1 site, and D120, C221, and H263 in the Zn2 site. A third zinc ion, Zn3, was observed bound to H285 on the enzyme surface. Two Cl ions were identified; one Cl1 between residues R224 and W64 in the R2 site, and the other Cl2 on the enzyme surface. The active site of TMB-1 is defined by residues V61, W64, V67, R224, S228 and Y233, resulting in a very hydrophobic binding site. The TMB-1 W64 residue in the L1 loop is likely to be involved in inhibitor binding, as seen in IMP-1 inhibitor complex crystal structures [84, 158]. W64 is in a very closed conformation in TMB-1 chain A structure and a slightly more open R2 site for chain B. TMB-1

contains a positively charged R224 residue in the R2 site, which may contribute in binding of β-lactam substrates (**paper IV**, **Figure 6**), as shown with the positively charged K224 residue in NDM-1 [99, 126, 152]. The S228 are contributing to a more open active site for substrates to bind more easily, as shown in VIM-26 [165]. Another important residue is the Y233 residue, which may affect the catalytic activity, as shown in GIM-1, through aromatic stacking. In general, new X-ray crystal structures provide valuable information of the MBL residue arrangements, and together with activity measurements, increase the understanding of the differences in catalytic efficiencies and SAR for MBLs.

Overall, none of the new mutant crystal structures of VIM-7 (**paper I**) or GIM-1 (**paper II**) showed to alter the structure significantly. Some changes were observed in the L1 and L3 loops, however, these differences could be due to the flexible nature of the loops. The new TMB-1 crystal structure (**paper IV**) was solved at high resolution describing the binding site accurately, and showed a closed R2 binding site due to the closed W64 conformation.

4.3. Inhibitor studies with VIM-2, NDM-1, GIM-1, and TMB-1

In order to identify inhibitors that preferably act on a wide variety of MBL enzymes, the inhibitors were tested against two wide-spread and clinically challenging MBLs (VIM-2 and NDM-1 **paper III**) and the two more geographically restricted MBLs, GIM-1 (**paper III**) and TMB-1 (**paper IV**). The half maximal inhibitory concentration (IC_{50}) tested on purified enzymes and whole cell assay experiments were performed for each inhibitor. The following synthetically-made thiol-based inhibitors were tested: mercaptophosphonate esters **2a-c**, mercaptophosphonic acids **3a-c** and mercapto-*N*H-tetrazol **4**, in addition to synthesis intermediates **7**, **10a-c**, **15a**, **15b** and **16**. The inhibitors are in a racemic mixture, containing 50/50% of both enantiomers. A previously reported VIM-2 inhibitor, compound **1c**, was included in the studies for benchmarking. Crystal structures obtained of VIM-2 in complex with inhibitor **2b**, **10a** and **10b** gave insight into the coordinating properties of the phosphonic acid group compared to the thiol in the enzyme.

4.3.1. Inhibitors preferably targets VIM-2

Our results included the previously reported compound **1c** [212] found an IC_{50} value in the same order as previously reported, validating our assay. In general, all inhibitors showed lower IC_{50} values towards VIM-2 compared to GIM-1 and NDM-1, with the exception of inhibitor **2a**,

which had a significantly better IC_{50} for GIM-1 compared to VIM-2 (**paper III**. **Table 2**). The substitution of carboxylic acid on previously reported compound **1c** with a *N*H-tetrazole (**4**) inhibitor showed a reduced inhibitory effect, while the phosphonate esters and phosphonic acid groups gave a similar (**2**, **10**) or improved (**3**) activity. By comparing the inhibitors containing alcohols (**7**, **9**) with corresponding thiols and thioacetates (**2**, **3**, **10**), shows that the sulfur atom of the inhibitor β-carbon is important for the inhibitory activity. Comparison of the mercapto and thioacetate substituted phosphonate esters and phosphonic acids **2**, **3**, **8** and **10**, the activity seems to depend on a subtle combination of the sulfur atom and a carboxylic acid bioisoster. The inhibitors showing the highest inhibitory effect on enzyme activity were the mercapto substituted phosphonate ester **3**, while the thioacetate substituted phosphonate ester **8** showed the lowest inhibitory effect of all four inhibitor series. This effect was not observed in phosphonic acids **2** and **10**, as thiol **2** and thioacetate **10** showed the same level of inhibition. This may indicate that the interaction of phosphonic acid with the enzyme is more important for the activity than the interaction with the thiol. This is in line with a study on mercaptophosphonic acids in the class B2 CphA MBL crystal structure showing that oxygen of the phosphonic acid is binding to the zinc ion, and not the sulfur atom of the thiol [179]. Overall, according to the IC_{50} values, the most efficient inhibitors contained a mercapto group and a phosphonate ester (inhibitor **3a-c**) or acid (inhibitor **2a** and **2b**), with two or three methyl groups connecting the phenyl group.

In order to investigate the inhibitory activity towards MBLs expressed in *E. coli*, the inhibitors were tested against the β-lactamase-negative *E. coli* SNO3 cells transformed with pET26b(+) containing the genes bla_{VIM-2}, bla_{GIM-1} or bla_{NDM-1} were tested. The calculated percent inhibition revealed high percent inhibition (>70%) for several compounds. This shows that the inhibitors are able to diffuse across the outer bacterial cell membrane of *E. coli*. The highest percent inhibition was observed for the inhibitors **3a-c** and **10a-c** with *E. coli* harboring VIM-2, which was in agreement with the low IC_{50} values. For *E. coli* containing GIM-1 or NDM-1, the percent inhibition was not as pronounced, although the IC_{50} values were low. Inhibitors **2a** and **2b** showed high IC_{50} values but lower percent inhibition with VIM-2 compared to inhibitors **3a-c** and **10a-c**. The most promising inhibitors were tested in a synergy assay with *E. coli* bacterial strain containing VIM-1 and meropenem, showing a reduced MIC for inhibitors **3b**, **10b** and **10c**. VIM-2 share 91% sequence identity with VIM-1, hence, it is likely that the

same effect would be observed with *E. coli* harboring VIM-2. In general, the percent inhibition was highest in *E. coli* with VIM-2 compared to GIM-1 and NDM-1, and reduced MIC for some inhibitors in *E. coli* synergy assays with VIM-1. Consequently, the selection of synthetic inhibitors seems to be better at inhibiting VIM-2, thus, not suited as broad-spectrum inhibitors, and here the **3** and **10** series are most promising.

4.3.2. VIM-2 inhibitor complex structures

The crystal structures of VIM-2 complexed with inhibitors shows that only one of the two enantiomers fit into in the observed electron density in the active site. The VIM-2 structure with inhibitors **2b**, **10b** or **10c** all showed the (*R*)-form in the active site, in agreement with the reported VIM-2 complexed with the (*S*)-form of compound **1c** [153], showing the stereoisomer with corresponding sterically arrangement of substituents (**paper III**, **Figure 2**). This might indicate that the (*R*)-enantiomer of the three inhibitors is the more efficient than the (*S*)-enantiomer. By separating the two enantiomers, lower IC_{50} values are likely to be obtained. Studies of pure stereoisomers of the mercaptocarboxylic acids captopril and bisthiazolidine showed a difference in 10-100 times in IC_{50} values between different stereoisomers [161, 184].

In the VIM-2 inhibitor **2b** complex, the sulfur atom in the thiol is bridging the zinc ions and replacing the hydroxide ion normally found in the VIM-2 structure. This has been observed in a number of other B1 MBL complexed with thiol inhibitors [84, 153, 161, 162, 208]. The inhibitor **2b** forms hydrogen bonds from the inhibitor P=O to the N233 residue, while the phenyl ring is in a T-shaped π-π stacking interaction with Y67, cation-π interaction with the positively charged R228, and a T-shaped stacking with H263. The phosphonate esters ethyl groups of the **2b** inhibitor make hydrophobic interactions with F61, Y67, W87 and D119 residues of VIM-2. The corresponding phosphonic acids **3** without the two ethyl groups, showed weaker IC_{50} values with VIM-2 compared to the phosphonate esters, indicating that the phosphonic acids are not involved in the corresponding favorable interactions.

Both crystal structures of VIM-2 complexed with inhibitor **10b** and **10c** show that the thioacetate sulfur atom is binding to the zinc differently than the typical thiol complexes, as seen in VIM-2 inhibitor **2b** structure (**paper III**, **Figure 3**). The thioacetate is interacting with the zinc and to the R228 through a water molecule in both, and in **10b** a sulfur is interacting with N233. The phosphonic acid is adjacent to W87 and interacting with the N233. The phenyl

ring is parallel to Y67, with the R228 stacking at the opposite side, and the H263 in a T-shaped orientation, which is also observed in the complex structure of VIM-2 and compound **1c** [153]. In addition to these interactions, the G232 are stacking opposite side to Y67 in our structure. Despite the inhibitor **10c** being longer than inhibitor **10b**, the phenyl ring is binding in approximately the same place, due to a twisting of the inhibitor carbon chain. Residue F61 differs between the **2b** and **10b/c** complexes, showing a closed conformation over the inhibitors **10b/c** interacting with the phosphonic acid group, while F61 in **2b** shows a more open conformation interacting with the ethyl groups (**paper III**, **Figure 4**).

4.3.3. Inhibitor studies in TMB-1 show results similar to GIM-1

To investigate the second sphere residues interacting with the inhibitors in GIM-1 and NDM-1, the inhibitors from the VIM-2 crystal structures were modelled into the structures (**paper III**, **Figure 4**). The modelling of inhibitor **2b**, **10b** and **10c** in GIM-1 shows that W228 and Y64 makes the R2 site smaller and more hydrophobic. The low difference in IC_{50} values between the shortest and longest inhibitors indicate that all compounds within the series may have the same favorable T-shaped stacking from W228 and cation-π interaction from R224 to the inhibitor phenyl groups. The NDM-1 inhibitor **2b**, **10b**, and **10c** modelling shows that the N233 residue can bind the inhibitors through the P=O group, as shown in VIM-2. However, the hydrophobic stabilization of the phenyl ring in the inhibitors are limited due to the A228 and K224 residues in the R2 site. The K224 in NDM-1 is shorter than the R228 in VIM-2 and R224 in GIM-1. Compared to VIM-2 and GIM-1, the NDM-1 binding site is more hydrophobic and different with few conserved second sphere residues, making the design of a broad-spectrum MBL inhibitor challenging.

The dose-respond IC_{50} values of GIM-1 and TMB-1 for the nine common inhibitor tested (series **2a-b**, **3**, **10** and **captopril**) are within the same range, which is not surprising as they share 51% sequence identity. The active site of GIM-1 (PDB-ID: 2YNW) and TMB-1 (**Figure 5d**, **paper IV**) show that the residue 228 is different, a tryptophan in GIM-1 and a serine in TMB-1. The crystal structure of VIM-2 in complex with inhibitor **2b** show that the positively charged residue R228 are involved in cation-π interaction with the phenyl ring of inhibitor **2b** (**paper III**). The tryptophan in GIM-1 may contribute in a π-π interaction with the inhibitor phenyl ring, while S228 in TMB-1 may not. However, TMB-1 has a W64 on the flexible L1 loop, as shown in modelling in **paper IV**, which can contribute in a π-π stacking edge-to-face interaction with the

phenyl ring, as observed in crystal structure of IMP-1-mercarboxylate inhibitor complex showing W64 in edge-to-face interaction with the inhibitor thiopene ring [84]. The interaction with the phenyl ring in TMB-1 may also include residues H263 and R224. The modelling in TMB-1 shows that the residues W87, W64 and E119 might make hydrophobic interactions to the ethyl groups on the inhibitor **2b**.

In general, the inhibitors showed the lowest IC_{50} values for VIM-2, then GIM-1 and TMB-1, while the lowest activity was observed with NDM-1. Inhibitors targeting a broad number of MBLs was not found, however, the thioacetate phosphonic acid **10b** did target both the clinically challenging VIM-2 and NDM-1 enzymes, and may be a template for further inhibitor optimization.

4.3.4. Binding studies of **captopril**, **2a** and **2b** inhibitors to TMB-1 using Surface Plasmon Resonance (SPR)

To investigate the binding of inhibitors in TMB-1 the binding affinity, K_D, of inhibitors with the lowest IC_{50} values, inhibitors **2a** and **2b**, were investigated using SPR (**paper IV**, **Figure 4**). **Captopril** was added to the assay as it is a well-characterized MBL inhibitor, which has been tested against a variety of MBLs [161]. **Captopril** and meropenem were used to verify the activity of immobilized TMB-1. Both inhibitors **2a** and **2b** showed binding to TMB-1, however, only the inhibitor **2a** data fit the 1:1 interaction model, and had sufficient data to determine a K_D. The inhibitor **2a** revealed a 10 times better binding affinity compared to **captopril**. The sensorgrams presented show some background noise (**paper IV**, **Figure 4**), and through further optimization of the assay, it is likely that also inhibitor **2b** would give data to fit the 1:1 interaction model, providing a K_D value. Overall, the SPR measurement revealed inhibitor **2a** to be a more potent inhibitor than **captopril**.

4.3.5. *In vitro* experiments versus cell-based experiments

Synergistic effects of meropenem and inhibitors in cell-based experiments with clinical bacterial strains containing VIM-1, VIM-2 or NDM-1 were only observed in *E. coli* harboring VIM-1 (**paper III**). Herein, VIM-1 and VIM-2 have 91% sequence identity. These results is different compared to the dose-response IC_{50} assay with purified enzyme. The inconsistency between results of an assay with purified enzyme and cell-based assays was also observed in MIC determination of GIM-1 and the different mutants (**paper II**). This could be due to a

different environment in the bacterial periplasm, where the MBLs break down β-lactams, compared to the controlled environment in the kinetic assays. This emphasizes the importance of cell-based experiments in evaluation of inhibitors and also against a variety of bacterial strains.

4.3.6. MBL inhibitors from the Barents Sea

Natural sources have given many marketed drugs, and through marine bioprospecting, searching in the Barents Sea where the biodiversity is enormous and adapted the extreme conditions, one may find new alternative antibiotics or inhibitors of resistance mechanisms. Marine microorganisms may have evolved the ability to produce compounds for protection against intruders, which we may utilize. Marine extracts were collected from the bottom of the Barents Sea. The extracts had previously been through a process of first round of testing with VIM-2 MBL to look for inhibitory effect. Extracts showing inhibitory effects were purified further using Flash chromatography method. The marine extracts in the second round of testing against purified VIM-2 enzyme showed inhibition, however, the extracts were not investigated further. The extracts were too complex to identify single compounds, as they contained a mixture of compounds. Further investigation or purification and testing against a variety of MBLs could have provided a starting point for optimization of MBL inhibitors, either through an identified scaffold or through a full functional inhibitor compound.

Structure activity relationship (SAR) and impact on inhibition properties

Through knowledge of the contribution of residues and SAR for the enzymatic activity and their involvement in substrate and inhibitor binding in the MBLs, specific inhibitors containing side groups which can target specific MBL residues and block their hydrolytic function can be designed. The identification of broad-spectrum MBL inhibitors remains unresolved. In this thesis, however, new and potent inhibitors against VIM-2 have been identified by bioisosteric replacement. Their inhibitory effect in the low micro- or nanomolar range and the presented information on the inhibitor binding to VIM-2 using crystallography contribute to future work on discovery of even more potent MBL inhibitors.

5. Concluding remarks

In this thesis, the substitution of a zinc-binding residue resulted in loss of one active site zinc and the ability for the enzyme to hydrolyze β-lactam antibiotics. Substitutions of second sphere residues contributed in tuning the substrate specificity of the MBL enzymes. Certain second sphere substitutions introduced more hydrogen bonds, which increased the catalytic activity and the temperature stability of the mutants. Other substitutions revealed a reduction in catalytic efficiency, showing that the residues are important, however, not essential for the enzyme activity.

The introduction of single point mutation did not affect the overall fold of the enzyme structures, as identified using crystallography. Slight changes in the active site were observed in the mutant structures due to the second sphere substitutions, and these may affect the distances between the zinc ions and, in some cases, the loss of a catalytically important zinc ion. The effect from mutations in the second sphere showed that interactions from metal binding residues are more important for the catalytic activity that the second sphere residues. The new TMB-1 crystal structure revealed a very closed enzyme conformation with the characteristic B1 MBL features; the αβ/βα fold, two zinc ions in the active site and flexible L1 and L3 loops adjoining the active site.

The different environment affects the enzyme activity, as demonstrated by the inhibitor testing against purified enzyme, through to cellular assay. The inhibition effects were not as profound in the cell bacterial assays as with purified enzyme, e.g. the necessity for inhibitors to cross the outer cell wall to enter the periplasmic space for enzyme binding.

The thiol-based synthesized inhibitors studied in this thesis revealed potent inhibitors with inhibitory effects in the low micro- and nanomolar range. These inhibitors are good starting points for further inhibitors optimization, preferably broad spectrum inhibitors.

6. Future Perspectives

MBL inhibitors can prevent the hydrolysis of β-lactam antibiotics, and when used in combination therapy is a promising strategy in combating β-lactam antibiotic resistance. Currently no clinically MBL inhibitor is available, thus the need for finding novel inhibitors for this class of enzymes is urgent. The search for inhibitors presented in this thesis can be further explored by investigating the inhibitory effect of the enantiomers individually and on a broader selection of MBLs. Toxicity tests of the thiol-based inhibitors and exploration of more bacterial strains to verify the ability to pass the outer cell membrane which is needed for an inhibitor, can be performed.

Another approach is to search for MBL inhibitors in natural sources, for example, to further explore extracts and organisms from the Barents Sea for MBL inhibitory effects. The biologic diversity in the sea remains roughly unexplored and the search for inhibitors in the extreme marine environment could provide information on possible broad-spectrum MBL inhibitors. Future hits with increased inhibition potential could arise after extract purification, leading up to a single active compound, or give an indication of possible scaffolds that could target a wide variety of MBLs.

7. References

1. **Goldsworthy, P.D. and McFarlane, A.C.** (2002) Howard Florey, Alexander Fleming and the fairy tale of penicillin. *Med J Aust*, **176**(4): p. 176-178.
2. **Tan, S.Y. and Tatsumura, Y.** (2015) Alexander Fleming (1881-1955): Discoverer of penicillin. *Singapore Med J*, **56**(7): p. 366-367.
3. **Duemling, W.W.** (1946) Clinical Experiences with Penicillin in the Navy. *Annals of the New York Academy of Sciences*, **48**(2): p. 201-218.
4. **Bush, K. and Bradford, P.A.** (2016) β-Lactams and β-Lactamase Inhibitors: An Overview. *Cold Spring Harb Perspect Med*, **6**(8).
5. **Levy, S.B. and Marshall, B.** (2004) Antibacterial resistance worldwide: causes, challenges and responses. *Nat Med*, **10**(12 Suppl): p. S122-129.
6. **Morar, M. and Wright, G.D.** (2010) The genomic enzymology of antibiotic resistance. *Annu Rev Genet*, **44**: p. 25-51.
7. **Clardy, J., Fischbach, M.A. and Currie, C.R.** (2009) The natural history of antibiotics. *Curr Biol*, **19**(11): p. R437-441.
8. **Davies, J. and Davies, D.** (2010) Origins and evolution of antibiotic resistance. *Microbiol Mol Biol Rev*, **74**(3): p. 417-433.
9. **Bush, K.** (2010) The coming of age of antibiotics: discovery and therapeutic value. *Ann N Y Acad Sci*, **1213**: p. 1-4.
10. **González, M.M. and Vila, A.J.** (2016) An Elusive Task: A Clinically Useful Inhibitor of Metallo-β-Lactamases. *Top. Med. Chem.*: p. 1-34.
11. **Palzkill, T.** (2013) Metallo-β-lactamase structure and function. *Ann N Y Acad Sci*, **1277**: p. 91-104.
12. **Pacifici, G.M.** (2010) Clinical Pharmacokinetics of Penicillins, Cephalosporins and Aminoglycosides in the Neonate: A Review. *Pharmaceuticals (Basel)*, **3**(8): p. 2568-2591.
13. **Chrystal, E.J.T.e., Wrigley, S.K.e., Thomas, R.e., Nicholson, N.e. and Hayes, M.e.**, Biodiversity : New Leads for the Pharmaceutical and Agrochemical Industries. 1st ed. 2000. 316.
14. **Brogden, R.N., Heel, R.C., Speight, T.M. and Avery, G.S.** (1979) Cefuroxime: a review of its antibacterial activity, pharmacological properties and therapeutic use. *Drugs*, **17**(4): p. 233-266.
15. **Sarap, M.D., Scher, K.S. and Jones, C.W.** (1986) Anaerobic coverage for wound prophylaxis. Comparison of cefazolin and cefoxitin. *Am J Surg*, **151**(2): p. 213-215.
16. **Richards, D.M. and Brogden, R.N.** (1985) Ceftazidime - a Review of Its Antibacterial Activity, Pharmacokinetic Properties and Therapeutic Use. *Drugs*, **29**(2): p. 105-161.
17. **Angelescu, M. and Apostol, A.** (2001) Cefepime (maxipime), large spectrum 4th generation cephalosporin, resistant to β-lactamases. *Chirurgia (Bucur)*, **96**(6): p. 547-552.
18. **Birnbaum, J., Kahan, F.M., Kropp, H. and MacDonald, J.S.** (1985) Carbapenems, a new class of β-lactam antibiotics. Discovery and development of imipenem/cilastatin. *Am J Med*, **78**(6A): p. 3-21.
19. **Papp-Wallace, K.M., Endimiani, A., Taracila, M.A. and Bonomo, R.A.** (2011) Carbapenems: past, present, and future. *Antimicrob Agents Chemother*, **55**(11): p. 4943-4960.

20. **Nukaga, M., Bethel, C.R., Thomson, J.M., Hujer, A.M., Distler, A., Anderson, V.E., Knox, J.R. and Bonomo, R.A.** (2008) Inhibition of class A β-lactamases by carbapenems: crystallographic observation of two conformations of meropenem in SHV-1. *J Am Chem Soc*, **130**(38): p. 12656-12662.
21. **Maveyraud, L., Mourey, L., Kotra, L.P., Pedelacq, J.D., Guillet, V., Mobashery, S. and Samama, J.P.** (1998) Structural basis for clinical longevity of carbapenem antibiotics in the face of challenge by the common class A β-lactamases from the antibiotic-resistant bacteria. *Journal of the American Chemical Society*, **120**(38): p. 9748-9752.
22. **Papadakis, M.A. and McPhee, S.J.** (2016) Current medical diagnosis & treatment 2016. *McGraw-Hill's AccessMedicine*: p. xii, 1,904 p.
23. **Massova, I. and Mobashery, S.** (1998) Kinship and diversification of bacterial penicillin-binding proteins and β-lactamases. *Antimicrob Agents Chemother*, **42**(1): p. 1-17.
24. **Goffin, C. and Ghuysen, J.M.** (1998) Multimodular penicillin-binding proteins: an enigmatic family of orthologs and paralogs. *Microbiol Mol Biol Rev*, **62**(4): p. 1079-1093.
25. **Sauvage, E., Kerff, F., Terrak, M., Ayala, J.A. and Charlier, P.** (2008) The penicillin-binding proteins: structure and role in peptidoglycan biosynthesis. *FEMS Microbiol Rev*, **32**(2): p. 234-258.
26. **Zapun, A., Contreras-Martel, C. and Vernet, T.** (2008) Penicillin-binding proteins and β-lactam resistance. *FEMS Microbiol Rev*, **32**(2): p. 361-385.
27. **Drawz, S.M. and Bonomo, R.A.** (2010) Three decades of β-lactamase inhibitors. *Clin Microbiol Rev*, **23**(1): p. 160-201.
28. **Bayles, K.W.** (2000) The bactericidal action of penicillin: new clues to an unsolved mystery. *Trends Microbiol*, **8**(6): p. 274-278.
29. **Aarestrup, F.M.**, Antimicrobial resistance in bacteria of animal origin. 2006, Washington, D.C.: *ASM Press*. xii, 442 p.
30. **Holland, H.D.** (1997) Evidence for life on Earth more than 3850 million years ago. *Science*, **275**(5296): p. 38-39.
31. **Molton, J.S., Tambyah, P.A., Ang, B.S., Ling, M.L. and Fisher, D.A.** (2013) The global spread of healthcare-associated multidrug-resistant bacteria: a perspective from Asia. *Clin Infect Dis*, **56**(9): p. 1310-1318.
32. **Mellon, M., Benbrook, C. and Benbrook, K.L.**, Hogging it : estimates of antimicrobial abuse in livestock. 2001, Cambridge, MA: *Union of Concerned Scientists*. xiv, 109 p.
33. **Levy, S.B.**, The antibiotic paradox : how miracle drugs are destroying the miracle. 1992, New York: *Plenum Press*. xiv, 279 p.
34. **Normark, B.H. and Normark, S.** (2002) Evolution and spread of antibiotic resistance. *J Intern Med*, **252**(2): p. 91-106.
35. **Nikaido, H.** (2001) Preventing drug access to targets: cell surface permeability barriers and active efflux in bacteria. *Semin Cell Dev Biol*, **12**(3): p. 215-223.
36. **Hall, R.M., Collis, C.M., Kim, M.J., Partridge, S.R., Recchia, G.D. and Stokes, H.W.** (1999) Mobile gene cassettes and integrons in evolution. *Ann N Y Acad Sci*, **870**: p. 68-80.
37. **Wang, H., Dzink-Fox, J.L., Chen, M.J. and Levy, S.B.** (2001) Genetic characterization of highly fluoroquinolone-resistant clinical *Escherichia coli* strains from China: Role of *acrR* mutations. *Antimicrobial Agents and Chemotherapy*, **45**(5): p. 1515-1521.

38. **Schneiders, T., Amyes, S.G.B. and Levy, S.B.** (2003) Role of AcrR and RamA in fluoroquinolone resistance in clinical *Klebsiella pneumoniae* isolates from Singapore. *Antimicrobial Agents and Chemotherapy*, **47**(9): p. 2831-2837.
39. **Anderson, R.M.** (1998) Tuberculosis: old problems and new approaches. *Proc Natl Acad Sci U S A*, **95**(23): p. 13352-13354.
40. **Boucher, H.W., Talbot, G.H., Bradley, J.S., Edwards, J.E., Gilbert, D., Rice, L.B., Scheld, M., Spellberg, B. and Bartlett, J.** (2009) Bad bugs, no drugs: no ESKAPE! An update from the Infectious Diseases Society of America. *Clin Infect Dis*, **48**(1): p. 1-12.
41. **Lim, D. and Strynadka, N.C.** (2002) Structural basis for the β-lactam resistance of PBP2a from methicillin-resistant *Staphylococcus aureus*. *Nat Struct Biol*, **9**(11): p. 870-876.
42. **Spika, J.S., Waterman, S.H., Hoo, G.W.S., Stlouis, M.E., Pacer, R.E., James, S.M., Bissett, M.L., Mayer, L.W., Chiu, J.Y., Hall, B., Greene, K., Potter, M.E., Cohen, M.L. and Blake, P.A.** (1987) Chloramphenicol-Resistant *Salmonella*-Newport Traced through Hamburger to Dairy Farms - a Major Persisting Source of Human Salmonellosis in California. *New England Journal of Medicine*, **316**(10): p. 565-570.
43. **Doumith, M., Ellington, M.J., Livermore, D.M. and Woodford, N.** (2009) Molecular mechanisms disrupting porin expression in ertapenem-resistant *Klebsiella* and *Enterobacter* spp. clinical isolates from the UK. *J Antimicrob Chemother*, **63**(4): p. 659-667.
44. **Webber, M.A. and Piddock, L.J.** (2003) The importance of efflux pumps in bacterial antibiotic resistance. *J Antimicrob Chemother*, **51**(1): p. 9-11.
45. **Poole, K.** (2004) Efflux-mediated multiresistance in Gram-negative bacteria. *Clin Microbiol Infect*, **10**(1): p. 12-26.
46. **Heritier, C., Poirel, L., Lambert, T. and Nordmann, P.** (2005) Contribution of acquired carbapenem-hydrolyzing oxacillinases to carbapenem resistance in *Acinetobacter baumannii*. *Antimicrob Agents Chemother*, **49**(8): p. 3198-3202.
47. **Paulsen, I.T., Brown, M.H. and Skurray, R.A.** (1996) Proton-dependent multidrug efflux systems. *Microbiol Rev*, **60**(4): p. 575-608.
48. **Abraham, E.P. and Chain, E.** (1940) An enzyme from bacteria able to destroy penicillin. *Nature*, **146**: p. 837-837.
49. **Abraham, E.P., Demain, A.L. and Solomon, N.A.**, Antibiotics containing the β-lactam structure. Handbook of experimental pharmacology. 1983, Berlin ; New York: *Springer-Verlag*. 360
50. **Knox, J.R., Moews, P.C. and Frere, J.M.** (1996) Molecular evolution of bacterial β-lactam resistance. *Chem Biol*, **3**(11): p. 937-947.
51. **Fisher, J.F., Meroueh, S.O. and Mobashery, S.** (2005) Bacterial resistance to β-lactam antibiotics: compelling opportunism, compelling opportunity. *Chem Rev*, **105**(2): p. 395-424.
52. **Medeiros, A.A.** (1997) Evolution and dissemination of β-lactamases accelerated by generations of β-lactam antibiotics. *Clin Infect Dis*, **24 Suppl 1**: p. S19-45.
53. **Bush, K.** (2013) The ABCD's of β-lactamase nomenclature. *J Infect Chemother*, **19**(4): p. 549-559.
54. **Bush, K., Jacoby, G.A. and Medeiros, A.A.** (1995) A functional classification scheme for β-lactamases and its correlation with molecular structure. *Antimicrob Agents Chemother*, **39**(6): p. 1211-1233.

55. **Bush, K. and Jacoby, G.A.** (2010) Updated functional classification of β-lactamases. *Antimicrob Agents Chemother*, **54**(3): p. 969-976.
56. **Jaurin, B. and Grundstrom, T.** (1981) ampC cephalosporinase of *Escherichia coli* K-12 has a different evolutionary origin from that of β-lactamases of the penicillinase type. *Proc Natl Acad Sci U S A*, **78**(8): p. 4897-4901.
57. **Huovinen, P., Huovinen, S. and Jacoby, G.A.** (1988) Sequence of PSE-2 β-lactamase. *Antimicrob Agents Chemother*, **32**(1): p. 134-136.
58. **Poirel, L., Naas, T. and Nordmann, P.** (2010) Diversity, epidemiology, and genetics of class D β-lactamases. *Antimicrob Agents Chemother*, **54**(1): p. 24-38.
59. **Yong, D., Toleman, M.A., Giske, C.G., Cho, H.S., Sundman, K., Lee, K. and Walsh, T.R.** (2009) Characterization of a new metallo-β-lactamase gene, bla_{NDM-1}, and a novel erythromycin esterase gene carried on a unique genetic structure in *Klebsiella pneumoniae* sequence type 14 from India. *Antimicrob Agents Chemother*, **53**(12): p. 5046-5054.
60. **Walsh, T.R., Toleman, M.A., Poirel, L. and Nordmann, P.** (2005) Metallo-β-lactamases: the quiet before the storm? *Clin Microbiol Rev*, **18**(2): p. 306-325.
61. **Cornaglia, G., Giamarellou, H. and Rossolini, G.M.** (2011) Metallo-β-lactamases: a last frontier for β-lactams? *Lancet Infect Dis*, **11**(5): p. 381-393.
62. **Bebrone, C.** (2007) Metallo-β-lactamases (classification, activity, genetic organization, structure, zinc coordination) and their superfamily. *Biochem Pharmacol*, **74**(12): p. 1686-1701.
63. **Poeylaut-Palena, A.A., Tomatis, P.E., Karsisiotis, A.I., Damblon, C., Mata, E.G. and Vila, A.J.** (2007) A minimalistic approach to identify substrate binding features in B1 Metallo-β-lactamases. *Bioorg Med Chem Lett*, **17**(18): p. 5171-5174.
64. **Sabath, L.D. and Abraham, E.P.** (1966) Zinc as a Cofactor for Cephalosporinase from *Bacillus Cereus* 569. *Biochemical Journal*, **98**(1): p. C11-&.
65. **Walsh, T.R., Hall, L., Assinder, S.J., Nichols, W.W., Cartwright, S.J., MacGowan, A.P. and Bennett, P.M.** (1994) Sequence analysis of the L1 metallo-β-lactamase from *Xanthomonas maltophilia*. *Biochim Biophys Acta*, **1218**(2): p. 199-201.
66. **Cuchural, G.J., Jr., Malamy, M.H. and Tally, F.P.** (1986) β-lactamase-mediated imipenem resistance in *Bacteroides fragilis*. *Antimicrob Agents Chemother*, **30**(5): p. 645-648.
67. **Rossolini, G.M., Franceschini, N., Riccio, M.L., Mercuri, P.S., Perilli, M., Galleni, M., Frere, J.M. and Amicosante, G.** (1998) Characterization and sequence of the *Chryseobacterium (Flavobacterium) meningosepticum* carbapenemase: a new molecular class B β-lactamase showing a broad substrate profile. *Biochem J*, **332 (Pt 1)**: p. 145-152.
68. **Bellais, S., Leotard, S., Poirel, L., Naas, T. and Nordmann, P.** (1999) Molecular characterization of a carbapenem-hydrolyzing β-lactamase from *Chryseobacterium (Flavobacterium) indologenes*. *FEMS Microbiol Lett*, **171**(2): p. 127-132.
69. **Moran-Barrio, J., Gonzalez, J.M., Lisa, M.N., Costello, A.L., Peraro, M.D., Carloni, P., Bennett, B., Tierney, D.L., Limansky, A.S., Viale, A.M. and Vila, A.J.** (2007) The metallo-β-lactamase GOB is a mono-Zn(II) enzyme with a novel active site. *J Biol Chem*, **282**(25): p. 18286-18293.
70. **Shannon, K., King, A. and Phillips, I.** (1986) β-lactamases with high activity against imipenem and Sch 34343 from *Aeromonas hydrophila*. *J Antimicrob Chemother*, **17**(1): p. 45-50.

71. **Walsh, T.R., Neville, W.A., Haran, M.H., Tolson, D., Payne, D.J., Bateson, J.H., MacGowan, A.P. and Bennett, P.M.** (1998) Nucleotide and amino acid sequences of the metallo-β-lactamase, ImiS, from *Aeromonas veronii* bv. sobria. *Antimicrob Agents Chemother*, **42**(2): p. 436-439.
72. **Ito, H., Arakawa, Y., Ohsuka, S., Wacharotayankun, R., Kato, N. and Ohta, M.** (1995) Plasmid-mediated dissemination of the metallo-β-lactamase gene *bla*$_{IMP}$ among clinically isolated strains of *Serratia marcescens*. *Antimicrob Agents Chemother*, **39**(4): p. 824-829.
73. **Nordmann, P., Naas, T. and Poirel, L.** (2011) Global spread of Carbapenemase-producing *Enterobacteriaceae*. *Emerg Infect Dis*, **17**(10): p. 1791-1798.
74. **Laraki, N., Galleni, M., Thamm, I., Riccio, M.L., Amicosante, G., Frere, J.M. and Rossolini, G.M.** (1999) Structure of In31, a *bla*$_{IMP}$-containing *Pseudomonas aeruginosa* integron phyletically related to In5, which carries an unusual array of gene cassettes. *Antimicrob Agents Chemother*, **43**(4): p. 890-901.
75. **Lauretti, L., Riccio, M.L., Mazzariol, A., Cornaglia, G., Amicosante, G., Fontana, R. and Rossolini, G.M.** (1999) Cloning and characterization of *bla*$_{VIM}$, a new integron-borne metallo-β-lactamase gene from a *Pseudomonas aeruginosa* clinical isolate. *Antimicrob Agents Chemother*, **43**(7): p. 1584-1590.
76. **Bennett, P.M.** (2008) Plasmid encoded antibiotic resistance: acquisition and transfer of antibiotic resistance genes in bacteria. *Br J Pharmacol*, **153 Suppl 1**: p. S347-357.
77. **Moran-Barrio, J., Limansky, A.S. and Viale, A.M.** (2009) Secretion of GOB metallo-β-lactamase in *Escherichia coli* depends strictly on the cooperation between the cytoplasmic DnaK chaperone system and the Sec machinery: completion of folding and Zn(II) ion acquisition occur in the bacterial periplasm. *Antimicrob Agents Chemother*, **53**(7): p. 2908-2917.
78. **Meini, M.R., Gonzalez, L.J. and Vila, A.J.** (2013) Antibiotic resistance in Zn(II)-deficient environments: metallo-β-lactamase activation in the periplasm. *Future Microbiol*, **8**(8): p. 947-979.
79. **Garau, G., Garcia-Saez, I., Bebrone, C., Anne, C., Mercuri, P., Galleni, M., Frere, J.M. and Dideberg, O.** (2004) Update of the standard numbering scheme for class B β-lactamases. *Antimicrob Agents Chemother*, **48**(7): p. 2347-2349.
80. **Pettinati, I., Brem, J., Lee, S.Y., McHugh, P.J. and Schofield, C.J.** (2016) The Chemical Biology of Human Metallo-β-Lactamase Fold Proteins. *Trends Biochem Sci*, **41**(4): p. 338-355.
81. **Carfi, A., Pares, S., Duee, E., Galleni, M., Duez, C., Frere, J.M. and Dideberg, O.** (1995) The 3-D structure of a zinc metallo-β-lactamase from *Bacillus cereus* reveals a new type of protein fold. *EMBO J*, **14**(20): p. 4914-4921.
82. **Concha, N.O., Rasmussen, B.A., Bush, K. and Herzberg, O.** (1996) Crystal structure of the wide-spectrum binuclear zinc β-lactamase from *Bacteroides fragilis*. *Structure*, **4**(7): p. 823-836.
83. **Carfi, A., Duee, E., Galleni, M., Frere, J.M. and Dideberg, O.** (1998) 1.85 Å resolution structure of the zinc (II) β-lactamase from *Bacillus cereus*. *Acta Crystallogr D Biol Crystallogr*, **54**(Pt 3): p. 313-323.
84. **Concha, N.O., Janson, C.A., Rowling, P., Pearson, S., Cheever, C.A., Clarke, B.P., Lewis, C., Galleni, M., Frere, J.M., Payne, D.J., Bateson, J.H. and Abdel-Meguid, S.S.** (2000) Crystal structure of the IMP-1 metallo β-lactamase from *Pseudomonas aeruginosa* and

its complex with a mercaptocarboxylate inhibitor: binding determinants of a potent, broad-spectrum inhibitor. *Biochemistry*, **39**(15): p. 4288-4298.

85. **Garcia-Saez, I., Hopkins, J., Papamicael, C., Franceschini, N., Amicosante, G., Rossolini, G.M., Galleni, M., Frere, J.M. and Dideberg, O.** (2003) The 1.5-Å structure of *Chryseobacterium meningosepticum* zinc β-lactamase in complex with the inhibitor, D-captopril. *J Biol Chem*, **278**(26): p. 23868-23873.
86. **Garcia-Saez, I., Docquier, J.D., Rossolini, G.M. and Dideberg, O.** (2008) The three-dimensional structure of VIM-2, a Zn-β-lactamase from *Pseudomonas aeruginosa* in its reduced and oxidised form. *J Mol Biol*, **375**(3): p. 604-611.
87. **Borra, P.S., Leiros, H.K., Ahmad, R., Spencer, J., Leiros, I., Walsh, T.R., Sundsfjord, A. and Samuelsen, Ø.** (2011) Structural and computational investigations of VIM-7: insights into the substrate specificity of VIM metallo-β-lactamases. *J Mol Biol*, **411**(1): p. 174-189.
88. **Murphy, T.A., Catto, L.E., Halford, S.E., Hadfield, A.T., Minor, W., Walsh, T.R. and Spencer, J.** (2006) Crystal structure of *Pseudomonas aeruginosa* SPM-1 provides insights into variable zinc affinity of metallo-β-lactamases. *J Mol Biol*, **357**(3): p. 890-903.
89. **King, D. and Strynadka, N.** (2011) Crystal structure of New Delhi metallo-β-lactamase reveals molecular basis for antibiotic resistance. *Protein Sci*, **20**(9): p. 1484-1491.
90. **Borra, P.S., Samuelsen, Ø., Spencer, J., Walsh, T.R., Lorentzen, M.S. and Leiros, H.K.** (2013) Crystal structures of *Pseudomonas aeruginosa* GIM-1: active-site plasticity in metallo-β-lactamases. *Antimicrob Agents Chemother*, **57**(2): p. 848-854.
91. **Garau, G., Bebrone, C., Anne, C., Galleni, M., Frere, J.M. and Dideberg, O.** (2005) A metallo-β-lactamase enzyme in action: crystal structures of the monozinc carbapenemase CphA and its complex with biapenem. *J Mol Biol*, **345**(4): p. 785-795.
92. **Ullah, J.H., Walsh, T.R., Taylor, I.A., Emery, D.C., Verma, C.S., Gamblin, S.J. and Spencer, J.** (1998) The crystal structure of the L1 metallo-β-lactamase from *Stenotrophomonas maltophilia* at 1.7 Å resolution. *J Mol Biol*, **284**(1): p. 125-136.
93. **Garcia-Saez, I., Mercuri, P.S., Papamicael, C., Kahn, R., Frere, J.M., Galleni, M., Rossolini, G.M. and Dideberg, O.** (2003) Three-dimensional structure of FEZ-1, a monomeric subclass B3 metallo-β-lactamase from *Fluoribacter gormanii*, in native form and in complex with D-captopril. *J Mol Biol*, **325**(4): p. 651-660.
94. **Leiros, H.K., Borra, P.S., Brandsdal, B.O., Edvardsen, K.S., Spencer, J., Walsh, T.R. and Samuelsen, Ø.** (2012) Crystal structure of the mobile metallo-β-lactamase AIM-1 from *Pseudomonas aeruginosa*: insights into antibiotic binding and the role of Gln157. *Antimicrob Agents Chemother*, **56**(8): p. 4341-4353.
95. **Docquier, J.D., Benvenuti, M., Calderone, V., Stoczko, M., Menciassi, N., Rossolini, G.M. and Mangani, S.** (2010) High-resolution crystal structure of the subclass B3 metallo-β-lactamase BJP-1: rational basis for substrate specificity and interaction with sulfonamides. *Antimicrob Agents Chemother*, **54**(10): p. 4343-4351.
96. **Meini, M.R., Llarrull, L.I. and Vila, A.J.** (2014) Evolution of Metallo-β-lactamases: Trends Revealed by Natural Diversity and in vitro Evolution. *Antibiotics (Basel)*, **3**(3): p. 285-316.
97. **Patel, G. and Bonomo, R.A.** (2013) "Stormy waters ahead": global emergence of carbapenemases. *Frontiers in Microbiology*, **4**.
98. **de Seny, D., Heinz, U., Wommer, S., Kiefer, M., Meyer-Klaucke, W., Galleni, M., Frere, J.M., Bauer, R. and Adolph, H.W.** (2001) Metal ion binding and coordination geometry

for wild type and mutants of metallo-β-lactamase from *Bacillus cereus* 569/H/9 (BcII): a combined thermodynamic, kinetic, and spectroscopic approach. *J Biol Chem*, **276**(48): p. 45065-45078.

99. **King, D.T., Worrall, L.J., Gruninger, R. and Strynadka, N.C.** (2012) New Delhi metallo-β-lactamase: structural insights into β-lactam recognition and inhibition. *J Am Chem Soc*, **134**(28): p. 11362-11365.
100. **Lim, H.M., Pene, J.J. and Shaw, R.W.** (1988) Cloning, nucleotide sequence, and expression of the *Bacillus cereus* 5/B/6 β-lactamase II structural gene. *J Bacteriol*, **170**(6): p. 2873-2878.
101. **Rasmussen, B.A., Gluzman, Y. and Tally, F.P.** (1990) Cloning and sequencing of the class B β-lactamase gene (ccrA) from *Bacteroides fragilis* TAL3636. *Antimicrob Agents Chemother*, **34**(8): p. 1590-1592.
102. **Zhao, W.H. and Hu, Z.Q.** (2011) IMP-type metallo-β-lactamases in Gram-negative bacilli: distribution, phylogeny, and association with integrons. *Crit Rev Microbiol*, **37**(3): p. 214-226.
103. **Castanheira, M., Toleman, M.A., Jones, R.N., Schmidt, F.J. and Walsh, T.R.** (2004) Molecular characterization of a β-lactamase gene, *bla*$_{GIM-1}$, encoding a new subclass of metallo-β-lactamase. *Antimicrob Agents Chemother*, **48**(12): p. 4654-4661.
104. **El Salabi, A., Borra, P.S., Toleman, M.A., Samuelsen, Ø. and Walsh, T.R.** (2012) Genetic and biochemical characterization of a novel metallo-β-lactamase, TMB-1, from an *Achromobacter xylosoxidans* strain isolated in Tripoli, Libya. *Antimicrob Agents Chemother*, **56**(5): p. 2241-2245.
105. **Toleman, M.A., Simm, A.M., Murphy, T.A., Gales, A.C., Biedenbach, D.J., Jones, R.N. and Walsh, T.R.** (2002) Molecular characterization of SPM-1, a novel metallo-β-lactamase isolated in Latin America: report from the SENTRY antimicrobial surveillance programme. *J Antimicrob Chemother*, **50**(5): p. 673-679.
106. **Bebrone, C., Delbruck, H., Kupper, M.B., Schlomer, P., Willmann, C., Frere, J.M., Fischer, R., Galleni, M. and Hoffmann, K.M.** (2009) The structure of the dizinc subclass B2 metallo-β-lactamase CphA reveals that the second inhibitory zinc ion binds in the histidine site. *Antimicrob Agents Chemother*, **53**(10): p. 4464-4471.
107. **Hall, B.G., Salipante, S.J. and Barlow, M.** (2003) The metallo-β-lactamases fall into two distinct phylogenetic groups. *Journal of Molecular Evolution*, **57**(3): p. 249-254.
108. **Massidda, O., Rossolini, G.M. and Satta, G.** (1991) The *Aeromonas hydrophila* cphA gene: molecular heterogeneity among class B metallo-β-lactamases. *J Bacteriol*, **173**(15): p. 4611-4617.
109. **Saavedra, M.J., Peixe, L., Sousa, J.C., Henriques, I., Alves, A. and Correia, A.** (2003) Sfh-I, a subclass B2 metallo-β-lactamase from a *Serratia fonticola* environmental isolate. *Antimicrob Agents Chemother*, **47**(7): p. 2330-2333.
110. **Bellais, S., Poirel, L., Leotard, S., Naas, T. and Nordmann, P.** (2000) Genetic diversity of carbapenem-hydrolyzing metallo-β-lactamases from *Chryseobacterium (Flavobacterium) indologenes*. *Antimicrob Agents Chemother*, **44**(11): p. 3028-3034.
111. **Boschi, L., Mercuri, P.S., Riccio, M.L., Amicosante, G., Galleni, M., Frere, J.M. and Rossolini, G.M.** (2000) The *Legionella (Fluoribacter) gormanii* metallo-β-lactamase: a new member of the highly divergent lineage of molecular-subclass B3 β-lactamases. *Antimicrob Agents Chemother*, **44**(6): p. 1538-1543.

112. **Avison, M.B., Higgins, C.S., von Heldreich, C.J., Bennett, P.M. and Walsh, T.R.** (2001) Plasmid location and molecular heterogeneity of the L1 and L2 β-lactamase genes of *Stenotrophomonas maltophilia*. *Antimicrob Agents Chemother*, **45**(2): p. 413-419.
113. **Yong, D., Toleman, M.A., Bell, J., Ritchie, B., Pratt, R., Ryley, H. and Walsh, T.R.** (2012) Genetic and biochemical characterization of an acquired subgroup B3 metallo-β-lactamase gene, *bla*$_{AIM-1}$, and its unique genetic context in *Pseudomonas aeruginosa* from Australia. *Antimicrob Agents Chemother*, **56**(12): p. 6154-6159.
114. **Moali, C., Anne, C., Lamotte-Brasseur, J., Groslambert, S., Devreese, B., Van Beeumen, J., Galleni, M. and Frere, J.M.** (2003) Analysis of the importance of the metallo-β-lactamase active site loop in substrate binding and catalysis. *Chem Biol*, **10**(4): p. 319-329.
115. **Carenbauer, A.L., Garrity, J.D., Periyannan, G., Yates, R.B. and Crowder, M.W.** (2002) Probing substrate binding to metallo-β-lactamase L1 from *Stenotrophomonas maltophilia* by using site-directed mutagenesis. *BMC Biochem*, **3**: p. 4.
116. **Spencer, J., Read, J., Sessions, R.B., Howell, S., Blackburn, G.M. and Gamblin, S.J.** (2005) Antibiotic recognition by binuclear metallo-β-lactamases revealed by X-ray crystallography. *J Am Chem Soc*, **127**(41): p. 14439-14444.
117. *The PyMOL Molecular Graphics System*, Schrödinger, LLC.
118. **de Seny, D., Prosperi-Meys, C., Bebrone, C., Rossolini, G.M., Page, M.I., Noel, P., Frere, J.M. and Galleni, M.** (2002) Mutational analysis of the two zinc-binding sites of the *Bacillus cereus* 569/H/9 metallo-β-lactamase. *Biochem J*, **363**(Pt 3): p. 687-696.
119. **Wommer, S., Rival, S., Heinz, U., Galleni, M., Frere, J.M., Franceschini, N., Amicosante, G., Rasmussen, B., Bauer, R. and Adolph, H.W.** (2002) Substrate-activated zinc binding of metallo-β-lactamases: physiological importance of mononuclear enzymes. *J Biol Chem*, **277**(27): p. 24142-24147.
120. **Vanhove, M., Zakhem, M., Devreese, B., Franceschini, N., Anne, C., Bebrone, C., Amicosante, G., Rossolini, G.M., Van Beeumen, J., Frere, J.M. and Galleni, M.** (2003) Role of Cys221 and Asn116 in the zinc-binding sites of the *Aeromonas hydrophila* metallo-β-lactamase. *Cell Mol Life Sci*, **60**(11): p. 2501-2509.
121. **Crawford, P.A., Yang, K.W., Sharma, N., Bennett, B. and Crowder, M.W.** (2005) Spectroscopic studies on cobalt(II)-substituted metallo-β-lactamase ImiS from *Aeromonas veronii* bv. *sobria*. *Biochemistry*, **44**(13): p. 5168-5176.
122. **Sharma, N.P., Hajdin, C., Chandrasekar, S., Bennett, B., Yang, K.W. and Crowder, M.W.** (2006) Mechanistic studies on the mononuclear ZnII-containing metallo-β-lactamase ImiS from *Aeromonas sobria*. *Biochemistry*, **45**(35): p. 10729-10738.
123. **Moran-Barrio, J., Lisa, M.N., Larrieux, N., Drusin, S.I., Viale, A.M., Moreno, D.M., Buschiazzo, A. and Vila, A.J.** (2016) Crystal Structure of the Metallo-β-Lactamase GOB in the Periplasmic Dizinc Form Reveals an Unusual Metal Site. *Antimicrob Agents Chemother*, **60**(10): p. 6013-6022.
124. **Costello, A., Periyannan, G., Yang, K.W., Crowder, M.W. and Tierney, D.L.** (2006) Site-selective binding of Zn(II) to metallo-β-lactamase L1 from *Stenotrophomonas maltophilia*. *J Biol Inorg Chem*, **11**(3): p. 351-358.
125. **Crowder, M.W., Spencer, J. and Vila, A.J.** (2006) Metallo-β-lactamases: novel weaponry for antibiotic resistance in bacteria. *Acc Chem Res*, **39**(10): p. 721-728.
126. **Zhang, H. and Hao, Q.** (2011) Crystal structure of NDM-1 reveals a common β-lactam hydrolysis mechanism. *FASEB J*, **25**(8): p. 2574-2582.

127. **Park, H., Brothers, E.N. and Merz, K.M., Jr.** (2005) Hybrid QM/MM and DFT investigations of the catalytic mechanism and inhibition of the dinuclear zinc metallo-β-lactamase CcrA from *Bacteroides fragilis*. *J Am Chem Soc*, **127**(12): p. 4232-4241.
128. **Wang, Z., Fast, W. and Benkovic, S.J.** (1999) On the mechanism of the metallo-β-lactamase from *Bacteroides fragilis*. *Biochemistry*, **38**(31): p. 10013-10023.
129. **Meini, M.R., Llarrull, L.I. and Vila, A.J.** (2015) Overcoming differences: The catalytic mechanism of metallo-β-lactamases. *FEBS Lett*, **589**(22): p. 3419-3432.
130. **Tioni, M.F., Llarrull, L.I., Poeylaut-Palena, A.A., Marti, M.A., Saggu, M., Periyannan, G.R., Mata, E.G., Bennett, B., Murgida, D.H. and Vila, A.J.** (2008) Trapping and characterization of a reaction intermediate in carbapenem hydrolysis by *B. cereus* metallo-β-lactamase. *J Am Chem Soc*, **130**(47): p. 15852-15863.
131. **Fonseca, F., Bromley, E.H., Saavedra, M.J., Correia, A. and Spencer, J.** (2011) Crystal structure of *Serratia fonticola* Sfh-I: activation of the nucleophile in mono-zinc metallo-β-lactamases. *J Mol Biol*, **411**(5): p. 951-959.
132. **Llarrull, L.I., Tioni, M.F., Kowalski, J., Bennett, B. and Vila, A.J.** (2007) Evidence for a dinuclear active site in the metallo-β-lactamase BcII with substoichiometric Co(II). A new model for metal uptake. *J Biol Chem*, **282**(42): p. 30586-30595.
133. **Yang, H., Aitha, M., Marts, A.R., Hetrick, A., Bennett, B., Crowder, M.W. and Tierney, D.L.** (2014) Spectroscopic and mechanistic studies of heterodimetallic forms of metallo-β-lactamase NDM-1. *J Am Chem Soc*, **136**(20): p. 7273-7285.
134. **Aitha, M., Marts, A.R., Bergstrom, A., Moller, A.J., Moritz, L., Turner, L., Nix, J.C., Bonomo, R.A., Page, R.C., Tierney, D.L. and Crowder, M.W.** (2014) Biochemical, mechanistic, and spectroscopic characterization of metallo-β-lactamase VIM-2. *Biochemistry*, **53**(46): p. 7321-7331.
135. **Garrity, J.D., Bennett, B. and Crowder, M.W.** (2005) Direct evidence that the reaction intermediate of metallo-β-lactamase L1 is metal bound. *Biochemistry*, **44**(3): p. 1078-1087.
136. **Bicknell, R., Schaffer, A., Waley, S.G. and Auld, D.S.** (1986) Changes in the coordination geometry of the active-site metal during catalysis of benzylpenicillin hydrolysis by *Bacillus cereus* β-lactamase II. *Biochemistry*, **25**(22): p. 7208-7215.
137. **Bicknell, R. and Waley, S.G.** (1985) Cryoenzymology of *Bacillus cereus* β-lactamase II. *Biochemistry*, **24**(24): p. 6876-6887.
138. **Llarrull, L.I., Tioni, M.F. and Vila, A.J.** (2008) Metal content and localization during turnover in *B. cereus* metallo-β-lactamase. *J Am Chem Soc*, **130**(47): p. 15842-15851.
139. **Wang, Z.G., Fast, W. and Benkovic, S.J.** (1998) Direct observation of an enzyme-bound intermediate in the catalytic cycle of the metallo-β-lactamase from *Bacteroides fragilis*. *Journal of the American Chemical Society*, **120**(41): p. 10788-10789.
140. **McManus-Munoz, S. and Crowder, M.W.** (1999) Kinetic mechanism of metallo-β-lactamase L1 from *Stenotrophomonas maltophilia*. *Biochemistry*, **38**(5): p. 1547-1553.
141. **Lisa, M.N., Hemmingsen, L. and Vila, A.J.** (2010) Catalytic role of the metal ion in the metallo-β-lactamase GOB. *J Biol Chem*, **285**(7): p. 4570-4577.
142. **Hu, Z., Periyannan, G., Bennett, B. and Crowder, M.W.** (2008) Role of the Zn1 and Zn2 sites in metallo-β-lactamase L1. *J Am Chem Soc*, **130**(43): p. 14207-14216.
143. **Hawk, M.J., Breece, R.M., Hajdin, C.E., Bender, K.M., Hu, Z., Costello, A.L., Bennett, B., Tierney, D.L. and Crowder, M.W.** (2009) Differential binding of Co(II) and Zn(II) to metallo-β-lactamase Bla2 from *Bacillus anthracis*. *J Am Chem Soc*, **131**(30): p. 10753-10762.

144. **Huntley, J.J., Fast, W., Benkovic, S.J., Wright, P.E. and Dyson, H.J.** (2003) Role of a solvent-exposed tryptophan in the recognition and binding of antibiotic substrates for a metallo-β-lactamase. *Protein Sci*, **12**(7): p. 1368-1375.
145. **Tripathi, R. and Nair, N.N.** (2015) Mechanism of Meropenem Hydrolysis by New Delhi Metallo β-Lactamase. *Acs Catalysis*, **5**(4): p. 2577-2586.
146. **Brem, J., Struwe, W.B., Rydzik, A.M., Tarhonskaya, H., Pfeffer, I., Flashman, E., van Berkel, S.S., Spencer, J., Claridge, T.D.W., McDonough, M.A., Benesch, J.L.P. and Schofield, C.J.** (2015) Studying the active-site loop movement of the Sao Paolo metallo-β-lactamase-1. *Chemical Science*, **6**(2): p. 956-963.
147. **Materon, I.C., Beharry, Z., Huang, W., Perez, C. and Palzkill, T.** (2004) Analysis of the context dependent sequence requirements of active site residues in the metallo-β-lactamase IMP-1. *J Mol Biol*, **344**(3): p. 653-663.
148. **Gonzalez, L.J., Moreno, D.M., Bonomo, R.A. and Vila, A.J.** (2014) Host-specific enzyme-substrate interactions in SPM-1 metallo-β-lactamase are modulated by second sphere residues. *PLoS Pathog*, **10**(1): p. e1003817.
149. **Yang, Y., Keeney, D., Tang, X., Canfield, N. and Rasmussen, B.A.** (1999) Kinetic properties and metal content of the metallo-β-lactamase CcrA harboring selective amino acid substitutions. *J Biol Chem*, **274**(22): p. 15706-15711.
150. **Haruta, S., Yamaguchi, H., Yamamoto, E.T., Eriguchi, Y., Nukaga, M., O'Hara, K. and Sawai, T.** (2000) Functional analysis of the active site of a metallo-β-lactamase proliferating in Japan. *Antimicrob Agents Chemother*, **44**(9): p. 2304-2309.
151. **Horton, L.B., Shanker, S., Mikulski, R., Brown, N.G., Phillips, K.J., Lykissa, E., Venkataram Prasad, B.V. and Palzkill, T.** (2012) Mutagenesis of zinc ligand residue Cys221 reveals plasticity in the IMP-1 metallo-β-lactamase active site. *Antimicrob Agents Chemother*, **56**(11): p. 5667-5677.
152. **Feng, H., Ding, J., Zhu, D., Liu, X., Xu, X., Zhang, Y., Zang, S., Wang, D.C. and Liu, W.** (2014) Structural and mechanistic insights into NDM-1 catalyzed hydrolysis of cephalosporins. *J Am Chem Soc*, **136**(42): p. 14694-14697.
153. **Yamaguchi, Y., Jin, W., Matsunaga, K., Ikemizu, S., Yamagata, Y., Wachino, J., Shibata, N., Arakawa, Y. and Kurosaki, H.** (2007) Crystallographic investigation of the inhibition mode of a VIM-2 metallo-β-lactamase from *Pseudomonas aeruginosa* by a mercaptocarboxylate inhibitor. *J Med Chem*, **50**(26): p. 6647-6653.
154. **Christopeit, T., Yang, K.W., Yang, S.K. and Leiros, H.K.** (2016) The structure of the metallo-β-lactamase VIM-2 in complex with a triazolylthioacetamide inhibitor. *Acta Crystallogr F Struct Biol Commun*, **72**(Pt 11): p. 813-819.
155. **Scrofani, S.D., Chung, J., Huntley, J.J., Benkovic, S.J., Wright, P.E. and Dyson, H.J.** (1999) NMR characterization of the metallo-β-lactamase from *Bacteroides fragilis* and its interaction with a tight-binding inhibitor: role of an active-site loop. *Biochemistry*, **38**(44): p. 14507-14514.
156. **Gonzalez, J.M., Buschiazzo, A. and Vila, A.J.** (2010) Evidence of Adaptability in Metal Coordination Geometry and Active-Site Loop Conformation among B1 Metallo-β-lactamases. *Biochemistry*, **49**(36): p. 7930-7938.
157. **Borgianni, L., Vandenameele, J., Matagne, A., Bini, L., Bonomo, R.A., Frere, J.M., Rossolini, G.M. and Docquier, J.D.** (2010) Mutational analysis of VIM-2 reveals an essential determinant for metallo-β-lactamase stability and folding. *Antimicrob Agents Chemother*, **54**(8): p. 3197-3204.

158. **Toney, J.H., Hammond, G.G., Fitzgerald, P.M.D., Sharma, N., Balkovec, J.M., Rouen, G.P., Olson, S.H., Hammond, M.L., Greenlee, M.L. and Gao, Y.D.** (2001) Succinic acids as potent inhibitors of plasmid-borne IMP-1 metallo-β-lactamase. *Journal of Biological Chemistry*, **276**(34): p. 31913-31918.
159. **Christopeit, T., Carlsen, T.J., Helland, R. and Leiros, H.K.** (2015) Discovery of Novel Inhibitor Scaffolds against the Metallo-β-lactamase VIM-2 by Surface Plasmon Resonance (SPR) Based Fragment Screening. *J Med Chem*, **58**(21): p. 8671-8682.
160. **Hiraiwa, Y., Saito, J., Watanabe, T., Yamada, M., Morinaka, A., Fukushima, T. and Kudo, T.** (2014) X-ray crystallographic analysis of IMP-1 metallo-β-lactamase complexed with a 3-aminophthalic acid derivative, structure-based drug design, and synthesis of 3,6-disubstituted phthalic acid derivative inhibitors. *Bioorg Med Chem Lett*, **24**(20): p. 4891-4894.
161. **Brem, J., van Berkel, S.S., Zollman, D., Lee, S.Y., Gileadi, O., McHugh, P.J., Walsh, T.R., McDonough, M.A. and Schofield, C.J.** (2015) Structural Basis of Metallo-β-Lactamase Inhibition by Captopril Stereoisomers. *Antimicrob Agents Chemother*, **60**(1): p. 142-150.
162. **Hinchliffe, P., Gonzalez, M.M., Mojica, M.F., Gonzalez, J.M., Castillo, V., Saiz, C., Kosmopoulou, M., Tooke, C.L., Llarrull, L.I., Mahler, G., Bonomo, R.A., Vila, A.J. and Spencer, J.** (2016) Cross-class metallo-β-lactamase inhibition by bisthiazolidines reveals multiple binding modes. *Proc Natl Acad Sci U S A*, **113**(26): p. E3745-3754.
163. **Materon, I.C. and Palzkill, T.** (2001) Identification of residues critical for metallo-β-lactamase function by codon randomization and selection. *Protein Science*, **10**(12): p. 2556-2565.
164. **Haruta, S., Yamamoto, E.T., Eriguchi, Y. and Sawai, T.** (2001) Characterization of the active-site residues asparagine 167 and lysine 161 of the IMP-1 metallo-β-lactamase. *FEMS Microbiol Lett*, **197**(1): p. 85-89.
165. **Leiros, H.K., Edvardsen, K.S., Bjerga, G.E. and Samuelsen, Ø.** (2015) Structural and biochemical characterization of VIM-26 shows that Leu224 has implications for the substrate specificity of VIM metallo-β-lactamases. *FEBS J*, **282**(6): p. 1031-1042.
166. **Merino, M., Perez-Llarena, F.J., Kerff, F., Poza, M., Mallo, S., Rumbo-Feal, S., Beceiro, A., Juan, C., Oliver, A. and Bou, G.** (2010) Role of changes in the L3 loop of the active site in the evolution of enzymatic activity of VIM-type metallo-β-lactamases. *J Antimicrob Chemother*, **65**(9): p. 1950-1954.
167. **Brem, J., van Berkel, S.S., Aik, W., Rydzik, A.M., Avison, M.B., Pettinati, I., Umland, K.D., Kawamura, A., Spencer, J., Claridge, T.D., McDonough, M.A. and Schofield, C.J.** (2014) Rhodanine hydrolysis leads to potent thioenolate mediated metallo-β-lactamase inhibition. *Nat Chem*, **6**(12): p. 1084-1090.
168. **Mojica, M.F., Mahler, S.G., Bethel, C.R., Taracila, M.A., Kosmopoulou, M., Papp-Wallace, K.M., Llarrull, L.I., Wilson, B.M., Marshall, S.H., Wallace, C.J., Villegas, M.V., Harris, M.E., Vila, A.J., Spencer, J. and Bonomo, R.A.** (2015) Exploring the Role of Residue 228 in Substrate and Inhibitor Recognition by VIM Metallo-β-lactamases. *Biochemistry*, **54**(20): p. 3183-3196.
169. **Castanheira, M., Deshpande, L.M., Mendes, R.E., Rodriguez-Noriega, E., Jones, R.N. and Morfin-Otero, R.** (2011) Comment on: role of changes in the L3 loop of the active site in the evolution of enzymatic activity of VIM-type metallo-β-lactamases. *J Antimicrob Chemother*, **66**(3): p. 684-685; author reply 686.

170. **Brown, N.G., Horton, L.B., Huang, W., Vongpunsawad, S. and Palzkill, T.** (2011) Analysis of the functional contributions of Asn233 in metallo-β-lactamase IMP-1. *Antimicrob Agents Chemother*, **55**(12): p. 5696-5702.
171. **Chiou, J., Leung, T.Y. and Chen, S.** (2014) Molecular mechanisms of substrate recognition and specificity of New Delhi metallo-β-lactamase. *Antimicrob Agents Chemother*, **58**(9): p. 5372-5378.
172. **Oelschlaeger, P., Mayo, S.L. and Pleiss, J.** (2005) Impact of remote mutations on metallo-β-lactamase substrate specificity: implications for the evolution of antibiotic resistance. *Protein Sci*, **14**(3): p. 765-774.
173. **Docquier, J.D., Riccio, M.L., Mugnaioli, C., Luzzaro, F., Endimiani, A., Toniolo, A., Amicosante, G. and Rossolini, G.M.** (2003) IMP-12, a new plasmid-encoded metallo-β-lactamase from a *Pseudomonas putida* clinical isolate. *Antimicrob Agents Chemother*, **47**(5): p. 1522-1528.
174. **Liscio, J.L., Mahoney, M.V. and Hirsch, E.B.** (2015) Ceftolozane/tazobactam and ceftazidime/avibactam: two novel β-lactam/β-lactamase inhibitor combination agents for the treatment of resistant Gram-negative bacterial infections. *Int J Antimicrob Agents*.
175. **Hampton, T.** (2013) Report reveals scope of US antibiotic resistance threat. *JAMA*, **310**(16): p. 1661-1663.
176. **Goto, M., Takahashi, T., Yamashita, F., Koreeda, A., Mori, H., Ohta, M. and Arakawa, Y.** (1997) Inhibition of the metallo-β-lactamase produced from *Serratia marcescens* by thiol compounds. *Biol Pharm Bull*, **20**(11): p. 1136-1140.
177. **Siemann, S., Clarke, A.J., Viswanatha, T. and Dmitrienko, G.I.** (2003) Thiols as classical and slow-binding inhibitors of IMP-1 and other binuclear metallo-β-lactamases. *Biochemistry*, **42**(6): p. 1673-1683.
178. **Bounaga, S., Laws, A.P., Galleni, M. and Page, M.I.** (1998) The mechanism of catalysis and the inhibition of the Bacillus cereus zinc-dependent β-lactamase. *Biochem J*, **331 (Pt 3)**: p. 703-711.
179. **Lassaux, P., Hamel, M., Gulea, M., Delbruck, H., Mercuri, P.S., Horsfall, L., Dehareng, D., Kupper, M., Frere, J.M., Hoffmann, K., Galleni, M. and Bebrone, C.** (2010) Mercaptophosphonate compounds as broad-spectrum inhibitors of the metallo-β-lactamases. *J Med Chem*, **53**(13): p. 4862-4876.
180. **Greenlee, M.L., Laub, J.B., Balkovec, J.M., Hammond, M.L., Hammond, G.G., Pompliano, D.L. and Epstein-Toney, J.H.** (1999) Synthesis and SAR of thioester and thiol inhibitors of IMP-1 metallo-β-lactamase. *Bioorg Med Chem Lett*, **9**(17): p. 2549-2554.
181. **Mollard, C., Moali, C., Papamicael, C., Damblon, C., Vessilier, S., Amicosante, G., Schofield, C.J., Galleni, M., Frere, J.M. and Roberts, G.C.** (2001) Thiomandelic acid, a broad spectrum inhibitor of zinc β-lactamases: kinetic and spectroscopic studies. *J Biol Chem*, **276**(48): p. 45015-45023.
182. **Heinz, U., Bauer, R., Wommer, S., Meyer-Klaucke, W., Papamichaels, C., Bateson, J. and Adolph, H.W.** (2003) Coordination geometries of metal ions in D- or L-captopril-inhibited metallo-β-lactamases. *Journal of Biological Chemistry*, **278**(23): p. 20659-20666.
183. **Li, N., Xu, Y., Xia, Q., Bai, C., Wang, T., Wang, L., He, D., Xie, N., Li, L., Wang, J., Zhou, H.G., Xu, F., Yang, C., Zhang, Q., Yin, Z., Guo, Y. and Chen, Y.** (2014) Simplified captopril analogues as NDM-1 inhibitors. *Bioorg Med Chem Lett*, **24**(1): p. 386-389.

184. **Gonzalez, M.M., Kosmopoulou, M., Mojica, M.F., Castillo, V., Hinchliffe, P., Pettinati, I., Brem, J., Schofield, C.J., Mahler, G., Bonomo, R.A., Llarrull, L.I., Spencer, J. and Vila, A.J.** (2015) Bisthiazolidines: A Substrate-Mimicking Scaffold as an Inhibitor of the NDM-1 Carbapenemase. *ACS Infect Dis*, **1**(11): p. 544-554.
185. **Fitzgerald, P.M., Wu, J.K. and Toney, J.H.** (1998) Unanticipated inhibition of the metallo-β-lactamase from Bacteroides fragilis by 4-morpholineethanesulfonic acid (MES): a crystallographic study at 1.85 Å resolution. *Biochemistry*, **37**(19): p. 6791-6800.
186. **Payne, D.J., Bateson, J.H., Gasson, B.C., Proctor, D., Khushi, T., Farmer, T.H., Tolson, D.A., Bell, D., Skett, P.W., Marshall, A.C., Reid, R., Ghosez, L., Combret, Y. and Marchand-Brynaert, J.** (1997) Inhibition of metallo-β-lactamases by a series of mercaptoacetic acid thiol ester derivatives. *Antimicrob Agents Chemother*, **41**(1): p. 135-140.
187. **Weide, T., Saldanha, S.A., Minond, D., Spicer, T.P., Fotsing, J.R., Spaargaren, M., Frere, J.M., Bebrone, C., Sharpless, K.B., Hodder, P.S. and Fokin, V.V.** (2010) NH-1,2,3-Triazole-based Inhibitors of the VIM-2 Metallo-β-Lactamase: Synthesis and Structure-Activity Studies. *ACS Med Chem Lett*, **1**(4): p. 150-154.
188. **Payne, D.J., Hueso-Rodriguez, J.A., Boyd, H., Concha, N.O., Janson, C.A., Gilpin, M., Bateson, J.H., Cheever, C., Niconovich, N.L., Pearson, S., Rittenhouse, S., Tew, D., Diez, E., Perez, P., de la Fuente, J., Rees, M. and Rivera-Sagredo, A.** (2002) Identification of a series of tricyclic natural products as potent broad-spectrum inhibitors of metallo-β-lactamases. *Antimicrobial Agents and Chemotherapy*, **46**(6): p. 1880-1886.
189. **Walter, M.W., Felici, A., Galleni, M., Soto, R.P., Adlington, R.M., Baldwin, J.E., Frere, J.M., Gololobov, M. and Schofield, C.J.** (1996) Trifluoromethyl alcohol and ketone inhibitors of metallo-β-lactamases. *Bioorganic & Medicinal Chemistry Letters*, **6**(20): p. 2455-2458.
190. **Siemann, S., Evanoff, D.P., Marrone, L., Clarke, A.J., Viswanatha, T. and Dmitrienko, G.I.** (2002) N-arylsulfonyl hydrazones as inhibitors of IMP-1 metallo-β-lactamase. *Antimicrobial Agents and Chemotherapy*, **46**(8): p. 2450-2457.
191. **Toney, J.H., Fitzgerald, P.M.D., Grover-Sharma, N., Olson, S.H., May, W.J., Sundelof, J.G., Vanderwall, D.E., Cleary, K.A., Grant, S.K., Wu, J.K., Kozarich, J.W., Pompliano, D.L. and Hammond, G.G.** (1998) Antibiotic sensitization using biphenyl tetrazoles as potent inhibitors of *Bacteroides fragilis* metallo-β-lactamase. *Chemistry & Biology*, **5**(4): p. 185-196.
192. **Toney, J.H., Cleary, K.A., Hammond, G.G., Yuan, X.L., May, W.J., Hutchins, S.M., Ashton, W.T. and Vanderwall, D.E.** (1999) Structure-activity relationships of biphenyl tetrazoles as metallo-β-lactamase inhibitors. *Bioorganic & Medicinal Chemistry Letters*, **9**(18): p. 2741-2746.
193. **Bounaga, S., Galleni, M., Laws, A.P. and Page, M.I.** (2001) Cysteinyl peptide inhibitors of *Bacillus cereus* zinc β-lactamase. *Bioorg Med Chem*, **9**(2): p. 503-510.
194. **Nagano, R., Adachi, Y., Hashizume, T. and Morishima, H.** (2000) In vitro antibacterial activity and mechanism of action of J-111,225, a novel 1β-methylcarbapenem, against transferable IMP-1 metallo-β-lactamase producers. *Journal of Antimicrobial Chemotherapy*, **45**(3): p. 271-276.
195. **Buynak, J.D., Chen, H.S., Vogeti, L., Gadhachanda, V.R., Buchanan, C.A., Palzkill, T., Shaw, R.W., Spencer, J. and Walsh, T.R.** (2004) Penicillin-derived inhibitors that

simultaneously target both metallo- and serine-β-lactamases. *Bioorganic & Medicinal Chemistry Letters*, **14**(5): p. 1299-1304.

196. **Tsang, W.Y., Dhanda, A., Schofield, C.J., Frere, J.M., Galleni, M. and Page, M.I.** (2004) The inhibition of metallo-β-lactamase by thioxo-cephalosporin derivatives. *Bioorganic & Medicinal Chemistry Letters*, **14**(7): p. 1737-1739.
197. **Hiraiwa, Y., Morinaka, A., Fukushima, T. and Kudo, T.** (2009) Metallo-β-lactamase inhibitory activity of phthalic acid derivatives. *Bioorg Med Chem Lett*, **19**(17): p. 5162-5165.
198. **Gilpin, M.L., Fulston, M., Payne, D., Cramp, R. and Hood, I.** (1995) Isolation and structure determination of two novel phenazines from a *Streptomyces* with inhibitory activity against metallo-enzymes, including metallo-β-lactamase. *J Antibiot (Tokyo)*, **48**(10): p. 1081-1085.
199. **Roll, D.M., Yang, Y., Wildey, M.J., Bush, K. and Lee, M.D.** (2010) Inhibition of metallo-β-lactamases by pyridine monothiocarboxylic acid analogs. *J Antibiot (Tokyo)*, **63**(5): p. 255-257.
200. **Lienard, B.M.R., Horsfall, L.E., Galleni, M., Frere, J.M. and Schofield, C.J.** (2007) Inhibitors of the FEZ-1 metallo-β-lactamase. *Bioorganic & Medicinal Chemistry Letters*, **17**(4): p. 964-968.
201. **Sanschagrin, F. and Levesque, R.C.** (2005) A specific peptide inhibitor of the class B metallo-β-lactamase L-1 from *Stenotrophomonas maltophilia* identified using phage display. *Journal of Antimicrobial Chemotherapy*, **55**(2): p. 252-255.
202. **Mohamed, M.S., Hussein, W.M., McGeary, R.P., Vella, P., Schenk, G. and Abd El-Hameed, R.H.** (2011) Synthesis and kinetic testing of new inhibitors for a metallo-β-lactamase from *Klebsiella pneumonia* and *Pseudomonas aeruginosa*. *Eur J Med Chem*, **46**(12): p. 6075-6082.
203. **Somboro, A.M., Tiwari, D., Bester, L.A., Parboosing, R., Chonco, L., Kruger, H.G., Arvidsson, P.I., Govender, T., Naicker, T. and Essack, S.Y.** (2015) NOTA: a potent metallo-β-lactamase inhibitor. *J Antimicrob Chemother*, **70**(5): p. 1594-1596.
204. **King, A.M., Reid-Yu, S.A., Wang, W., King, D.T., De Pascale, G., Strynadka, N.C., Walsh, T.R., Coombes, B.K. and Wright, G.D.** (2014) Aspergillomarasmine A overcomes metallo-β-lactamase antibiotic resistance. *Nature*, **510**(7506): p. 503-506.
205. **Ishii, Y., Eto, M., Mano, Y., Tateda, K. and Yamaguchi, K.** (2010) In Vitro Potentiation of Carbapenems with ME1071, a Novel Metallo-β-Lactamase Inhibitor, against Metallo-β-Lactamase-Producing *Pseudomonas aeruginosa* Clinical Isolates. *Antimicrobial Agents and Chemotherapy*, **54**(9): p. 3625-3629.
206. **Bush, K.** (2015) A resurgence of β-lactamase inhibitor combinations effective against multidrug-resistant Gram-negative pathogens. *Int J Antimicrob Agents*, **46**(5): p. 483-493.
207. **Klingler, F.M., Wichelhaus, T.A., Frank, D., Cuesta-Bernal, J., El-Delik, J., Muller, H.F., Sjuts, H., Gottig, S., Koenigs, A., Pos, K.M., Pogoryelov, D. and Proschak, E.** (2015) Approved Drugs Containing Thiols as Inhibitors of Metallo-β-lactamases: Strategy To Combat Multidrug-Resistant Bacteria. *J Med Chem*, **58**(8): p. 3626-3630.
208. **Lienard, B.M., Garau, G., Horsfall, L., Karsisiotis, A.I., Damblon, C., Lassaux, P., Papamicael, C., Roberts, G.C., Galleni, M., Dideberg, O., Frere, J.M. and Schofield, C.J.** (2008) Structural basis for the broad-spectrum inhibition of metallo-β-lactamases by thiols. *Org Biomol Chem*, **6**(13): p. 2282-2294.

209. **Miriagou, V., Carattoli, A. and Fanning, S.** (2006) Antimicrobial resistance islands: resistance gene clusters in *Salmonella* chromosome and plasmids. *Microbes Infect*, **8**(7): p. 1923-1930.
210. **Vella, P., Hussein, W.M., Leung, E.W., Clayton, D., Ollis, D.L., Mitic, N., Schenk, G. and McGeary, R.P.** (2011) The identification of new metallo-β-lactamase inhibitor leads from fragment-based screening. *Bioorg Med Chem Lett*, **21**(11): p. 3282-3285.
211. **Bebrone, C., Lassaux, P., Vercheval, L., Sohier, J.S., Jehaes, A., Sauvage, E. and Galleni, M.** (2010) Current challenges in antimicrobial chemotherapy: focus on β-lactamase inhibition. *Drugs*, **70**(6): p. 651-679.
212. **Jin, W., Arakawa, Y., Yasuzawa, H., Taki, T., Hashiguchi, R., Mitsutani, K., Shoga, A., Yamaguchi, Y., Kurosaki, H., Shibata, N., Ohta, M. and Goto, M.** (2004) Comparative study of the inhibition of metallo-β-lactamases (IMP-1 and VIM-2) by thiol compounds that contain a hydrophobic group. *Biol Pharm Bull*, **27**(6): p. 851-856.
213. **Cragg, G.M. and Newman, D.J.** (2013) Natural products: a continuing source of novel drug leads. *Biochim Biophys Acta*, **1830**(6): p. 3670-3695.
214. **Cragg, G.M., Grothaus, P.G. and Newman, D.J.** (2009) Impact of natural products on developing new anti-cancer agents. *Chem Rev*, **109**(7): p. 3012-3043.
215. **Capon, R.J.** (2001) Marine bioprospecting - Trawling for treasure and pleasure. *European Journal of Organic Chemistry*, (4): p. 633-645.
216. **D'Amico, S., Collins, T., Marx, J.C., Feller, G. and Gerday, C.** (2006) Psychrophilic microorganisms: challenges for life. *EMBO Rep*, **7**(4): p. 385-389.
217. **Svenson, J.** (2013) MabCent: Arctic marine bioprospecting in Norway. *Phytochem Rev*, **12**: p. 567-578.
218. **Kubanek, J., Jensen, P.R., Keifer, P.A., Sullards, M.C., Collins, D.O. and Fenical, W.** (2003) Seaweed resistance to microbial attack: a targeted chemical defense against marine fungi. *Proc Natl Acad Sci U S A*, **100**(12): p. 6916-6921.
219. **Matz, C., Webb, J.S., Schupp, P.J., Phang, S.Y., Penesyan, A., Egan, S., Steinberg, P. and Kjelleberg, S.** (2008) Marine biofilm bacteria evade eukaryotic predation by targeted chemical defense. *PLoS One*, **3**(7): p. e2744.
220. **Crisp, J., Conners, R., Garrity, J.D., Carenbauer, A.L., Crowder, M.W. and Spencer, J.** (2007) Structural basis for the role of Asp-120 in metallo-β-lactamases. *Biochemistry*, **46**(37): p. 10664-10674.
221. **Samuelsen, Ø., Castanheira, M., Walsh, T.R. and Spencer, J.** (2008) Kinetic characterization of VIM-7, a divergent member of the VIM metallo-β-lactamase family. *Antimicrob Agents Chemother*, **52**(8): p. 2905-2908.
222. **Baker, E.N. and Hubbard, R.E.** (1984) Hydrogen-Bonding in Globular-Proteins. *Progress in Biophysics & Molecular Biology*, **44**(2): p. 97-179.
223. **Pace, C.N., Fu, H., Lee Fryar, K., Landua, J., Trevino, S.R., Schell, D., Thurlkill, R.L., Imura, S., Scholtz, J.M., Gajiwala, K., Sevcik, J., Urbanikova, L., Myers, J.K., Takano, K., Hebert, E.J., Shirley, B.A. and Grimsley, G.R.** (2014) Contribution of hydrogen bonds to protein stability. *Protein Sci*, **23**(5): p. 652-661.
224. **Oelschlaeger, P. and Mayo, S.L.** (2005) Hydroxyl groups in the ββ sandwich of metallo-β-lactamases favor enzyme activity: a computational protein design study. *J Mol Biol*, **350**(3): p. 395-401.
225. **Pegg, K.M., Liu, E.M., Lacuran, A.E. and Oelschlaeger, P.** (2013) Biochemical characterization of IMP-30, a metallo-β-lactamase with enhanced activity toward ceftazidime. *Antimicrob Agents Chemother*, **57**(10): p. 5122-5126.

226. **Docquier, J.D., Lamotte-Brasseur, J., Galleni, M., Amicosante, G., Frere, J.M. and Rossolini, G.M.** (2003) On functional and structural heterogeneity of VIM-type metallo-β-lactamases. *J Antimicrob Chemother*, **51**(2): p. 257-266.
227. **Poirel, L., Rodriguez-Martinez, J.M., Al Naiemi, N., Debets-Ossenkopp, Y.J. and Nordmann, P.** (2010) Characterization of DIM-1, an integron-encoded metallo-β-lactamase from a *Pseudomonas stutzeri* clinical isolate in the Netherlands. *Antimicrob Agents Chemother*, **54**(6): p. 2420-2424.
228. **Tomatis, P.E., Rasia, R.M., Segovia, L. and Vila, A.J.** (2005) Mimicking natural evolution in metallo-β-lactamases through second-shell ligand mutations. *Proc Natl Acad Sci U S A*, **102**(39): p. 13761-13766.
229. **Oelschlaeger, P., Schmid, R.D. and Pleiss, J.** (2003) Insight into the mechanism of the IMP-1 metallo-β-lactamase by molecular dynamics simulations. *Protein Eng*, **16**(5): p. 341-350.